Cardiology Research and Practice

Diagnostic and Prognostic Role of Cardiac Magnetic Resonance in Cardiomyopathies

Lead Guest Editor: George Bazoukis
Guest Editors: Gary Tse and Vassilios Vassiliou

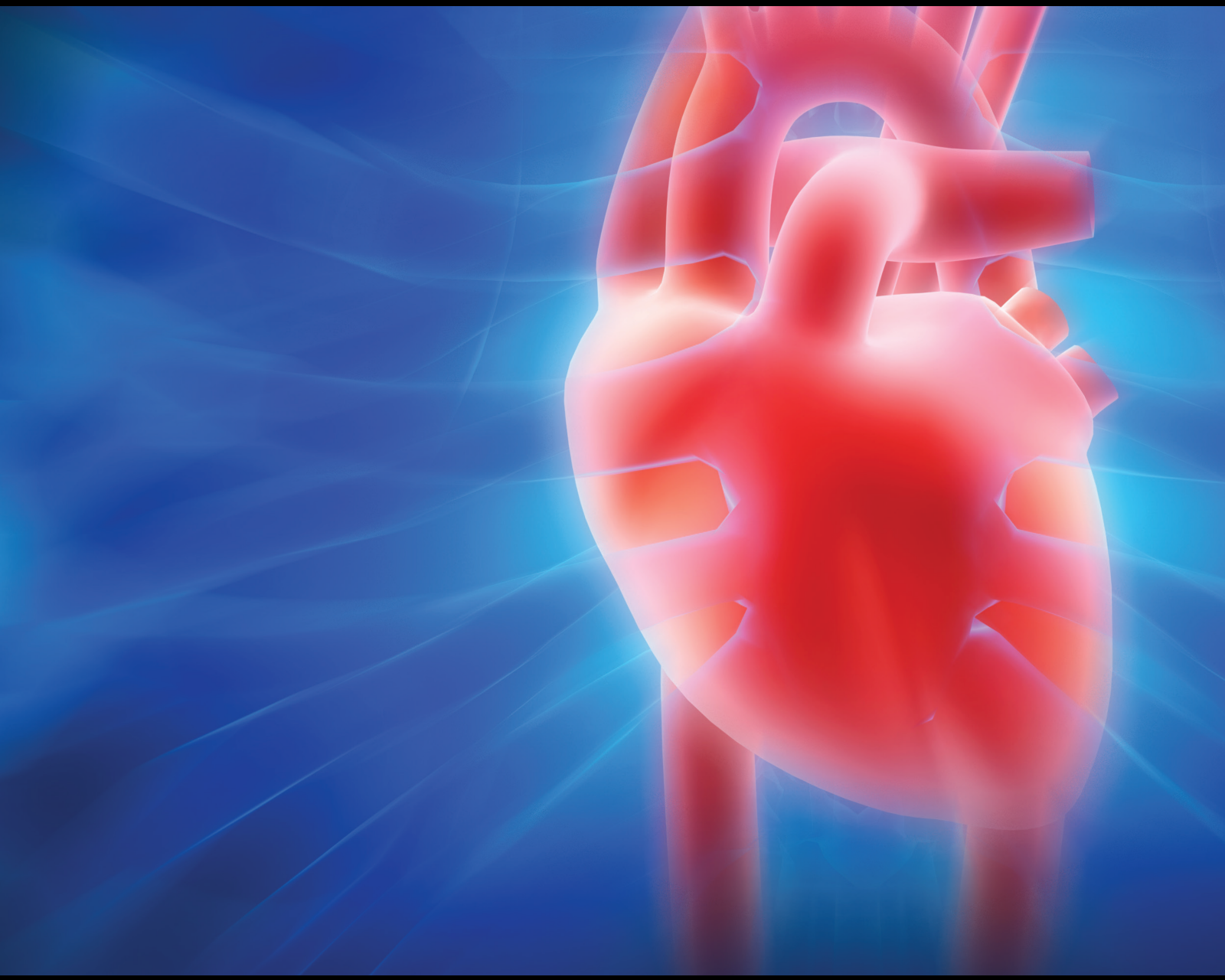

Diagnostic and Prognostic Role of Cardiac Magnetic Resonance in Cardiomyopathies

Cardiology Research and Practice

Diagnostic and Prognostic Role of Cardiac Magnetic Resonance in Cardiomyopathies

Lead Guest Editor: George Bazoukis
Guest Editors: Gary Tse and Vassilios Vassiliou

Contents

Hindawi
Cardiology Research and Practice
Volume 2022, Article ID 1910841, 14 pages
https://doi.org/10.1155/2022/1910841

Review Article

Herceptin-Mediated Cardiotoxicity: Assessment by Cardiovascular Magnetic Resonance

Jin Jiang,[1] **Boyang Liu**,[1,2] **and Sandeep S Hothi**[1,2]

[1]*Heart and Lung Centre, New Cross Hospital, Wolverhampton, UK*
[2]*Institute of Cardiovascular Sciences, College of Medical and Dental Sciences, University of Birmingham, Birmingham, UK*

Correspondence should be addressed to Sandeep S Hothi; sandeephothi@gmail.com

Received 1 May 2021; Revised 12 October 2021; Accepted 20 January 2022; Published 27 February 2022

Academic Editor: Francesco Paciullo

Herceptin (trastuzumab) is a recombinant, humanized, monoclonal antibody that targets the human epidermal growth factor receptor 2 (HER2) and is used in the treatment of HER2-positive breast and gastric cancers. However, it carries a risk of cardiotoxicity, manifesting as left ventricular (LV) systolic dysfunction, conventionally assessed for by transthoracic echocardiography. Clinical surveillance of cardiac function and discontinuation of trastuzumab at an early stage of LV systolic dysfunction allow for the timely initiation of heart failure drug therapies that can result in the rapid recovery of cardiac function in most patients. Often considered the reference standard for the noninvasive assessment of cardiac volume and function, cardiac magnetic resonance (CMR) imaging has superior reproducibility and accuracy compared to other noninvasive imaging modalities. However, due to limited availability, it is not routinely used in the serial assessment of cardiac function in patients receiving trastuzumab. In this article, we review the diagnostic and prognostic role of CMR in trastuzumab-mediated cardiotoxicity.

1. Introduction

Herceptin (trastuzumab) is a recombinant, humanized, monoclonal antibody directed against the extracellular domain IV of the human epidermal growth factor receptor 2 (HER2) and is indicated for the treatment of HER2-positive breast and gastric cancers [1–3]. HER2 positivity is relatively frequent, found in around one-fifth of breast and gastric cancer patients [4, 5]. Trastuzumab has been transformational for the prognosis of these patients, acting through its mechanisms of preventing HER2 dimerization and downstream signalling, HER2 internalization and degradation, and antibody-dependent cellular cytotoxicity [6, 7].

Although the chemotherapeutic mechanisms of trastuzumab are well characterised, the molecular aspects of trastuzumab-induced cardiotoxicity, recognised since its phase III trial [8], remain incompletely understood. Early studies have reported trastuzumab-related cardiotoxicity to be largely reversible with endomyocardial biopsies demonstrating an absence of the typical anthracycline-induced cardiomyocyte vacuolization or dropout [9]. However, in vivo mice studies have found trastuzumab to alter the expression of 15 genes involved in cardiac contractility, adaptation to stress, as well as DNA repair, cellular proliferation, healing, and mitochondrial function [10]. Furthermore, trastuzumab-mediated phosphorylation of HER1 and HER2 has been reported to activate the autophagy inhibitory Erk signalling pathway in human primary cardiomyocytes, inducing cardiotoxicity by disrupting the cardiomyocyte's ability to recycle cellular toxins [11]. These data, together with analyses of major trastuzumab trials, have highlighted the potential for trastuzumab to induce persistent left ventricular (LV) systolic dysfunction (LVSD) despite drug cessation [12]. This is of concern particularly as heart failure induced by cancer therapy is associated with worse outcomes than that of more common heart failure patients [13]. Despite this, it is important to recognise that close clinical surveillance and discontinuation of trastuzumab at an early stage of LVSD will allow the timely initiation of heart

failure drug therapies that can result in the rapid recovery of cardiac function in most patients [1, 14].

Consequently, a distinct multidisciplinary clinical subspecialty, cardio-oncology, has emerged with the aim of preventing, monitoring, and treating cancer therapeutics-related cardiac dysfunction (CTRCD) [15]. In current cardio-oncology practice, transthoracic echocardiography (TTE) remains the first line for cardiac surveillance among oncology patients due to its widespread availability and lack of radiation exposure [16–19]. However, with a reported temporal inter- and intra-observer variability of 10% in the assessment of left ventricular ejection fraction (LVEF) by 2D TTE [20], cardiac magnetic resonance (CMR) is gaining an increasingly prominent role in cardio-oncology. Often considered the reference standard for the assessment of cardiac volume and function, CMR has demonstrated superior reproducibility and accuracy compared to other conventional methods [21]. However, due to limited availability, it is not widely used in the serial monitoring for cardio-oncology assessment. Here in this article, we aim to review the diagnostic and prognostic role of CMR in trastuzumab-mediated cardiotoxicity.

2. Volumetric Assessment and CMR

The assessment of cardiac function before, during, and after therapy is essential for all cancer patients undergoing potentially cardiotoxic therapy [16]. Whilst CMR is widely considered as the reference standard for cardiac volumetric assessment, its current role remains reserved for patients with inadequate echocardiographic windows due to limitations in availability, higher cost, and the requirement of patient cooperation with breath-holding and an absence of claustrophobia [1, 16, 21]. Conversely, echocardiography with its wider availability and cost-effectiveness is highly suited for serial surveillance. Consequently, given that definitions of cardiotoxicity in many oncology trials are based on a reduction of LVEF, TTE-derived LVEF remains the first-line method for the detection of CTRCD according to consensus guidelines [1, 16–19] (Figure 1). One of the key limitations of 2D TTE is its significant inter- and intra-observer variation, often quoted at 10% [16, 20]. Therefore, it can be challenging to discern whether a change in LVEF, for instance from 55 to 45%, represents true dysfunction or merely inter-study variation. This variability can be improved with the use of LV opacification contrast and is better still with 3D TTE [20, 23]. Similarly, 3D TTE has been reported to possess superior sensitivity (53%) to 2D TTE (25–29%) for the identification of LVEF <50% in adult survivors of childhood cancer when using CMR quantification as the reference standard [24]. However, it is evident from a recent survey of 96 echocardiographic laboratories from 22 different countries across Europe that there are wide variations in the adoption of 3D TTE with only 32% of centres routinely capturing 3D data for all TTE studies, and 20% of centres not performing any 3D TTE [25]. Furthermore, the feasibility of 3D TTE can be suboptimal even under research conditions. In a study of 100 breast cancer patients undergoing baseline and surveillance TTE during chemotherapy, 3D TTE was reported to be feasible in only 66% of studies, with factors such as increasing age, weight, smoking, mastectomy, and concomitant radiotherapy contributing to poor 3D image quality [26].

Multigated acquisition (MUGA) scanning was once a commonly used method for serial evaluation of cardiotoxicity. Despite low inter- and intra-observer variability, such methodology may be rendered obsolete in modern times due to low sensitivity to subtle changes and radiation exposure [27] (Table 1).

The superior accuracy and lower variability of CMR lend it clinical significance not only for the timely diagnosis of CTRCD, via detection of true positives cases, but also for its ability to avoid false negatives, thereby preventing unnecessary treatment interruptions. This is evident from a retrospective cohort study of 369 patients receiving trastuzumab therapy for breast cancer where trastuzumab was withheld for at least 4 weeks in patients who had experienced a decline in LVEF ≥16%, or decline ≥10% whilst below normal LVEF limits [28]. This treatment interruption allowed time for cardiology review and cardioprotective therapy initiation. Despite trastuzumab being recommenced in those whose LVEF recovered to normal, patients experiencing any treatment interruption possessed significantly worse outcomes in terms of both disease-free survival (adjusted hazards ratio of 4.4, $P = 0.001$) and overall survival (adjusted hazards ratio 4.8, $P < 0.001$) [28].

In the absence of randomized prospective studies directly comparing patient outcomes from CMR and TTE derived LVEF, guidance from the British Society for Echocardiography (BSE) and British Cardio-Oncology Society (BCOS) recognises the addition of recent pilot data on the safe use of trastuzumab in patients with asymptomatic reductions in TTE-derived LVEF down to 40% [17, 29, 30]. These guidelines may help to compensate for the variability associated with TTE derived LVEF discussed above, emphasising the ESC's personalized approach to cardiac surveillance by cardio-oncology services [16], and support echocardiography in remaining at the core of cardio-oncology diagnostics.

3. Myocardial Strain and CMR

While LVEF has historically been used as a standard measure of systolic function, there is increasing interest in the use of more sensitive markers that can detect "subclinical" signs of LV dysfunction that can aid earlier initiation of cardioprotective therapy. The extent of myocardial deformation which occurs following application of contractile and relaxation forces can be quantified as strain, defined as the percent change in myocardial length from the relaxed to the contractile state. This deformation represents a fundamental property of the tissue [31] and there is increasing evidence for a causative relationship between the development of myocardial fibrosis and a reduction in ventricular deformation across a range of conditions [32–34]. Deformation imaging may, therefore, act as a functional imaging biomarker of myocardial fibrosis and offer additional prognostic information for the personalized

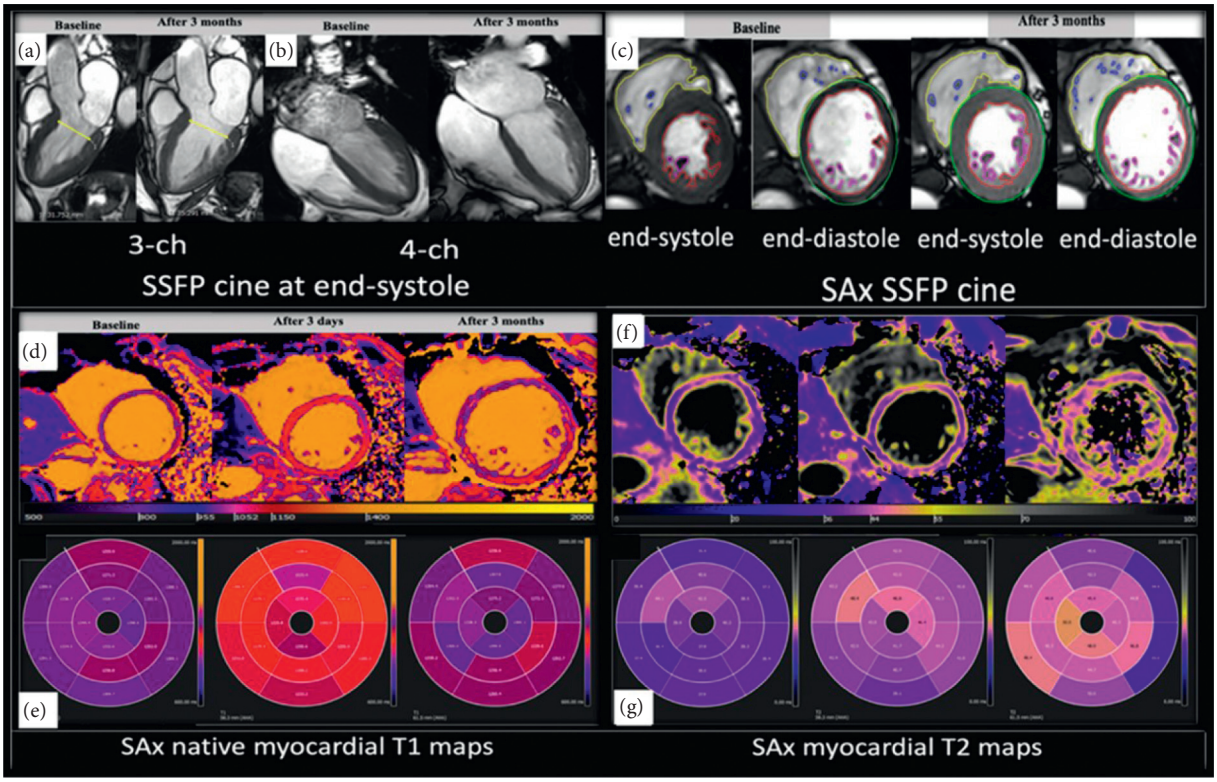

Figure 1: Representative images of trastuzumab-induced cardiotoxicity. Cine 3-chamber (a) and 4-chamber views (b) as well as short axis view (c) during baseline study (LVEF = 66%) and 3 months thereafter (LVEF = 54%). Native T1 (d) shows reduction of global left ventricular value after 3 days (baseline = 1196 ms, 1st follow-up = 1172 ms, and 2nd follow-up = 1277 ms). Myocardial T2 (f) shows subtle elevation of global value after 3 months (baseline = 40 ms, 1st follow-up = 43 ms, and 2nd follow-up = 44 ms). The average segmental T1 and T2 times are displayed as "bull's eye" images (e, g). The colour maps represent continuous T1 and T2 values. LVEF, left ventricular ejection fraction; reproduced with permission from Abdelmonem Atia et al. [22].

Table 1: Advantages and disadvantages of imaging modalities.

Imaging modalities	Cardiac MRI	Echocardiography	Multigated acquisition scan
Advantages	High spatial and temporal resolution Superior signal-to-noise ratio Free choice of imaging plane No geometric assumptions required	Widespread availability and feasibility Low cost Portable Current standard and guideline-recommended	Low inter- and intra-observer variability (<5%) No need for geometric confirmation LVEF calculation highly reproducible
Disadvantages	Expensive Lack of portability Claustrophobic patients unable to tolerate Contraindicated in patients with ferromagnetic metallic implants Potential for nephrogenic systemic fibrosis	Operator dependence Suboptimal acoustic windows Use of geometric assumption High temporal and observer variability	Repeated exposure to radiation (5–10 millisieverts) Exposure to radioactive isotope tracers Requires venepuncture The gamma camera may be suboptimal for critical measurements of EF

management of patients receiving trastuzumab. Unlike the inherent flaws of a simplistic measurement such as LVEF, strain allows quantification of the different spatial components of contractile function in either longitudinal (GLS), circumferential (GCS), or radial (GRS) directions, both globally and regionally.

Most myocardial strain studies in patients receiving trastuzumab have used GLS derived from 2D speckle tracking echocardiography (STE). A meta-analysis of 9 studies found reduced GLS to be associated with a higher CTRCD risk (odds ratio 12.27; 95% CI 5.84–42.85; area under the hierarchical summary receiver operating

characteristic curves 0.86; 95% CI, 0.83–0.89) [35]. However, there remains uncertainty regarding whether a strain-guided management approach offers incremental prognostic value compared to an LVEF-guided approach. In an observational study where 24 out of 81 consecutive women receiving trastuzumab developed CTRCD, GLS reduction was the strongest predictor of cardiotoxicity [36]. However, in the only prospective randomized controlled trial where 331 anthracycline-treated patients were randomized to either LVEF or GLS guided therapy, there were no significant differences in the primary outcome of change in LVEF between the two different study arms [37]. Despite this, it is important to recognise that the GLS-guided approach led to greater use of cardioprotective therapy, higher final LVEF, and lower incidence of CTRCD [37]. The current limitation of STE derived GLS is in its significant inter-vendor variability [38] with guideline quoted normal GLS values of $<-17\%$ for men and $<-18\%$ for women being specific to General Electric (United States) analysis software [17] alongside the demands for good image quality. Strain analysis of 3D STE datasets is also feasible. However, as a relatively novel technique, there is a lack of data for its use in CTRCD and it generally demands patients to breath-hold as well as a regular cardiac rhythm to enable multi-beat 3D acquisition [39].

Myocardial strain quantification is also feasible with CMR and is traditionally performed with one of many dedicated "tagging" sequences (such as spatial modulation of magnetization (SPAMM), harmonic phase (HARP), displacement encoding (DENSE), and strain encoding (SENC). These sequences magnetise temporary tags into the myocardium which are prominent during systole and fade during diastole. These tags can be tracked throughout the cardiac cycle to highlight myocardial movement. CMR-tagging derived GLS and GCS have been noted to be worse (less negative) than STE derived strain in a study of 46 cancer survivors exposed to anthracycline therapy with normal range LVEF, suggesting CMR to be more sensitive to subclinical LV dysfunction compared to TTE [40]. Looking beyond cardio-oncology, CMR-tagging GCS was again found to offer incremental predictive value to the traditional parameters of LVEF, left ventricular mass, and cardiovascular risk factors, for the future onset of heart failure in 1768 asymptomatic individuals from the Multi-Ethnic Study of Atherosclerosis (MESA) cohort [41].

The main disadvantage of dedicated deformation CMR sequences is their time-consuming nature. To overcome this, it is possible to derive strain from feature-tracking of steady-state free precession (SSFP) cine images, with important distinctions being made between 2D (average strain value of three long-axis studies) and 3D derived strain values [42]. Whereas 3D STE is adversely affected by both poor spatial and temporal resolution (leading to coarser speckle patterns) and requires stitching together of volumes to achieve adequate frame rates for analysis at higher heart rates, CMR cine stack datasets are intrinsically three-dimensional with strain quantification highly feasible [42]. Theoretically, 3D strain quantification (either by CMR or STE) overcomes the overestimation of myocardial movement that results from the through-plane loss of features into the third dimension which plagues 2D myocardial deformation techniques [43]. This means that the absolute values of 3D strain are usually lower than that of 2D strain and are likely provide a closer representation of underlying myocardial mechanics [42]. Being relatively novel techniques, the incremental value of CMR feature-tracking derived strain is not well known, with only one study confirming feasibility of 2D CMR feature tracking and its correlation with CMR derived LVEF [44].

A large meta-analysis comprising 65 studies and 2888 patients compared the most used noninvasive imaging modalities to the reference standard CMR in the last two decades [45]. The findings revealed significant negative bias in LV end-diastolic volume (LVEDV) and LV end-systolic volume (LVESV) for 2DE ± contrast and 3DE, demonstrating that echocardiography-based techniques tend to underestimate these values, whereas computed tomography (CT) correlates closely, when compared to CMR (Figure 2). In an earlier study involving 114 patients, echocardiography was compared to CMR imaging, focusing on the reference standard for LV function [24]. The study reported that LV volume was consistently underestimated in 2DE and 3DE compared to CMR, and cardiac mass was higher in 2DE than CMR. Compared to CMR, the echocardiographic methods correlated rather poorly, specifically 2D TTE, which demonstrated a low sensitivity (25%) and high false-positive rate (75%) with a mean LVEF 5% higher than CMR. While 3D TTE compared more favourably to CMR and demonstrated less variability, the authors concluded the technique lacks the desired accuracy to detect subtle changes that may have important therapeutic implication.

4. Varying Definitions of Cardiotoxicity

Cardiotoxicity is a broad term that refers to any direct untoward toxic effects on cardiac structure and function or the acceleration of cardiovascular disease (CVD) among patients with cardiovascular risk factors or preexisting CVD as a result of cancer therapy [46]. A universal definition for cardiotoxicity is lacking and often oversimplified, resulting in the term being shrouded with controversy due to a lack of clarity. Since the earliest definition of cardiotoxicity was defined [47], definitions used for clinical decisions have varied among different consensus guidelines and clinical trials, usually based on variable cut-off values for LVEF in various imaging modalities [48] (Table 2).

More recently, the European Association of Cardiovascular Imaging (EACVI) and the American Society of Echocardiography (ASE) defined cardiotoxicity as $\geq 10\%$ decline in LVEF to a final LVEF $<53\%$ by echocardiography, multigated acquisition scan (MUGA), and cardiac magnetic resonance imaging (CMR), as well as being the first reported guidelines to include global longitudinal strain (GLS) reduction defined as $>15\%$ [16, 19]. The British Society of Echocardiography (BSE) and the British Cardio-Oncology Society (BCOS) have jointly published similar guidelines for adult cancer patients, specifically patients receiving anthracycline ± trastuzumab therapy [17]. The consensus guideline classified cardiotoxicity into three categories: (1)

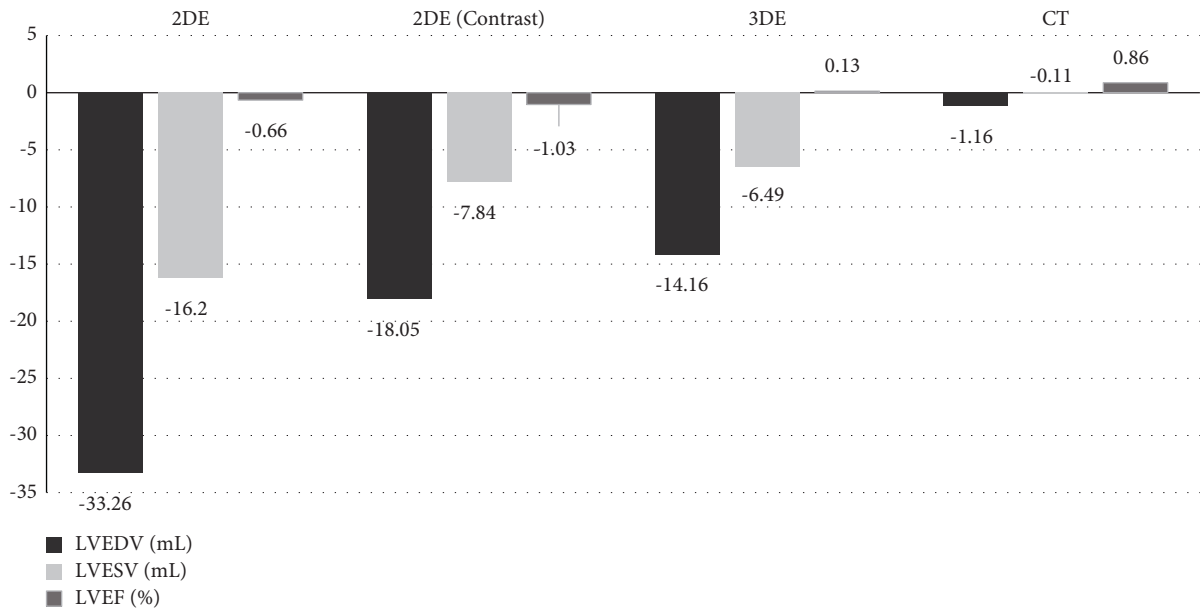

Figure 2: Mean bias associated with LV quantification by multimodality imaging compared to reference CMR using data derived from Rigolli et al. [45].

cardiotoxicity, (2) probable subclinical cardiotoxicity, and (3) possible subclinical cardiotoxicity, which should ideally be achieved via advanced echocardiographic measures (2D/3D LVEF and GLS). Additionally, technical considerations should be accounted for due to various factors (clear visualisation endocardial border and timing of measurement during cardiac cycle) that could influence GLS values, thereby further limiting efforts to define abnormal GLS. Establishing a definitive description of cardiotoxicity is vitally important with major clinical implications because while failing to detect cardiotoxicity promptly is harmful, overdiagnosis is equally detrimental, potentially causing interruption to a patient's cancer treatment and thereby impacting upon oncological outcomes.

Trastuzumab has demonstrated effectiveness when used either as monotherapy or in combination with other substances [52]. However, rarely is trastuzumab administered as a single agent, but is instead more commonly combined with surgery, chemotherapy, and radiotherapy as adjuvant therapy. To date, most patients treated with trastuzumab monotherapy have previously been exposed to other forms of treatment such as anthracycline, either prior to, or concurrently with trastuzumab administration. Consequently, the assessment of trastuzumab-related cardiotoxicity is often confounded by the lack of patients with no prior anthracycline exposure. This is important as trastuzumab and anthracycline are considered to have different mechanisms of action. Trastuzumab tends to cause cellular dysfunction in most patients and is perceived to be largely reversible (type 2 cardiotoxicity), whereas anthracycline cardiomyopathy is associated with irreversible myocyte necrosis in the form of apoptosis (type 1 cardiotoxicity) (Table 3) [9]. However, this distinction may be further complicated as recent evidence suggests that trastuzumab could share some common mechanisms with anthracycline-mediated cardiotoxicity, with equally profound toxicity, particularly amongst the elderly population with near-normal ejection fraction and risk factors for CVD. While anthracycline cardiotoxicity is often perceived to be irreversible, there have been reports of partial recovery of cardiac function. Trastuzumab-induced cardiotoxicity is not always reversible [67, 68]. Hence, the classifications of cardiotoxicity so far are oversimplifications, failing to reflect the nuance of its complex pathophysiology and natural history.

5. Mechanisms of Trastuzumab Cardiotoxicity

The mechanisms of trastuzumab-induced cardiotoxicity remain to be definitively identified. Limited data from myocardial biopsies reveal rather different mechanisms between trastuzumab and anthracycline, and the prompt recovery of trastuzumab-induced toxicity upon treatment discontinuation further supports this [9]. Different mechanisms have been proposed relating to the cardiotoxic mechanism, while potentially multifactorial and likely attributed to the anti-HER2 activity; this remains a topic for extensive discussion. *In vivo* work in HER2-deleted mice showed interruption to the HER2 signalling pathway resulted in the spontaneous development of dilated cardiomyopathy [75], supporting the notion that HER2 signalling is an important modifier in heart failure. Preclinical studies revealed an overactive HER pathway characterised as overexpression of HER2 receptor on a breast tumour cell or multiple copies of HER2 gene in the nucleus of the cell being the potential underlying mechanism of HER2+ breast cancer [76]. Presently, disruption to NRG/ErbB signalling is recognised as the most likely mechanism of trastuzumab-induced cardiotoxicity. Trastuzumab is known to selectively bind to the juxtamembrane domain IV of HER2 - a section

Table 2: Definitions of cardiotoxicity.

Author and year of publication	Testing modality	Definition of cardiotoxicity	Additional information
Alexander et al. 1979 [47]	Multigated acquisition (MUGA) scan	Mild: decline in LVEF >10% Moderate: decline in LVEF >15% to final LVEF <45% Severe: congestive HF	Anthracycline
Cardiac review and evaluation committee, Seidman et al. 2002 [49]	Echocardiography and MUGA	Drop in global LVEF or more severe in septum ≥5% decline to final EF <55% with symptoms of congestive HF Asymptomatic decline of ≥10% to final EF <55%	Trastuzumab ± anthracycline
American society of echocardiography (ASE), Plana et al. 2014 [19]	Echocardiography	≥10% decline in LVEF to final LVEF <53% Reduction in global longitudinal strain (GLS) > 15% from baseline	First guideline to include GLS >15% reduction as definition of cardiotoxicity Trastuzumab
Barthur et al. 2017 [50]	Cardiac magnetic resonance	EF < 50%	Trastuzumab
NICE (National Guideline Alliance, 2018) [18]	Echocardiography	LVEF drops by 10 percentage (ejection) points or more from baseline and to below 50%	Chemotherapeutic agents
Keramida et al. 2019 [51]	Echocardiography	≥10% decline in LVEF to final LVEF <50%	GLS reduction >15% Trastuzumab
European association of cardiovascular imaging (EACVI), Čelutkienė et al. 2020 [16]	Echocardiography	≥10% decline in LVEF to final LVEF <53% Relative reduction in global longitudinal strain (GLS) reduction by >15% from baseline	
British Society of Echocardiography (BSE) jointly with British Cardio-Oncology Society (BCOS), Dobson et al. 2021 [17]	Echocardiography	The definition is categorised into three groups Cardiotoxicity: LVEF: a decline in LVEF by >10 absolute percentage points to a value <50% Probable subclinical cardiotoxicity: LVEF: a decline in LVEF by >10 absolute percentage points to a value ≥50% with an accompanying fall in GLS >15% from baseline Possible subclinical cardiotoxicity: LVEF: a decline in LVEF by <10 absolute percentage points to a value <50%	Trastuzumab ± anthracycline

Adapted from Lambert, J. and Thavendiranathan, P., 2016. *Controversies in the Definition of Cardiotoxicity: Do We Care? American College of Cardiology*. [online] American College of Cardiology. Available at <https://www.acc.org/latest-in-cardiology/articles/2016/07/07/14/59/controversies-in-the-definition-of-cardiotoxicity> (Accessed 25 August 2021).

of the extracellular domain essential for HER2 - ErbB4 and HER2-ErbB4 dimerization within the cardiomyocytes. Upon binding, the antibody downregulates the expression of HER2 which initiates a cascade of downstream signalling of the PI3K-AKT-mTOR pathway, which is an important contributor in cellular growth, proliferation, and survival [77]. In patients preexposed to anthracycline, it is probable these patients have begun to undergo subclinical or clinical apoptotic/necrotic process, thereby increasing susceptibility to further myocardial damage. Trastuzumab-associated heart failure is likely the cause of ongoing attrition of myocytes over time.

6. Prognosis and Reversibility of Trastuzumab-Induced Cardiotoxicity

In contrast to anthracycline, the clinical outcome for trastuzumab-induced cardiotoxicity is generally considered to be more favourable since LV dysfunction appears largely reversible upon the discontinuation of trastuzumab, and the inclusion of standard cardioprotective therapy seems to accelerate the recovery process [78]. A right ventricular- (RV-) focused CMR study by Barthur et al. [50] found that while RVEF and LVEF had declined with increased RVEDV and RVESV during therapy, all parameters had normalised

Table 3: Clinical features differentiating herceptin- and anthracycline-related cardiac dysfunction.

Characteristics	Herceptin (trastuzumab)	Anthracycline (doxorubicin)
Cardiotoxicity	Myocardial dysfunction, also referred to as type II cardiotoxicity	Myocardial damage, also referred to as type I cardiotoxicity
Incidence	2–27%* [49]	3–26% [53, 54]
Mechanisms	Not definitively understood, though may be multifactorial. The most likely mechanism may be the consequence of attenuated NRG/HER-2 mediated signal transduction pathway and increased susceptibility to anthracycline exposure [55]	Incompletely understood, though may be multifactorial. Potential mechanisms include the following: Type IIB topoisomerases-doxorubicin binding [56] Disruption of Ca^{2+} homeostasis [57] The upregulation of DRs, including TNFR1, Fas, DR4, and DR5 [57] Disruption in HER2/HER4 and NRG-1 signalling Such mechanisms lead to mitochondrial dysfunction, free radical generation, myocardial oxidative stress, and causing cell apoptosis
Dose effect	Dose-independent [58, 59]	Cumulative, dose-dependent [59, 60]
Features	No ultrastructural changes observed [9, 61]	Ultrastructural changes detected [62]
Clinical course and reversibility	Mostly reversible upon the discontinuation of the agent [9, 63]	Mostly irreversible [64]
Response to cardioprotective therapy	ACEi and β-blockers appear to mitigate the risk of HIC [9, 29, 30]	β-blockers (particularly carvedilol) have shown promising results in preserving cardiac function. ACEi could mitigate oxidate stress, LV remodelling, and apoptosis. Statins consist of antioxidant and anti-inflammatory properties [65] Dexrazoxane may, in part, prevent toxicity by binding to type IIB topoisomerases [66]
Recommencement of agent	Considered relatively safe [9, 46]	High probability of recurrence of dysfunction or cardiotoxicity [9]

ACEi, angiotensin converting enzyme inhibitor; NRG-1, neuregulin-1; HIC, herceptin-induced cardiotoxicity; DRs, death receptors; TNFR1, TNF receptor 1; LV, left ventricular. *The patient cohort in these trials may have been preexposed to anthracycline.

at 18 months, six months following the cessation of therapy. Consistent with these findings is another study by Ong et al. [72] which utilised feature tracking (FT) strain analysis. The authors reported a reduction in LVEF, FT-GLS, and FT-GCS at 6 and 12 months into therapy. By 18 months, with treatment completed 6 months prior, the parameters returned to near baseline level. Ewer et al. [9] reported on the reversibility of trastuzumab-related LVEF reduction, showing improvements in cardiac function typically at 4 to 6 weeks (before, 0.61 ± 0.13; during, 0.43 ± 0.16; after, 0.56 ± 0.11) following the withdrawal of therapy [79].

Trastuzumab-mediated cardiotoxicity is generally considered to not cause ultrastructural changes, though benign ultrastructural changes were observed from endomyocardial biopsy samples in a trial by Ewer and Ewer [80]. It should be noted that while this is a sensitive method for the evaluation of chemotherapeutic drug-induced cardiotoxicity, its invasive nature and questionable ability to predict clinical outcome renders it impractical for routine clinical use. Moreover, abnormalities uncovered from cardiac biopsy only reflect recent and ongoing changes rather than earlier insults.

Additionally, an earlier trial comprising 160 patients by Fallah-Rad et al. [81] identified 10 trastuzumab-induced cardiotoxic patients with subepicardial linear LGE in the lateral portion of the LV. Interestingly, at 6-month follow-up evaluation, despite EF recovery in 6 of the 10 patients, these LGE findings persisted, suggesting persistent myocardial injury. Such findings were amplified in a study by Wadhwa et al. [82] where of the 36 patients that developed mostly asymptomatic cardiotoxicity, subepicardial linear LGE of the LV was observed in 34 patients. Elevation of troponin-I was also reported in 4 patients following >6 cycles of treatment in another trial [83], implying ongoing myocardial necrosis. The underlying mechanism for the presence of LGE is unclear, particularly in the subepicardial lateral portion of the LV, perhaps merely a typical distribution and location associated with this agent (Figure 3).

Relatively little is currently known about the long-term prognosis of trastuzumab-induced cardiotoxicity. To our knowledge, CMR studies to date have seldom followed up patients beyond 18 months. From the available data [50, 72, 73], despite most CMR parameters having demonstrated statistically significant changes at 18 months, the magnitude of reductions is small. This raises the question as to whether these statistically significant reductions are also truly clinically significant for previously cardiotoxic patients or whether they might potentially pose a greater risk of cardiac functional deterioration in the coming years. These findings suggest trastuzumab-mediated cardiotoxicity could be associated with long-term marked impairment of cardiac function and may contribute to increased risk of late-occurring cardiovascular disease in survivors of HER2-positive breast cancer.

One long-term study aimed to determine whether trastuzumab-induced cardiotoxicity recovers and explore

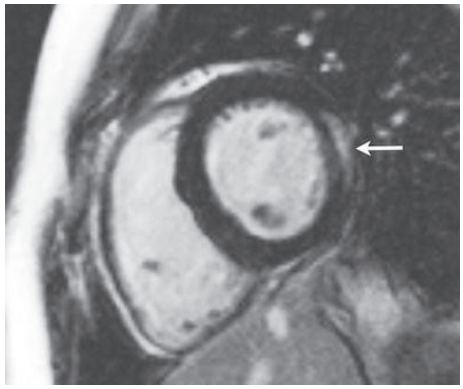

Figure 3: Short axis reconstructed IR-TrueFISP image through the mid-ventricle demonstrates subepicardial linear delayed enhancement (arrow) in the lateral wall of a patient who had received trastuzumab [69]; reprinted with permission from Wadhwa et al. [82].

any association with long-term cardiopulmonary dysfunction in survivors of HER2+ breast cancer [84]. The trial enrolled 57 patients after completion of trastuzumab-based therapy (median, 7.0 years after therapy). Patients were assessed in three groups using speckle-tracking echocardiography: (1) developed cardiotoxicity during therapy (TOX) group, (2) no evidence of cardiotoxicity during therapy (NTOX) group, and (3) healthy control (HC) group. The study reported significantly lower LVEF in the TOX group (56.9% [5.2%]) compared with the NTOX (62.4% [4.0%]) and HC (65.3% [2.9%]) groups. Similar results were found for GLS (TOX group, −17.8% [2.2%]; NTOX group, −19.8% [2.2%]; HC group, −21.3% [1.8%]) ($P < 0.001$).

A large meta-analysis of randomized and cohort studies of over 29,000 women with breast cancer observed the frequency of severe cardiotoxicity up to 3 years following trastuzumab initiation [85]. Among the 58 studies, severe cardiotoxicity occurred in 844 breast cancer patients, accounting for 3% (95% CI 2.41–3.64) of the total sample. 557 incident cases occurred in the early breast cancer group, 203 in the metastatic breast cancer group, and 84 in the mixed population. Mild or asymptomatic cardiotoxicity was reported in 45 studies with a total incidence case of 2251 (out of 20,491 patients). Two years following the initiation of trastuzumab therapy, severe cardiotoxicity was reported in approximately 3% of the total patient cohort. The incidence rate observed from cohort studies is higher compared to randomized control trials, possibly due to such trials excluding patients at higher risk of adverse events. Accordingly, this renders those studies less reflective of real-world settings. Variability of incident cases between studies was high with frequencies ranging from 0 to 9.8% in the early breast cancer group and 0 to 16.1% in the metastatic group. Such variability of cardiotoxic events is likely associated with patient selection, definition of cardiotoxicity, and methods of assessment.

Based on these findings, the consensus is that trastuzumab-mediated cardiotoxicity is largely reversible, or at least partially reversible, particularly from a functional standpoint. Though the true prevalence and extent of reversibility is debatable, late toxicity remains a possibility. With the toxicity profile of trastuzumab yet to be fully established, treatment necessitates close monitoring, and in the face of new, emerging data, such issues warrant revisiting.

An important limitation to these studies, from the CMR perspective, other than the small sample sizes, is the lack of CMR imaging for evaluating cardiotoxicity, whilst cardiac biomarkers, myocardial biopsy (in some cases), and echocardiography, or other imaging modalities, were adopted instead. Large, prospective CMR-studies are warranted to enable a more definitive conclusion on the diagnostic and prognostic role of trastuzumab-induced cardiotoxicity. Collectively, these studies highlight the potential need for the utilisation of cardiac MRI in the early detection of subclinical cardiotoxicity, as well its extended toxicity profile.

Establishing a validated risk stratification tool to distinguish patients that are at increased risk of developing cardiotoxicity to those of lower risk may be necessary so that monitoring by and utilisation of CMR can be reserved for those at higher risk. From the present data, a multitude of risk factors are associated with increased risk of trastuzumab-treated cardiac events, including age (2.31% in <50 years to 4.91% in >60 years 95% CI 3.22–6.94), postmenopausal status (0.013 OR: 4.39 CI: 1.28–15.02), smoking status (5.3%, 95% CI 2.15–9.75), body mass index ≥25 (6.49%, 95% CI 2.34–12.51), hypertension (5.47%, 95% CI 3.40–7.99), dyslipidaemia (4.43%, 95% CI 2.54–6.78), diabetes (6.19, 95% CI 0.85–15.93), and previous positive cardiac history (19.12%, 95% CI 11.85–27.63) [72, 73]. A scoring system based on these parameters may be valuable for estimating the risk of developing cardiotoxicity during therapy. Additionally, it is important to establish the length of follow-up for previously cardiotoxic patients that are deemed to be at potential higher risk for late toxicity. It is yet to be established if "recovered" patients with mild-to-moderate cardiotoxicity with asymptomatic or oligosymptomatic status possess a higher risk of late toxicity compared to those that developed severe toxicity with intense clinical symptomology.

7. Tissue Characterisation and CMR

Chemotherapy associated myocardial oedema, diffuse interstitial fibrosis (collagen deposition in the absence of myocyte loss), and coarse replacement fibrosis (collagen deposition in the presence of myocyte necrosis) can be uniquely imaged with CMR based T2 mapping, T1 mapping, and late-gadolinium enhancement (LGE) sequences, respectively [86] (Table 4). Given the lack of consensus of a precise LVEF-based definition of CTRCD, increasing evidence for deformation imaging to provide incremental prognostic information, and a potential causative relationship between myocardial fibrosis development and reduced myocardial strain [32–34], there is increasing appeal for direct myocardial characterisation in the earlier detection of CTRCD. To date, only the presence of absence of LGE has been studied following trastuzumab therapy [69]. While T1 and ECV increase

Table 4: CMR findings in herceptin ± anthracycline-treated patients.

	Study design	Size (*N*)	Serial measurement	Definition of cardiotoxicity/CRTCD	Left ventricular function								Right ventricular function			Incidence of cardiotoxicity/ CRTCD
					EDV	ESV	EF	MMI	FTGLS	FTGCS	TGLS	TGCS	EDV	ESV	EF	
Fallah-rad et al. [69]	Single centre, prospective	42	12M after treatment initiation	Decline in LVEF of at least 10% below 55%, with accompanying signs or symptoms of CHF	↑	↑	↓	↔								10 (25%)
Grover et al. [70]	Single centre, prospective	15	0, 1, 4, and 12M after treatment initiation	Not reported but significant functional changes characterised as decline in EF of 10%	Mainly ↔ ↑12M	↓	↓						Mainly ↔ ↑12M	↑	↓	Not stated
Nakano et al. [71]	Single centre, prospective	9	0, 3, 6, and 12M after treatment initiation	Cardiac review and evaluation committee criteria			↔3M ↓6&12M									None
Barthur et al. [50]	Multicentre, prospective	41	Three-monthly F/U after treatment initiation for 12M Including an 18m F/U	Not reported			↓6&12M ↔18M						↑6M ↔18M	↑6&12M ↔18M	↓6&12M ↔18M	1, treatment withheld for 1 cycle
Ong et al. [72]	Multicentre, prospective	41	Six-monthly F/U after treatment initiation for 18M	Not reported			↓6&12M ↔18M		↓6&12M ↔18M	↓6&12M ↔18M						1, treatment withheld for 1 cycle
Dhir et al. [73]	Multicentre, prospective	41	Six-monthly F/U after treatment initiation for 18M	LVEF decrease ≥15% from baseline, or LVEF <50% and signs and symptoms of CHF (NYHA class III or IV)	↓6&12M ↔18M	↓6&12M ↔18M	↓6&12M ↔18M									1, treatment withheld for 1 cycle
Houbois et al. [74]	Single centre, prospective	125	Three-monthly F/U after treatment initiation for 12M	Cardiac review and evaluation committee criteria	↑	↑	↓	↑	↓	↓	↓	↓				28% by CMR 22% by 2DE

CRTCD, cancer therapy-related cardiac dysfunction; EDV, end-diastolic volume; ESV, end-systolic volume; EF, ejection fraction; MMI, myocardial mass index; FTGLS, feature tracking global longitudinal strain; FTGCS, feature tracking global circumferential strain; TGLS, tagging global longitudinal strain; TGCS, global circumferential strain; LVEF, left ventricular ejection fraction; F/U, follow-up; M, month; CMR, cardiac magnetic resonance; 2DE, two-dimensional echocardiography; CHF, congestive heart failure; NYHA, New York Heart Association.

Table 5: CMR characteristics of chemotherapeutic agents.

	T1	T2	EGE	LGE	ECV	↓ LVEF	↑LV volume	↓ RVEF	Cardiotoxicity/cardiac dysfunction
Herceptin		✓ [89]		✓ [69, 81, 82, 90]		✓ [50]	✓ [73]	✓ [50]	2–27%* [49]
Anthracycline (doxorubicin)	✓ [87]	✓ [87, 91]	✓ [87]	✓ [90]	✓ [92, 93]	✓ [91]	✓ [70, 94]	✓ [70]	3–26% [53, 54]
Pertuzumab						✓ [56]			6.6% [95]
Lapatinib						✓ [57, 65]			2.7% [96]
Epirubicin			✓ [97]			✓ [97]	✓ [98]	✓ [99]	0.7–11.4% [100]

EGE, early gadolinium enhancement; T1, T1 mapping; T2, T2 mapping; ECV, extracellular volume; LGE, late gadolinium enhancement; LV, left ventricular; ↓ LVEF, reduction in left ventricular ejection fraction; ↓ RVEF, reduction in right ventricular ejection fraction. *The patient cohort in these trials may have been preexposed to anthracycline.

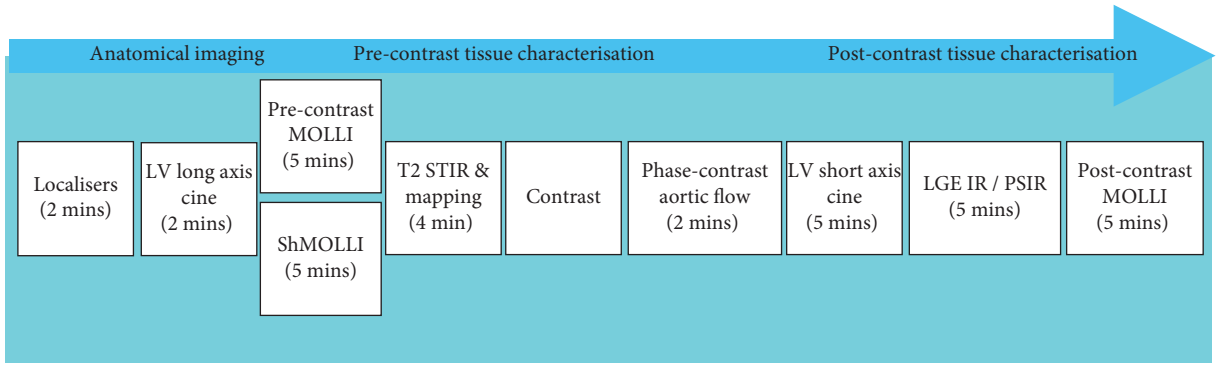

Figure 4: Proposed 30-minute cardiac magnetic resonance imaging protocol for the assessment of trastuzumab cardiotoxicity. LV, left ventricle; MOLLI, modified look-locker inversion recovery; ShMOLLI, shortened modified look-locker inversion recovery; STIR, short tau inversion recovery; IR, inversion recovery; PSIR, phase-sensitive inversion recovery.

following anthracycline therapy [87, 88], this has not been characterised for trastuzumab (Table 5).

8. Summary: When Should You Do a CMR for Trastuzumab?

In the 2016 ESC position paper, there was recognition of the value of CMR for the following: evaluating cardiac structure and function, identifying the cause of LV dysfunction, and distinguishing left and right ventricular function in difficult cases where other imaging modalities are unsuccessful [1]. Consistent with this are the consensus recommendations from the European Society for Medical Oncology (ESMO) and the joint guidelines from BSE and BCOS, which recommends the utilisation of CMR if significant and unexplained discrepancies exist in echo-derived measures of LVEF and GLS [17, 101]. While CMR is the reference standard procedure for assessing cardiotoxicity, it remains largely underutilised for breast cancer cardiotoxicity surveillance [16]. The choice of imaging modality depends on local expertise and availability; it is strongly encouraged that the imaging modality utilised for baseline assessment remains the same for the remainder of the treatment pathway. A potential protocol for CMR assessment of trastuzumab cardiotoxicity is illustrated in Figure 4.

CMR is demonstrably superior to echo-based imaging of left ventricular function, whether by assessment of LVEF or strain, offering greater sensitivity and specificity in the detection of cardiotoxicity in patients receiving trastuzumab. Furthermore, it offers the ability to assess for myocardial oedema, diffuse interstitial fibrosis, or replacement fibrosis. It also carries some limitations. Thus, currently published normal LVEF reference ranges show an overlap of normal ranges. Application of CMR to patients would require a baseline CMR and regular surveillance scans with associated healthcare costs and requires gadolinium administration.

There are several important lines of enquiry to guide future research. Firstly, whether CMR-based detection of cardiotoxicity as assessed by LVEF and strain leads to improved outcomes compared to their detection by echo remains to be determined. Secondly, whether CMR-based identification of oedema and fibrosis, particularly the type and distribution of the latter, leads to improved risk stratification in trastuzumab cardiotoxicity is unknown. Thirdly, can CMR offer detection of features that would suggest a greater likelihood of recovery from cardiotoxicity by tissue characterisation findings? Given the greater availability of echocardiography than CMR, these three questions are central to further research into the optimum detection, follow-up, and surveillance of cardiotoxicity in trastuzumab patients. In the interim, we agree on the current echo-based

methodology of current guidance, with the use of CMR where echo images are poor despite left ventricular opacification with echo contrast agents.

Conflicts of Interest

The authors declare that they have no conflicts of interest.

Authors' Contributions

Jin Jiang and Boyang Liu contributed equally to the manuscript.

References

[1] J. L. Zamorano, P. Lancellotti, D. Rodriguez Muñoz et al., "ESC position paper on cancer treatments and cardiovascular toxicity developed under the auspices of the ESC committee for practice guidelines: thetask force for cancer treatments and cardiovascular toxicity of the European Society of Cardiology (ESC)," *European Heart Journal*, vol. 37, no. 36, pp. 2768–2801, 2016.

[2] F. Cardoso, S. Kyriakides, S. Ohno et al., "Early breast cancer: ESMO Clinical Practice Guidelines for diagnosis, treatment and follow-up," *Annals of Oncology*, vol. 30, no. 8, pp. 1194–1220, 2019.

[3] E. C. Smyth, M. Verheij, W. Allum, D. Cunningham, A. Cervantes, and D. Arnold, "Gastric cancer: ESMO clinical practice guidelines for diagnosis, treatment and follow-up," *Annals of Oncology*, vol. 27, pp. v38–v49, 2016.

[4] D. Zhao, S. J. Klempner, and J. Chao, "Progress and challenges in HER2-positive gastroesophageal adenocarcinoma," *Journal of Hematology & Oncology*, vol. 12, no. 1, p. 50, 2019.

[5] K. Goutsouliak, J. Veeraraghavan, V. Sethunath et al., "Towards personalized treatment for early stage HER2-positive breast cancer," *Nature Reviews Clinical Oncology*, vol. 17, no. 4, pp. 233–250, 2020.

[6] T. Vu and F. X. Claret, "Trastuzumab: updated mechanisms of action and resistance in breast cancer," *Frontiers in Oncology*, vol. 2, p. 62, 2012.

[7] M. J. Piccart-Gebhart, M. Procter, B. Leyland-Jones et al., "Trastuzumab after adjuvant chemotherapy in HER2-positive breast cancer," *New England Journal of Medicine*, vol. 353, no. 16, pp. 1659–1672, 2005.

[8] D. J. Slamon, B. Leyland-Jones, S. Shak et al., "Use of chemotherapy plus a monoclonal antibody against HER2 for metastatic breast cancer that overexpresses HER2," *New England Journal of Medicine*, vol. 344, no. 11, pp. 783–792, 2001.

[9] M. S. Ewer, M. T. Vooletich, J.-B. Durand et al., "Reversibility of trastuzumab-related cardiotoxicity: new insights based on clinical course and response to medical treatment," *Journal of Clinical Oncology*, vol. 23, no. 31, pp. 7820–7826, 2005.

[10] M. K. ElZarrad, P. Mukhopadhyay, N. Mohan et al., "Trastuzumab alters the expression of genes essential for cardiac function and induces ultrastructural changes of cardiomyocytes in mice," *PLoS One*, vol. 8, no. 11, Article ID e79543, 2013.

[11] N. Mohan, Y. Shen, Y. Endo, M. K. ElZarrad, and W. J. Wu, "Trastuzumab, but not pertuzumab, dysregulates HER2 signaling to mediate inhibition of autophagy and increase in reactive oxygen species production in human cardiomyocytes," *Molecular Cancer Therapeutics*, vol. 15, no. 6, pp. 1321–1331, 2016.

[12] M. L. Telli, S. A. Hunt, R. W. Carlson, and A. E. Guardino, "Trastuzumab-related cardiotoxicity: calling into question the concept of reversibility," *Journal of Clinical Oncology*, vol. 25, no. 23, pp. 3525–3533, 2007.

[13] W. Nadruz Jr., E. West, M. Sengeløv et al., "Cardiovascular phenotype and prognosis of patients with heart failure induced by cancer therapy," *Heart*, vol. 105, no. 1, pp. 34–41, 2019.

[14] T. M. Suter, M. Procter, D. J. van Veldhuisen et al., "Trastuzumab-associated cardiac adverse effects in the herceptin adjuvant trial," *Journal of Clinical Oncology*, vol. 25, no. 25, pp. 3859–3865, 2007.

[15] P. Lancellotti, T. M. Suter, T. López-Fernández et al., "Cardio-oncology services: rationale, organization, and implementation," *European Heart Journal*, vol. 40, no. 22, pp. 1756–1763, 2019.

[16] J. Čelutkienė, R. Pudil, T. López-Fernández et al., "Role of cardiovascular imaging in cancer patients receiving cardiotoxic therapies: a position statement on behalf of the heart failure association (HFA), the European association of cardiovascular imaging (EACVI) and the cardio-oncology council of the European society of cardiology (ESC)," *European Journal of Heart Failure*, vol. 22, pp. 1504–1524, 2020.

[17] R. Dobson, A. K. Ghosh, B. Ky et al., "BSE and BCOS guideline for transthoracic echocardiographic assessment of adult cancer patients receiving anthracyclines and/or trastuzumab," *Journal of the American College of Cardiology: CardioOncology*, vol. 3, no. 1, pp. 1–16, 2021.

[18] A. National Guideline, *National Institute for Health and Care Excellence: Clinical Guidelines. Early and Locally Advanced Breast Cancer: Diagnosis and Management*, National Institute for Health and Care Excellence (UK) Copyright © NICE, London, UK, 2018.

[19] J. C. Plana, M. Galderisi, A. Barac et al., "Expert consensus for multimodality imaging evaluation of adult patients during and after cancer therapy: a report from the American Society of Echocardiography and the European Association of Cardiovascular Imaging," *European Heart Journal-Cardiovascular Imaging*, vol. 15, no. 10, pp. 1063–1093, 2014.

[20] P. Thavendiranathan, A. D. Grant, T. Negishi, J. C. Plana, Z. B. Popović, and T. H. Marwick, "Reproducibility of echocardiographic techniques for sequential assessment of left ventricular ejection fraction and volumes: application to patients undergoing cancer chemotherapy," *Journal of the American College of Cardiology*, vol. 61, no. 1, pp. 77–84, 2013.

[21] B. I. Gardner, S. E. Bingham, M. R. Allen, D. D. Blatter, and J. L. Anderson, "Cardiac magnetic resonance versus transthoracic echocardiography for the assessment of cardiac volumes and regional function after myocardial infarction: an intrasubject comparison using simultaneous intrasubject recordings," *Cardiovascular Ultrasound*, vol. 7, no. 1, p. 38, 2009.

[22] N. Abdelmonem Atia, L. Lehmann, M. Adel Eltomey et al., "State-of-the-art CMR mapping techniques in the detection of subclinical chemotherapy-induced cardiotoxicity in breast cancer patients," *International Journal of Medical Imaging*, vol. 9, no. 1, pp. 29–35, 2021.

[23] S. Malm, S. Frigstad, E. Sagberg, H. Larsson, and T. Skjaerpe, "Accurate and reproducible measurement of left ventricular volume and ejection fraction by contrast echocardiography: a comparison with magnetic resonance imaging," *Journal of the American College of Cardiology*, vol. 44, no. 5, pp. 1030–1035, 2004.

[24] G. T. Armstrong, J. C. Plana, N. Zhang et al., "Screening adult survivors of childhood cancer for cardiomyopathy: comparison of echocardiography and cardiac magnetic resonance imaging," *Journal of Clinical Oncology*, vol. 30, no. 23, pp. 2876–2884, 2012.

[25] N. Ajmone Marsan, B. Michalski, M. Cameli et al., "EACVI survey on standardization of cardiac chambers quantification by transthoracic echocardiography," *European Heart Journal-Cardiovascular Imaging*, vol. 21, no. 2, pp. 119–123, 2020.

[26] C. Santoro, G. Arpino, R. Esposito et al., "2D and 3D strain for detection of subclinical anthracycline cardiotoxicity in breast cancer patients: a balance with feasibility," *European Heart Journal-Cardiovascular Imaging*, vol. 18, no. 8, pp. 930–936, 2017.

[27] B. C. Kolla, S. S. Roy, S. Duval, D. Weisdorf, U. Valeti, and A. Blaes, "Cardiac imaging methods for chemotherapy-related cardiotoxicity screening and related radiation exposure: current practice and trends," *Anticancer Research*, vol. 37, no. 5, pp. 2445–2449, 2017.

[28] S. Sardesai, J. Sukumar, M. Kassem et al., "Clinical impact of interruption in adjuvant trastuzumab therapy in patients with operable HER-2 positive breast cancer," *Cardio-Oncology*, vol. 6, no. 1, p. 26, 2020.

[29] F. Lynce, A. Barac, X. Geng et al., "Prospective evaluation of the cardiac safety of HER2-targeted therapies in patients with HER2-positive breast cancer and compromised heart function: the SAFE-HEaRt study," *Breast Cancer Research and Treatment*, vol. 175, no. 3, pp. 595–603, 2019.

[30] D. P. Leong, T. Cosman, M. M. Alhussein et al., "Safety of continuing trastuzumab despite mild cardiotoxicity," *Journal of the American College of Cardiology: CardioOncology*, vol. 1, no. 1, pp. 1–10, 2019.

[31] I. Mirsky and W. W. Parmley, "Assessment of passive elastic stiffness for isolated heart muscle and the intact heart," *Circulation Research*, vol. 33, no. 2, pp. 233–243, 1973.

[32] K. Shan, R. J. Bick, B. J. Poindexter et al., "Relation of tissue Doppler derived myocardial velocities to myocardial structure and beta-adrenergic receptor density in humans," *Journal of the American College of Cardiology*, vol. 36, no. 3, pp. 891–896, 2000.

[33] S.-J. Kang, H.-S. Lim, B.-J. Choi et al., "Longitudinal strain and torsion assessed by two-dimensional speckle tracking correlate with the serum level of tissue inhibitor of matrix metalloproteinase-1, a marker of myocardial fibrosis, in patients with hypertension," *Journal of the American Society of Echocardiography*, vol. 21, no. 8, pp. 907–911, 2008.

[34] Z. Y. Fang, S. Yuda, V. Anderson, L. Short, C. Case, and T. H. Marwick, "Echocardiographic detection of early diabetic myocardial disease," *Journal of the American College of Cardiology*, vol. 41, no. 4, pp. 611–617, 2003.

[35] E. K. Oikonomou, D. G. Kokkinidis, P. N. Kampaktsis et al., "Assessment of prognostic value of left ventricular global longitudinal strain for early prediction of chemotherapy-induced cardiotoxicity: a systematic review and meta-analysis," *JAMA Cardiology*, vol. 4, no. 10, pp. 1007–1018, 2019.

[36] K. Negishi, T. Negishi, J. L. Hare, B. A. Haluska, J. C. Plana, and T. H. Marwick, "Independent and incremental value of deformation indices for prediction of trastuzumab-induced cardiotoxicity," *Journal of the American Society of Echocardiography*, vol. 26, no. 5, pp. 493–498, 2013.

[37] P. Thavendiranathan, T. Negishi, E. Somerset et al., "Strain-guided management of potentially cardiotoxic cancer therapy," *Journal of the American College of Cardiology*, vol. 77, no. 4, pp. 392–401, 2021.

[38] S. Ünlü, O. Mirea, S. Bézy et al., "Inter-vendor variability in strain measurements depends on software rather than image characteristics," *The International Journal of Cardiovascular Imaging*, vol. 37, no. 5, pp. 1689–1697, 2021.

[39] D. Muraru, A. Niero, H. Rodriguez-Zanella, D. Cherata, and L. Badano, "Three-dimensional speckle-tracking echocardiography: benefits and limitations of integrating myocardial mechanics with three-dimensional imaging," *Cardiovascular Diagnosis and Therapy*, vol. 8, no. 1, pp. 101–117, 2018.

[40] O. H. Toro-Salazar, E. Gillan, M. T. O'Loughlin et al., "Occult cardiotoxicity in childhood cancer survivors exposed to anthracycline therapy," *Circulation: Cardiovascular Imaging*, vol. 6, no. 6, pp. 873–880, 2013.

[41] E.-Y. Choi, B. D. Rosen, V. R. S. Fernandes et al., "Prognostic value of myocardial circumferential strain for incident heart failure and cardiovascular events in asymptomatic individuals: the multi-ethnic study of atherosclerosis," *European Heart Journal*, vol. 34, no. 30, pp. 2354–2361, 2013.

[42] B. Liu, A. M. Dardeer, W. E. Moody et al., "Reference ranges for three-dimensional feature tracking cardiac magnetic resonance: comparison with two-dimensional methodology and relevance of age and gender," *The International Journal of Cardiovascular Imaging*, vol. 34, no. 5, pp. 761–775, 2017.

[43] R. Jasaityte, B. Heyde, V. Ferferieva et al., "Comparison of a new methodology for the assessment of 3D myocardial strain from volumetric ultrasound with 2D speckle tracking," *The International Journal of Cardiovascular Imaging*, vol. 28, no. 5, pp. 1049–1060, 2012.

[44] M.-P. Jolly, J. H. Jordan, G. C. Meléndez, G. R. McNeal, R. B. D'Agostino Jr., and W. G. Hundley, "Automated assessments of circumferential strain from cine CMR correlate with LVEF declines in cancer patients early after receipt of cardio-toxic chemotherapy," *Journal of Cardiovascular Magnetic Resonance*, vol. 19, no. 1, p. 59, 2017.

[45] M. Rigolli, S. Anandabaskaran, J. P. Christiansen, and G. A. Whalley, "Bias associated with left ventricular quantification by multimodality imaging: a systematic review and meta-analysis," *Open Heart*, vol. 3, no. 1, Article ID e000388, 2016.

[46] D. L. Keefe, "Trastuzumab-associated cardiotoxicity," *Cancer*, vol. 95, no. 7, pp. 1592–1600, 2002.

[47] J. Alexander, N. Dainiak, H. J. Berger et al., "Serial assessment of doxorubicin cardiotoxicity with quantitative radionuclide angiocardiography," *New England Journal of Medicine*, vol. 300, no. 6, pp. 278–283, 1979.

[48] R. Chung, A. K. Ghosh, and A. Banerjee, "Cardiotoxicity: precision medicine with imprecise definitions," *Open Heart*, vol. 5, no. 2, Article ID e000774, 2018.

[49] A. Seidman, C. Hudis, M. K. Pierri et al., "Cardiac dysfunction in the trastuzumab clinical trials experience," *Journal of Clinical Oncology*, vol. 20, no. 5, pp. 1215–1221, 2002.

[50] A. Barthur, C. Brezden-Masley, K. A. Connelly et al., "Longitudinal assessment of right ventricular structure and function by cardiovascular magnetic resonance in breast cancer patients treated with trastuzumab: a prospective observational study," *Journal of Cardiovascular Magnetic Resonance*, vol. 19, no. 1, p. 44, 2017.

[51] K. Keramida, D. Farmakis, J. Bingcang et al., "Longitudinal changes of right ventricular deformation mechanics during trastuzumab therapy in breast cancer patients," *European Journal of Heart Failure*, vol. 21, no. 4, pp. 529–535, 2019.

[52] C. Melcher, C. Scholz, B. Jäger, C. Hagenbeck, B. Rack, and W. Janni, "Breast cancer: state of the art and new findings,"

Geburtshilfe und Frauenheilkunde, vol. 72, no. 3, pp. 215–224, 2012.

[53] S. M. Swain, F. S. Whaley, and M. S. Ewer, "Congestive heart failure in patients treated with doxorubicin: a retrospective analysis of three trials," *Cancer*, vol. 97, no. 11, pp. 2869–2879, 2003.

[54] M. Lotrionte, G. Biondi-Zoccai, A. Abbate et al., "Review and meta-analysis of incidence and clinical predictors of anthracycline cardiotoxicity," *The American Journal of Cardiology*, vol. 112, no. 12, pp. 1980–1984, 2013.

[55] L. Pentassuglia, F. Timolati, F. Seifriz, K. Abudukadier, T. M. Suter, and C. Zuppinger, "Inhibition of ErbB2/neuregulin signaling augments paclitaxel-induced cardiotoxicity in adult ventricular myocytes," *Experimental Cell Research*, vol. 313, no. 8, pp. 1588–1601, 2007.

[56] C. C. Portera, J. M. Walshe, D. R. Rosing et al., "Cardiac toxicity and efficacy of trastuzumab combined with pertuzumab in patients with trastuzumab-insensitive human epidermal growth factor receptor 2-positive metastatic breast cancer," *Clinical Cancer Research*, vol. 14, no. 9, pp. 2710–2716, 2008.

[57] E. A. Perez, C. Barrios, W. Eiermann et al., "Trastuzumab emtansine with or without pertuzumab versus trastuzumab plus taxane for human epidermal growth factor receptor 2-positive, advanced breast cancer: primary results from the phase III MARIANNE study," *Journal of Clinical Oncology*, vol. 35, no. 2, pp. 141–148, 2017.

[58] Z. Jawa, R. M. Perez, L. Garlie et al., "Risk factors of trastuzumab-induced cardiotoxicity in breast cancer: a meta-analysis," *Medicine*, vol. 95, no. 44, Article ID e5195, 2016.

[59] A. Nohria, "β-adrenergic blockade for anthracycline- and trastuzumab-induced cardiotoxicity: is prevention better than cure?" *Circulation: Heart Failure*, vol. 6, no. 3, pp. 358–361, 2013.

[60] P. A. Henriksen, "Anthracycline cardiotoxicity: an update on mechanisms, monitoring and prevention," *Heart*, vol. 104, no. 12, pp. 971–977, 2018.

[61] S. Di Cosimo, "Heart to heart with trastuzumab: a review on cardiac toxicity," *Targeted Oncology*, vol. 6, no. 4, pp. 189–195, 2011.

[62] H. Farhad, P. V. Staziaki, D. Addison et al., "Characterization of the changes in cardiac structure and function in mice treated with anthracyclines using serial cardiac magnetic resonance imaging," *Circulation Cardiovascular Imaging*, vol. 9, no. 12, Article ID e003584, 2016.

[63] P. Vejpongsa and E. T. Yeh, "Topoisomerase 2β: a promising molecular target for primary prevention of anthracycline-induced cardiotoxicity," *Clinical Pharmacology & Therapeutics*, vol. 95, pp. 45–52, 2014.

[64] L. Zhao and B. Zhang, "Doxorubicin induces cardiotoxicity through upregulation of death receptors mediated apoptosis in cardiomyocytes," *Scientific Reports*, vol. 7, no. 1, Article ID 44735, 2017.

[65] M. Piccart-Gebhart, E. Holmes, J. Baselga et al., "Adjuvant lapatinib and trastuzumab for early human epidermal growth factor receptor 2-positive breast cancer: results from the randomized phase III adjuvant lapatinib and/or trastuzumab treatment optimization trial," *Journal of Clinical Oncology*, vol. 34, no. 10, pp. 1034–1042, 2016.

[66] S. Langer, "Dexrazoxane for the treatment of chemotherapy-related side effects," *Cancer Management and Research*, vol. 6, pp. 357–363, 2014.

[67] K. Ohtani, T. Ide, K.-i. Hiasa et al., "Cardioprotective effect of renin-angiotensin inhibitors and β-blockers in trastuzumab-related cardiotoxicity," *Clinical Research in Cardiology*, vol. 108, no. 10, pp. 1128–1139, 2019.

[68] E. H. Romond, J.-H. Jeong, P. Rastogi et al., "Seven-year follow-up assessment of cardiac function in NSABP B-31, a randomized trial comparing doxorubicin and cyclophosphamide followed by paclitaxel (ACP) with ACP plus trastuzumab as adjuvant therapy for patients with node-positive, human epidermal growth factor receptor 2-positive breast cancer," *Journal of Clinical Oncology*, vol. 30, no. 31, pp. 3792–3799, 2012.

[69] N. Fallah-Rad, J. R. Walker, A. Wassef et al., "The utility of cardiac biomarkers, tissue velocity and strain imaging, and cardiac magnetic resonance imaging in predicting early left ventricular dysfunction in patients with human epidermal growth factor receptor II-positive breast cancer treated with adjuvant trastuzumab therapy," *Journal of the American College of Cardiology*, vol. 57, no. 22, pp. 2263–2270, 2011.

[70] S. Grover, D. P. Leong, A. Chakrabarty et al., "Left and right ventricular effects of anthracycline and trastuzumab chemotherapy: a prospective study using novel cardiac imaging and biochemical markers," *International Journal of Cardiology*, vol. 168, no. 6, pp. 5465–5467, 2013.

[71] S. Nakano, M. Takahashi, F. Kimura et al., "Cardiac magnetic resonance imaging-based myocardial strain study for evaluation of cardiotoxicity in breast cancer patients treated with trastuzumab: a pilot study to evaluate the feasibility of the method," *Cardiology Journal*, vol. 23, no. 3, pp. 270–280, 2016.

[72] G. Ong, C. Brezden-Masley, V. Dhir et al., "Myocardial strain imaging by cardiac magnetic resonance for detection of subclinical myocardial dysfunction in breast cancer patients receiving trastuzumab and chemotherapy," *International Journal of Cardiology*, vol. 261, pp. 228–233, 2018.

[73] V. Dhir, A. T. Yan, R. Nisenbaum et al., "Assessment of left ventricular function by CMR versus MUGA scans in breast cancer patients receiving trastuzumab: a prospective observational study," *The International Journal of Cardiovascular Imaging*, vol. 35, no. 11, pp. 2085–2093, 2019.

[74] C. P. Houbois, M. Nolan, E. Somerset et al., "Serial cardiovascular magnetic resonance strain measurements to identify cardiotoxicity in breast cancer: comparison with echocardiography," *Journal of the American College of Cardiology: Cardiovascular Imaging*, vol. 14, no. 5, pp. 962–974, 2021.

[75] S. A. Crone, Y.-Y. Zhao, L. Fan et al., "ErbB2 is essential in the prevention of dilated cardiomyopathy," *Nature Medicine*, vol. 8, no. 5, pp. 459–465, 2002.

[76] C. García-García, Y. H. Ibrahim, V. Serra et al., "Dual mTORC1/2 and HER2 blockade results in antitumor activity in preclinical models of breast cancer resistant to anti-HER2 therapy," *Clinical Cancer Research: An Official Journal of the American Association for Cancer Research*, vol. 18, no. 9, pp. 2603–2612, 2012.

[77] E. Paplomata and R. O'Regan, "The PI3K/AKT/mTOR pathway in breast cancer: targets, trials and biomarkers," *Therapeutic Advances in Medical Oncology*, vol. 6, no. 4, pp. 154–166, 2014.

[78] M. Guglin, R. Cutro, and J. D. Mishkin, "Trastuzumab-induced cardiomyopathy," *Journal of Cardiac Failure*, vol. 14, no. 5, pp. 437–444, 2008.

[79] M. S. Ewer and E. Tan-Chiu, "Reversibility of trastuzumab cardiotoxicity: is the concept alive and well?" *Journal of Clinical Oncology*, vol. 25, no. 34, pp. 5532-5533, 2007.

[80] M. S. Ewer and S. M. Ewer, "Troponin I provides insight into cardiotoxicity and the anthracycline-trastuzumab interaction," *Journal of Clinical Oncology*, vol. 28, no. 25, pp. 3901–3904, 2010.

[81] N. Fallah-Rad, M. Lytwyn, T. Fang, I. Kirkpatrick, and D. S. Jassal, "Delayed contrast enhancement cardiac magnetic resonance imaging in trastuzumab induced cardiomyopathy," *Journal of Cardiovascular Magnetic Resonance*, vol. 10, no. 1, p. 5, 2008.

[82] D. Wadhwa, N. Fallah-Rad, D. Grenier et al., "Trastuzumab mediated cardiotoxicity in the setting of adjuvant chemotherapy for breast cancer: a retrospective study," *Breast Cancer Research and Treatment*, vol. 117, no. 2, pp. 357–364, 2009.

[83] D. Cardinale, A. Colombo, R. Torrisi et al., "Trastuzumab-induced cardiotoxicity: clinical and prognostic implications of troponin I evaluation," *Journal of Clinical Oncology*, vol. 28, no. 25, pp. 3910–3916, 2010.

[84] A. F. Yu, J. R. Flynn, C. S. Moskowitz et al., "Long-term cardiopulmonary consequences of treatment-induced cardiotoxicity in survivors of ERBB2-positive breast cancer," *JAMA Cardiology*, vol. 5, no. 3, pp. 309–317, 2020.

[85] S. Mantarro, M. Rossi, M. Bonifazi et al., "Risk of severe cardiotoxicity following treatment with trastuzumab: a meta-analysis of randomized and cohort studies of 29,000 women with breast cancer," *Internal and Emergency Medicine*, vol. 11, no. 1, pp. 123–140, 2016.

[86] G. C. Meléndez and W. G. Hundley, "Is myocardial fibrosis a new frontier for discovery in cardiotoxicity related to the administration of anthracyclines?" *Circulation Cardiovascular imaging*, vol. 9, no. 12, Article ID e005797, 2016.

[87] F. Muehlberg, S. Funk, L. Zange et al., "Native myocardial T1 time can predict development of subsequent anthracycline-induced cardiomyopathy," *ESC Heart Failure*, vol. 5, no. 4, pp. 620–629, 2018.

[88] J. H. Jordan, S. Vasu, T. M. Morgan et al., "Anthracycline-associated T1 mapping characteristics are elevated independent of the presence of cardiovascular comorbidities in cancer survivors," *Circulation. Cardiovascular imaging*, vol. 9, no. 8, Article ID e004325, 2016.

[89] P. Thavendiranathan, E. Amir, P. Bedard et al., "Regional myocardial edema detected by T2 mapping is a feature of cardiotoxicity in breast cancer patients receiving sequential therapy with anthracyclines and trastuzumab," *Journal of Cardiovascular Magnetic Resonance*, vol. 16, no. S1, Article ID P273, 2014.

[90] K. Modi, S. Joppa, K.-H. A. Chen et al., "Myocardial damage assessed by late gadolinium enhancement on cardiovascular magnetic resonance imaging in cancer patients treated with anthracyclines and/or trastuzumab," *European Heart Journal - Cardiovascular Imaging*, vol. 22, no. 4, pp. 427–434, 2021.

[91] C. Galán-Arriola, M. Lobo, J. P. Vílchez-Tschischke et al., "Serial magnetic resonance imaging to identify early stages of anthracycline-induced cardiotoxicity," *Journal of the American College of Cardiology*, vol. 73, no. 7, pp. 779–791, 2019.

[92] E. B. Tham, M. J. Haykowsky, K. Chow et al., "Diffuse myocardial fibrosis by T1-mapping in children with subclinical anthracycline cardiotoxicity: relationship to exercise capacity, cumulative dose and remodeling," *Journal of Cardiovascular Magnetic Resonance*, vol. 15, no. 1, p. 48, 2013.

[93] Z. Zhou, R. Wang, H. Wang et al., "Myocardial extracellular volume fraction quantification in an animal model of the doxorubicin-induced myocardial fibrosis: a synthetic hematocrit method using 3T cardiac magnetic resonance," *Quantitative Imaging in Medicine and Surgery*, vol. 11, no. 2, pp. 510–520, 2021.

[94] B. C. Drafts, K. M. Twomley, R. D'Agostino Jr et al., "Low to moderate dose anthracycline-based chemotherapy is associated with early noninvasive imaging evidence of subclinical cardiovascular disease," *JACC: Cardiovascular Imaging*, vol. 6, no. 8, pp. 877–885, 2013.

[95] S. M. Swain, D. Miles, S. B. Kim et al., "Pertuzumab, trastuzumab, and docetaxel for HER2-positive metastatic breast cancer (CLEOPATRA): end-of-study results from a double-blind, randomised, placebo-controlled, phase 3 study," *The Lancet Oncology*, vol. 21, pp. 519–530, 2020.

[96] H. D. Choi and M. J. Chang, "Cardiac toxicities of lapatinib in patients with breast cancer and other HER2-positive cancers: a meta-analysis," *Breast Cancer Research and Treatment*, vol. 166, no. 3, pp. 927–936, 2017.

[97] P. Kotwinski, G. Smith, J. Sanders et al., "The breast cancer, early disease: toxicity from therapy with epirubicin regimens - cardiac assessment and risk evaluation (BETTER-CARE) study: CMR with early gadolinium relative enhancement, but not high-sensitivity troponin T, predicts the risk of chronic anthracycline cardiotoxicity," *Journal of Cardiovascular Magnetic Resonance*, vol. 15, no. S1, p. O94, 2013.

[98] R. Wassmuth, S. Lentzsch, U. Erdbruegger et al., "Subclinical cardiotoxic effects of anthracyclines as assessed by magnetic resonance imaging-a pilot study," *American Heart Journal*, vol. 141, no. 6, pp. 1007–1013, 2001.

[99] A. Kimball, S. Patil, B. Koczwara et al., "Late characterisation of cardiac effects following anthracycline and trastuzumab treatment in breast cancer patients," *International Journal of Cardiology*, vol. 261, pp. 159–161, 2018.

[100] J. V. McGowan, R. Chung, A. Maulik, I. Piotrowska, J. M. Walker, and D. M. Yellon, "Anthracycline chemotherapy and cardiotoxicity," *Cardiovascular Drugs and Therapy*, vol. 31, no. 1, pp. 63–75, 2017.

[101] G. Curigliano, D. Lenihan, M. Fradley et al., "Management of cardiac disease in cancer patients throughout oncological treatment: ESMO consensus recommendations," *Annals of Oncology*, vol. 31, no. 2, pp. 171–190, 2020.

Hindawi
Cardiology Research and Practice
Volume 2022, Article ID 3144386, 9 pages
https://doi.org/10.1155/2022/3144386

Review Article

Valvular Cardiomyopathy: The Value of Cardiovascular Magnetic Resonance Imaging

Vasiliki Tsampasian,[1,2] **Sandeep S. Hothi**,[3] **Thuwarahan Ravindrarajah**,[2] **Andrew J. Swift**,[4] **Pankaj Garg**,[1,2,4] **and Vassilios S. Vassiliou**[1,2]

[1]*Norwich Medical School, University of East Anglia, Norwich Research Park, Norwich, UK*
[2]*Norfolk and Norwich University Hospital, Norwich, UK*
[3]*The Institute of Cardiovascular Sciences, College of Medical and Dental Sciences, University of Birmingham, Birmingham, UK*
[4]*Department of Infection, Immunity and Cardiovascular Disease, University of Sheffield, Sheffield, UK*

Correspondence should be addressed to Vasiliki Tsampasian; vasiliki.tsampasian@nnuh.nhs.uk and Pankaj Garg; p.garg@uea.ac.uk

Received 30 April 2021; Accepted 2 February 2022; Published 22 February 2022

Academic Editor: Michael Spartalis

Cardiovascular magnetic resonance (CMR) imaging has had a vast impact on the understanding of a wide range of disease processes and pathophysiological mechanisms. More recently, it has contributed significantly to the diagnosis and risk stratification of patients with valvular heart disease. With its increasing use, CMR allows for a detailed, reproducible, qualitative, and quantitative evaluation of left ventricular volumes and mass, thereby enabling assessment of the haemodynamic impact of a valvular lesion upon the myocardium. Postprocessing of the routinely acquired images with feature tracking CMR methodology can give invaluable information about myocardial deformation and strain parameters that suggest subclinical ventricular impairment that remains undetected by conventional measures such as the ejection fraction (EF). T1 mapping and late gadolinium enhancement (LGE) imaging provide deep myocardial tissue characterisation that is changing the approach towards risk stratification of patients as an increasing body of evidence suggests that the presence of fibrosis is related to adverse events and prognosis. This review summarises the current evidence regarding the utility of CMR in the left ventricular assessment of patients with aortic stenosis or mitral regurgitation and its value in diagnosis, risk stratification, and management.

1. Introduction

Valvular heart disease (VHD) has a high prevalence worldwide with mild disease affecting up to one in two people over the age of 65 [1, 2]. A substantial number of individuals in the primary care setting with symptoms of heart failure suffer from clinically significant VHD, most commonly aortic stenosis and mitral regurgitation [3]. Undoubtedly, prompt diagnosis and appropriate management are vital in positively influencing the prognosis and future course of the disease.

Traditionally, and still dominating much of cardiovascular medicine now, valvular heart disease assessment, and myocardial function has relied heavily upon echocardiographic data. Over recent years, as our knowledge and understanding of the pathophysiological mechanisms underlying VHD expands, it has become apparent that perhaps assessing the severity of valvular disease alone without the impact this has on the myocardium may be insufficient to guide prognostication and explain consequent VHD-related cardiomyopathy, morbidity, and mortality. This is evident in patients with similar degrees of valvular stenosis, but differences in clinical presentation and outcomes that relate to myocardial dysfunction. In this respect, cardiovascular magnetic resonance (CMR) has an invaluable role as, with its high spatial resolution, it allows accurate qualitative and quantitative assessment of left ventricular wall thickness, mass, volumes, and ejection fraction, which are of high prognostic value and thus allows accurate assessment, diagnosis, and risk stratification.

Table 1: Techniques available with CMR and comparison with echocardiography. Symbol "+" represents "good" and "++" represents "very good." Symbol "–" is used when there is no means to assess the particular method.

Assessment methods	CMR	Echocardiography
Chamber quantification (wall thickness, mass, and volumes)	++ The high spatial resolution allows accurate qualitative and quantitative assessment of cardiac chambers	+ Measurements are dependent on several parameters (acoustic windows, endocardial definition, on-axis/off-axis views, and sonographer)
Assessment of myocardial deformation (most commonly global longitudinal strain)	++ Dedicated accurate sequences can be used for CMR strain. Furthermore, reproducible method of myocardial deformation assessment using feature tracking postprocessing of SSFP cine images	++ A reproducible method that provides valuable information, as long as certain requirements are fulfilled (clear endocardial definition and frame rate >50)
Comprehensive assessment of valvular anatomy and structure	++ Unlimited imaging planes and high spatial resolution help in the detailed assessment of simple and complex valvular anatomy	+ Comprehensive anatomical assessment that is, however, limited in a certain number of imaging planes and by spatial resolution, which is lower compared to CMR
Qualitative and quantitative assessment of valvular lesions (regurgitation/stenosis)	++ CMR is very useful in the assessment of the severity of valvular lesions that are difficult to be quantified with echocardiography (e.g., very eccentric jets)	++ High temporal resolution and assessment with colour and continuous wave Doppler offers a detailed evaluation of the severity of valvular lesions
Tissue characterisation (LGE and T1 mapping)	++ CMR is the gold standard method for direct assessment of fibrosis with the use of LGE and T1 mapping techniques	– Not available with echocardiography. Echocardiography backscatter can associate with myocardial fibrosis, but it is not an accurate method.

CMR has proved to successfully fill in gaps and answer both scientific and clinical questions, not only because it can provide a detailed evaluation of the valve function and anatomy but also because it can assess the haemodynamic consequences of the valvular lesions on the myocardium that is directly associated with the valve. T1 mapping and late gadolinium enhancement (LGE) allow direct assessment of myocardial fibrosis and changes in extracellular volume, while feature tracking CMR allows accurate evaluation of myocardial deformation. Table 1 summarises the strengths of CMR and how these compare with echocardiography.

This review provides an overview of the role of CMR in the assessment and diagnosis of cardiomyopathy related to two of the commonest forms of valvular heart disease, aortic stenosis (AS), and mitral regurgitation (MR).

2. Aortic Stenosis

According to the current guidelines, valvular intervention is recommended for symptomatic patients with severe AS and asymptomatic patients with evidence of LV decompensation as noted by EF <50% or elevated BNP/NT-pro-BNP level more than twice the upper limit of normal [4]. The assessment of the aortic stenosis severity is conventionally performed with echocardiographic two-dimensional (2D) and Doppler assessment, with the main parameters being the peak jet velocity, the transvalvular mean gradient, and the valve area (as obtained by the continuity equation), while the ventricular function is routinely conducted with the echocardiographic assessment of the ejection fraction [5, 6]. Left ventricular ejection fraction (LVEF) has been traditionally one of the important prognostic markers of the disease, as patients with early left ventricular decompensation as evidenced by EF <60% have an increased risk of mortality, even after valve replacement [7] leading the National Institute for Health and Care Excellence (NICE) in the UK to recommend consideration of intervention when the LVEF <60% when the decline is attributed to the AS in their initial guidance in March 2021 [8]. While echocardiography remains the gold standard technique for the assessment and grading of aortic stenosis, new techniques and methodologies have emerged for better and detailed assessment of the left ventricular myocardium with CMR having a central role.

Over recent years, however, assessment of myocardial deformation using strain imaging has been found to be of major significance in the evaluation of left ventricular function, especially for the large proportion of patients with aortic stenosis and preserved EF [9]. Several studies have suggested that global longitudinal strain (GLS) is of great prognostic importance and can detect subtle changes in LV function pre- and postaortic valve intervention, even with LVEF in the normal range [10]. Feature tracking (FT) CMR methodology is based on tracking the endocardial and epicardial borders of the ventricle on postprocessing of steady-state free precession (SSFP) cine images [11]. GLS obtained by FT CMR is a highly reproducible quantification technique that provides invaluable information about myocardial function without requiring any additional imaging acquisitions over and above the routinely acquired CMR images [12]. Evidence suggests that patients with

asymptomatic severe AS and apparently normal LVEF do have in fact, impaired GLS, comparable to that of symptomatic patients with severe AS awaiting valve intervention [13]. This finding highlights the value of myocardial deformation analysis in this patient population. Abnormal GLS indicates the presence of potentially subclinical, impaired myocardial function, and that could help in the clinical decision-making process regarding the timing of intervention so as to avoid further potentially irreversible myocardial damage. Additionally, FT-derived GLS correlates well with the presence and extent of LGE, as strain values deteriorate when LGE is present [11, 14]. As the analysis of GLS is not dependent on gadolinium administration and does not require dedicated sequences (for example, when feature tracking is performed), it can therefore be assessed even in a noncontrast study during the postprocessing. This makes it a very useful measurement, specifically for the patients to whom MRI contrast agents may be contraindicated.

CMR is also the gold standard method for tissue characterisation as it allows the detection of changes of the myocardium on a cellular level [11]. In aortic stenosis, the left ventricular response to chronic pressure overload consists of an initial hypertrophic phase followed by cell apoptosis and eventually myocardial fibrosis [15]. Myocardial fibrosis is an early and fundamental part of this maladaptive response that determines changes in left ventricular function and heralds the presentation of symptoms and adverse events and therefore has prognostic implications [16].

Myocardial fibrosis in AS has a complex but characteristic pattern, formed mainly in two patterns which can be evaluated with the use of CMR, replacement (focal) and reactive (diffuse) fibrosis [17]. It has been demonstrated that both replacement and diffuse fibrosis are associated with the magnitude of LV hypertrophy, LV dysfunction, symptoms, and prognosis [18]. Interestingly enough, they are only weakly associated with the severity of the valve disease [18].

LGE is the paradigm method for the assessment of replacement (focal) fibrosis. Replacement fibrosis is the late phase of the disease process and represents cellular death that is followed by focal fibrosis (scar). This process is irreversible and is a strong predictor of adverse prognosis [19]. Replacement fibrosis can be detected and quantified with the use of CMR and LGE. This distinct pattern of midwall myocardial fibrosis signals the transition from the hypertrophic response to a decompensated phase with the occurrence of symptoms [15]. The poor prognosis associated with this irreversible stage persists even after aortic valve intervention and is strongly associated with all-cause and cardiovascular mortality [20]. Interestingly, this correlation appears to be "dose-dependent," related to the scar burden. A large study conducted by the British Society for Cardiovascular Magnetic Resonance Valve Consortium, including six hundred seventy-four patients, demonstrated that for every 1% increase in myocardial scar burden, there was an 11% increase in all-cause mortality and an 8% increase in cardiovascular mortality [20].

While LGE is a well-established method for identifying replacement fibrosis, quantification can be challenging when diffuse fibrosis is present. The added value of T1 mapping-derived measurements enables the detection and quantification of reactive (diffuse) interstitial fibrosis, which is an early and importantly reversible stage of the disease process [11]. CMR with T1 mapping has the strength of differentiating changes on a cellular level from changes on an extracellular level. Given that reactive fibrosis represents the expansion of the extracellular matrix, T1 mapping-derived techniques can be used to assess diffuse fibrosis by quantifying the extracellular volume fraction (ECV%) and the indexed extracellular volume (iECV), which represents the total fibrosis burden [21, 22]. Combined with the LV mass, these parameters can provide a comprehensive assessment of LV remodelling regarding both the cellular and the extracellular compartments [19]. Since diffuse fibrosis is potentially reversible, the contribution of CMR is invaluable as thorough assessment and quantification of the diffuse fibrosis are essential to identify early decompensation and allow prompt intervention [22]. In a recent study by Everett et al. that included more than four hundred patients with severe aortic stenosis undergoing aortic valve replacement, diffuse fibrosis as assessed by T1 mapping was found to be an independent predictor of all-cause mortality [22]. Like the midwall fibrosis data, a dose dependency was also found, with every 1% increase in the ECV% followed by a 10% rise in the risk of death [22].

These findings have triggered questions in the scientific community about the appropriate timing of intervention and whether this should be driven by early markers of LV decompensation rather than the development of symptoms when irreversible damage may have possibly already occurred. The EVOLVED (Early Valve Replacement Guided by Biomarkers of Left Ventricular Decompensation in Asymptomatic Patients with Severe Aortic Stenosis) trial is a multicentre randomised controlled trial in which patients with asymptomatic severe (AS), LVEF $\geq$50%, and midwall LGE are randomised either to an early intervention or conventional "watch and wait" approach (NCT03094143) [23]. It aims in this way, to investigate whether an intervention based on objective evidence of early LV decompensation will be better for the patients clinically and prognostically.

Additionally, 4D flow is an emerging CMR tool that is becoming increasingly popular as an alternative tool for the assessment of aortic stenosis. This noninvasive tool can provide an accurate evaluation of the valvular lesion as the measurements acquired are not subject to the common errors and restrictions that accompany the two-dimensional echocardiography [24]. Furthermore, 4D flow CMR can provide invaluable information and comprehensive evaluation of aortic flow patterns and the haemodynamic consequences of severe aortic stenosis to the left ventricle and the aorta [25]. Figures 1 and 2 illustrate examples of CMR assessment of severe aortic stenosis with the CMR modalities discussed.

Undoubtedly, for patients with AS, CMR with both its conventional and emerging methods will continue to have a huge impact not only in diagnosis but also in prognosis, risk

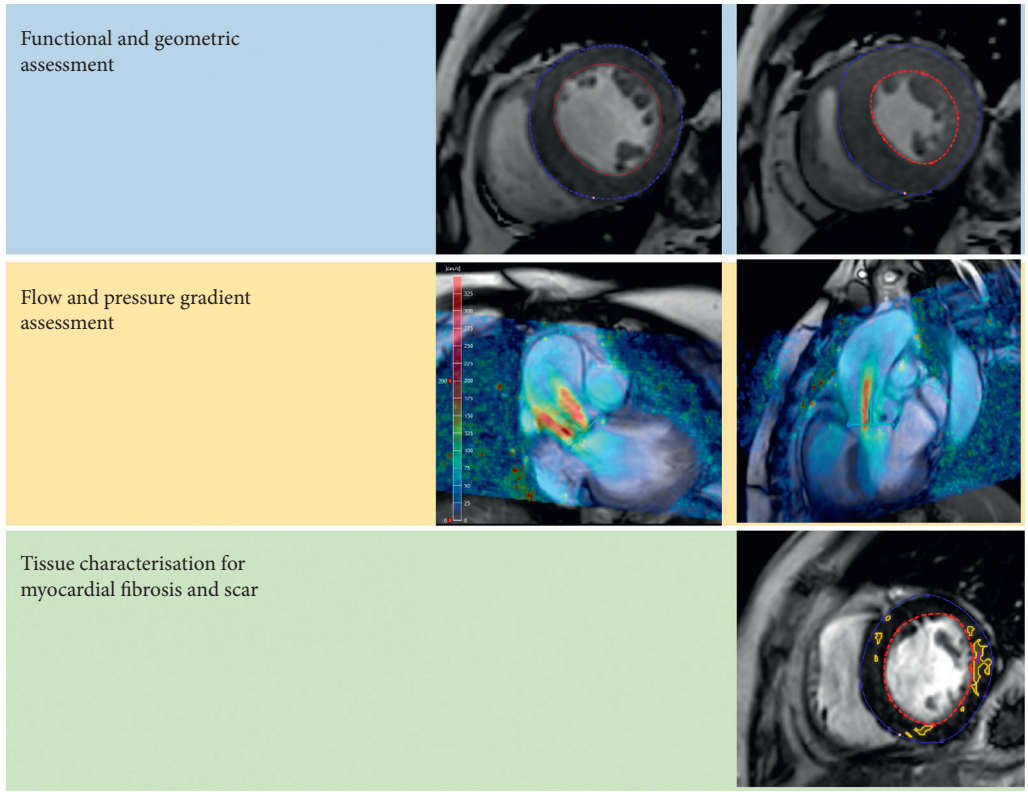

Figure 1: A case of severe aortic stenosis. (a) CMR assessment of left ventricular function and geometry. (b) 4D flow assessment of the severity of the aortic stenosis. (c) Tissue characterisation and assessment of myocardial fibrosis.

stratification, and potential decisions about the appropriate timing of intervention.

3. Mitral Regurgitation

Echocardiography is the primary investigation for the assessment of severity and mechanism of mitral regurgitation (MR). Transthoracic echocardiography may often be followed by a transoesophageal echocardiographic study for better assessment of the severity and mechanism of the mitral regurgitation. Standard 2D and Doppler echocardiographic methods of quantification of the severity include the vena contracta, proximal isovelocity surface area (PISA) method, and qualitative assessment of the continuous wave Doppler of the MR jet [26, 27]. Nevertheless, complex valvular anatomy or morphology or mechanism of regurgitation (multiple jets or very eccentric jets) may present a limitation of these techniques and may limit their diagnostic yield.

CMR has a central role in the evaluation of MR as it provides a comprehensive assessment of the valve anatomy, morphology, and accurate quantification of the MR [28]. MR can be either primary, where one or more structures of the valve apparatus are affected or secondary (functional), where regurgitation results from increased tethering forces stemming from either left ventricular or left atrial geometric alterations and subsequent annular dilatation [4]. CMR offers unlimited imaging planes that aid in the comprehensive assessment of the complex mitral valve apparatus and is an excellent tool that can be utilised if diagnostic uncertainty remains after echocardiography [29, 30]. This is reflected in clinical guidelines that suggest CMR assessment in patients where ventricular function and dimensions are insufficiently evaluated by echocardiography [4].

The haemodynamic impact of the mitral regurgitation on the myocardium is essential and traditionally this is evaluated with the 2D and volumetric assessment of the left ventricle and the left atrium [26, 27]. The LV end-diastolic and end-systolic volumes acquired from the standard volume quantification methods, together with forward flow measurements of the aorta or pulmonary artery, are used for the calculation of the regurgitant volume (MR regurgitant volume = LVSV–forward flow) and also determine the degree of LV dilatation resulting from the MR [28, 30]. In this way, the impact of chronic volume overload can be thoroughly assessed, and the haemodynamic effects of the mitral regurgitation on the left ventricle can be appreciated [31]. Current guidelines highlight the importance of LVEF and end-systolic cavity size in decision-making regarding the timing of intervention with LVEF $\leq$60% and LVESD $\geq$40 mm being markers of ventricular decompensation and worse outcomes, triggering, therefore, the referral for intervention regardless of symptoms [4]. There is, however, much debate regarding this matter, as, similar to aortic stenosis, there is evidence suggesting the occurrence of subtle myocardial impairment in the presence of normal LVEF and normal cavity size [31]. Such observations lead to a hypothesis in which LV remodelling, and indeed

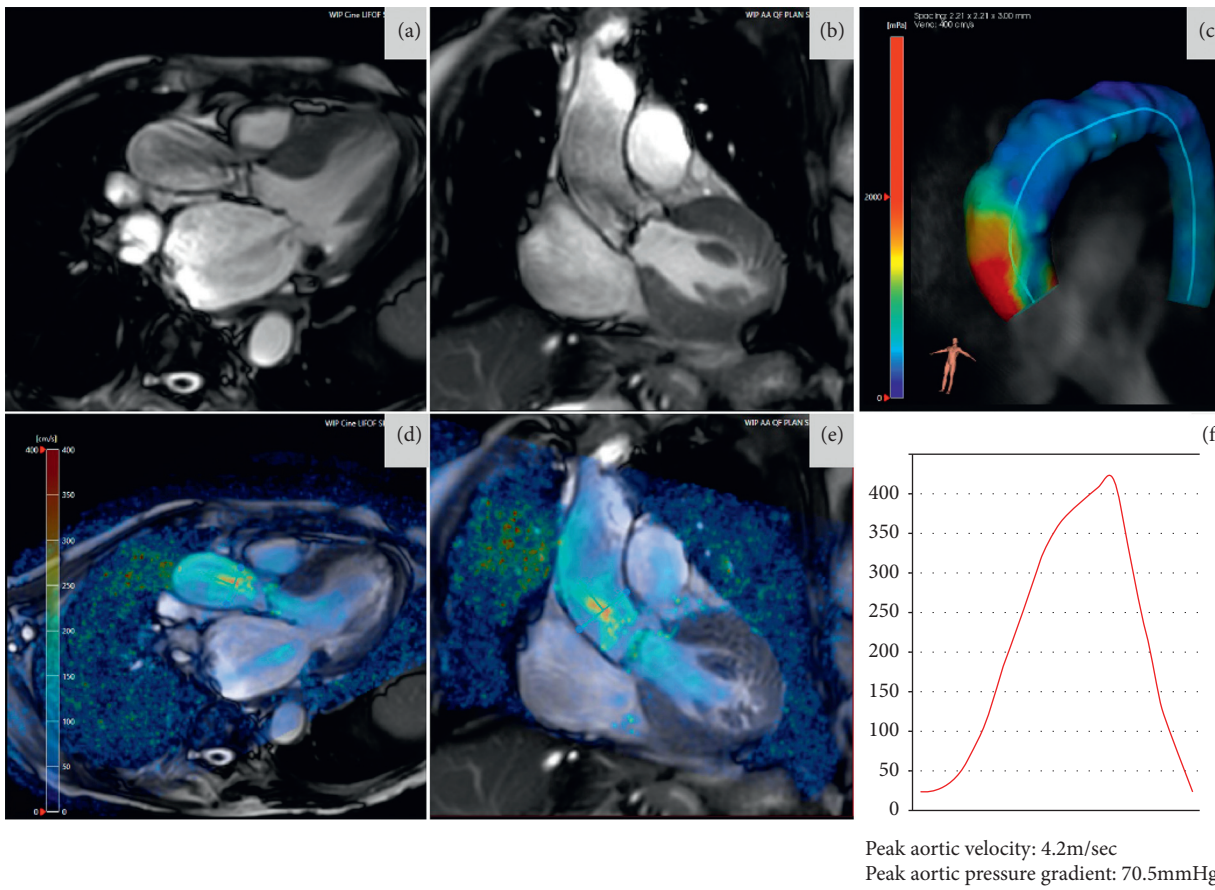

Figure 2: A case of aortic stenosis assessment using four-dimensional flow CMR. (a, b) Cine views demonstrating thickened and restrictive opening of aortic valve leaflets with flow acceleration in the aortic root. (c) Increased wall sheer stress on the anterior wall of the aortic sinus and ascending aorta due to eccentric jet through the stenosed valve. (d, e) Cine views with velocity overlay demonstrating flow acceleration greater than 4 m/sec and a two-dimensional plane through that to quantify peak velocity. (f) Peak velocity was consistent with severe aortic stenosis in this case.

myocardial fibrosis, can occur before a decline in LVEF and even before the development of symptoms [11]. Thus, in a small study of 35 patients with asymptomatic primary moderate or severe MR, diffuse interstitial fibrosis as measured by ECV was noted to occur before the occurrence of conventional indications for valvular intervention [32]. This was correlated with impaired myocardial deformation and reduced exercise tolerance assessed by cardiopulmonary exercise testing [32]. This finding has been confirmed in another large study comprised of 120 patients with chronic primary MR, which demonstrated that fibrosis, as quantified by ECV, occurs before the onset of symptoms [33].

Whereas early studies suggest a diffuse interstitial fibrosis pattern, more recent studies indicate there may also be a coexistent focal replacement fibrosis model. Recently, Kitkugvan et al. investigated the pattern of fibrosis and whether diffuse interstitial fibrosis was the result or the cause of the MR in a study that included more than four hundred patients with chronic primary MR [34]. The presence of diffuse fibrosis and raised ECV correlated with the severity of MR and was independently associated with symptoms and clinical events that included mitral surgery and cardiovascular death [34]. While diffuse interstitial fibrosis with raised ECV was raised in a similar fashion in patients with and without MVP, it was noted that replacement fibrosis with increased LGE was more prevalent in the individuals with MVP [34]. This finding was in agreement with a further study that included four hundred patients with MVP of variable severity [35]. This found that replacement fibrosis is common in patients with MVP and is independently associated with adverse cardiovascular events [35].

Although the pattern and spectrum of fibrosis in MR remain complex, the consequences of it remain rather clear. More specifically, it has been found that in young and middle-aged patients with mitral valve prolapse (MVP), there is a clear association of replacement fibrosis, as assessed by LGE, with life-threatening arrhythmias and risk of sudden cardiac death [36]. The myocardial scarring in this patient population targets specific myocardial regions, including the papillary muscles and the inferobasal LV wall [36, 37]. The presence of this nonischaemic pattern of LGE that appears to be in high prevalence in patients with MVP is not directly associated with the severity of the MR but has been repeatedly found to be a substrate for arrhythmic events [36–38]. The negative prognostic value of the presence of fibrosis may persist even after the intervention,

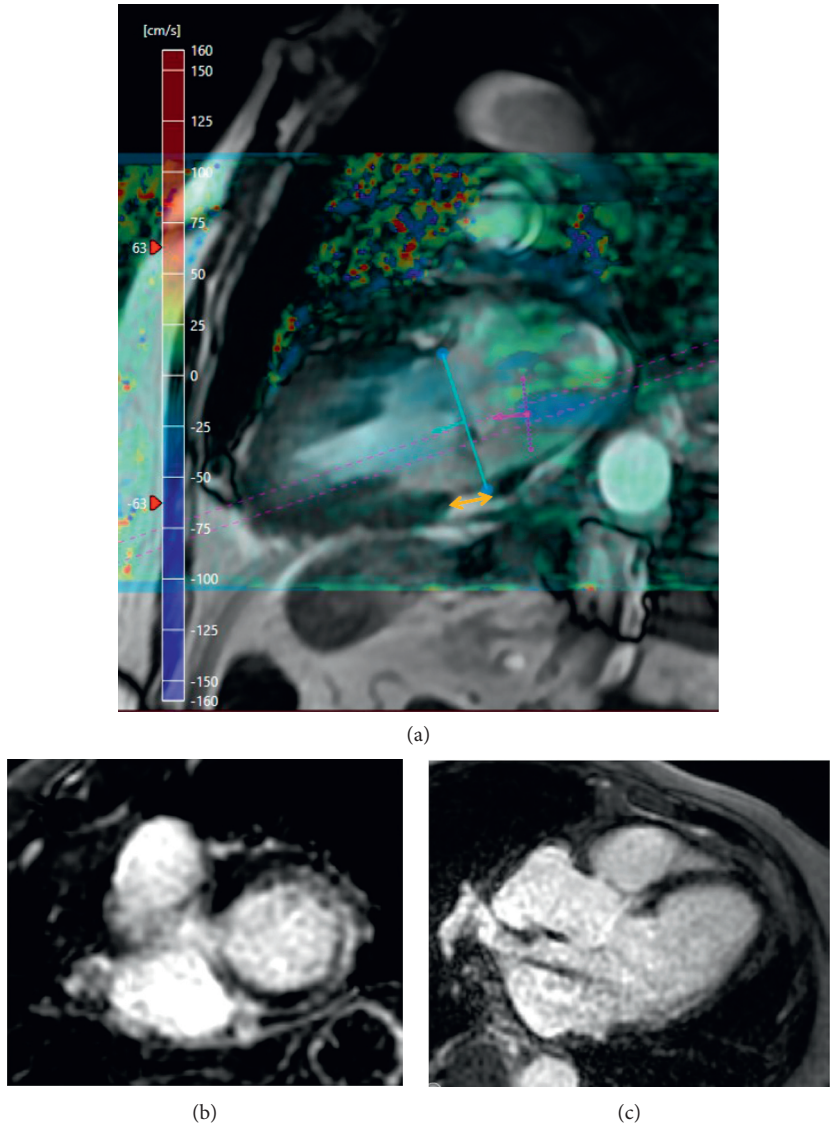

(a)

(b)

(c)

Figure 3: A case of mitral annular disjunction (a) (yellow arrow) with associated fibrosis in the basal lateral wall (b, c) (late gadolinium enhancement imaging) and moderate mitral regurgitation (a) (blue flow in the left atrium).

although further large studies are needed to confirm a causal relationship between LGE and adverse events [39].

CMR has also contributed significantly to the identification of the entity of mitral annular disjunction as a common cause of arrhythmias [37]. Mitral annular disjunction is defined as an atrial displacement of the hinge point of the mitral valve away from the ventricular myocardium, leading to paradoxical haemodynamics and acting as an arrhythmic trigger [37, 40]. Whereas this pathological finding was thought to be linked with MVP, it has been demonstrated that the two are separate, although commonly coexistent entities [37, 40]. Figure 3 demonstrates the CMR assessment of a case of mitral annular disjunction with myocardial fibrosis and moderate mitral regurgitation.

More recently, 4D flow CMR assessment and quantification of mitral valve regurgitation is increasingly used in clinical practice as it offers a much improved and detailed method of evaluation, especially for challenging cases, such as complicated anatomical lesions, multiple coexistent lesions or shunts [28]. The severity of the mitral regurgitation can be evaluated with 4D flow CMR either with direct quantification of the MR flow with retrospective mitral valve tracking or with indirect method, which is the mitral forward flow minus the aortic forward volume [28] (Figure 4). The exact mechanism and pathophysiology behind the findings may remain complicated and unclear, but CMR has undoubtedly the potential to support researchers in the quest to uncover the clinical and prognostic implications of the complex anatomical features and the presence of the different types of fibrosis.

4. Conclusions

The assessment and management of valvular heart disease have long centred on a triad of the presence or absence of symptoms, valvular functional parameters confirming

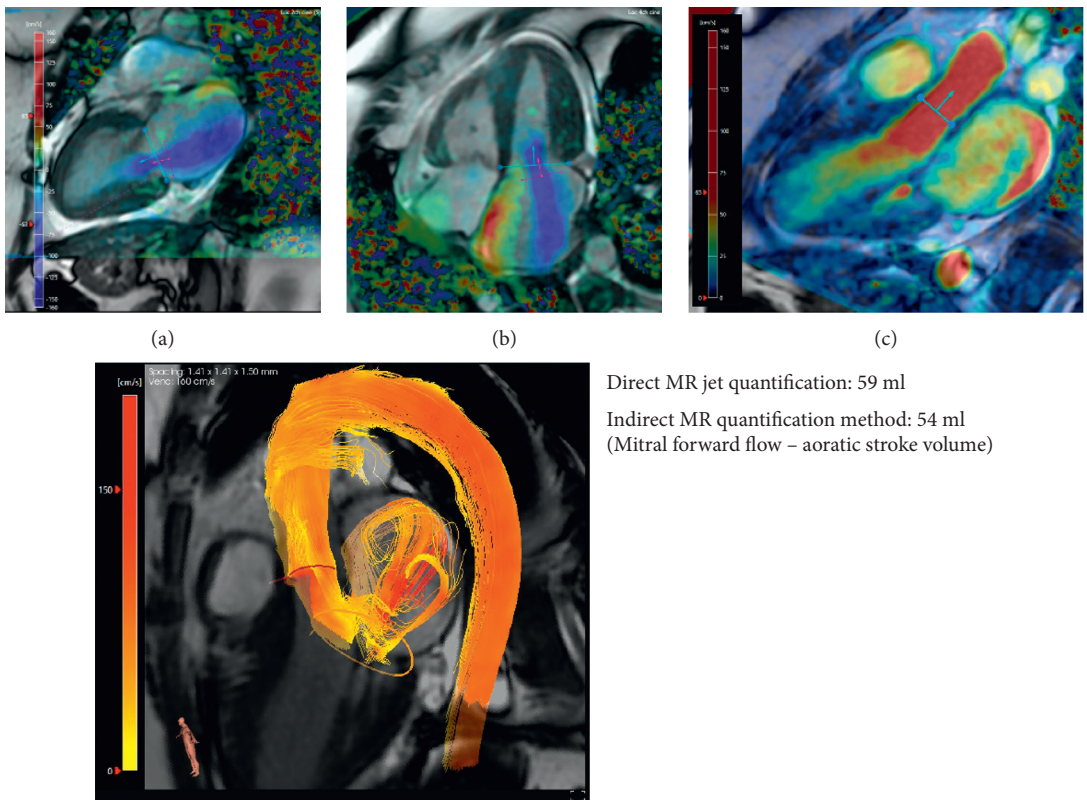

Figure 4: A case of mitral regurgitation assessment using four-dimensional flow CMR. (a) Two-chamber cine view with velocity overlay demonstrating mitral regurgitation (blue flow in the left atrium). (b) Four-chamber cine view shows the same mitral regurgitation jet which is swirling in the whole left atrium. (c) A three-chamber cine view used to quantify aortic stroke volume by valve tracking. (d) Three-dimensional streamlines of blood flow during systole demonstrating aortic forward flow and the mitral regurgitation swirling in the left atrium.

severity, and the presence or absence of LV dilatation or dysfunction assessed by LVEF. Furthermore, the assessment of valvular function and LV dysfunction has long been dominated by echocardiography. The utility of CMR in VHD-related cardiomyopathy offers more accurate and incremental information than that derived from echo. The ability to image in any plane also offers structural analysis, particularly important in mitral valvular assessment. Through its delivery of accurate and highly reproducible chamber quantification CMR provides a gold standard for volumetric assessment, and in turn, myocardial mass measurement. Moreover, with LGE imaging and T1 mapping, CMR also offers deep tissue characterisation, which is emerging as a powerful technique in the identification of myocardial fibrosis with potential implications for risk stratification and timing of valvular intervention. Whether the timing of valvular intervention based on these early markers of LV decompensation results in improved clinical outcomes remains, however, to be determined and is the subject of active clinical trials.

Data Availability

No data were used to support this study.

Consent

Since this is a review of already published data, no consent required.

Conflicts of Interest

PG has an advisor role in Pie Medical Imaging and Medis Medical Imaging.

Acknowledgments

This work was partly funded by Wellcome Trust grants (220703/Z/20/Z and 215799/Z/19/Z).References

References

[1] V. T. Nkomo, J. M. Gardin, T. N. Skelton, J. S. Gottdiener, C. G. Scott, and M. Enriquez-Sarano, "Burden of valvular heart diseases: a population-based study," *The Lancet*, vol. 368, no. 9540, pp. 1005–1011, 2006.

[2] J. L. D'Arcy, "Large-scale community echocardiographic screening reveals a major burden of undiagnosed valvular heart disease in older people: the OxVALVE Population Cohort Study," *European Heart Journal*, vol. 37, pp. 3515–3522a, 2016.

[3] A. Marciniak, K. Glover, and R. Sharma, "Cohort profile: prevalence of valvular heart disease in community patients with suspected heart failure in UK," *BMJ Open*, vol. 7, pp. e012240–4, 2017.

[4] A. Vahanian, "2021 ESC/EACTS Guidelines for the management of valvular heart disease," *European Heart Journal*, vol. 28, pp. 1–72, 2021.

[5] H. Baumgartner, J. Hung, J. Bermejo et al., "Recommendations on the echocardiographic assessment of aortic valve stenosis: a focused update from the european association of cardiovascular imaging and the american society of echocardiography," *European Heart Journal-Cardiovascular Imaging*, vol. 18, no. 3, pp. 254–275, 2017.

[6] L. Ring, B. N. Shah, S. Bhattacharyya et al., "Echocardiographic assessment of aortic stenosis: a practical guideline from the British Society of Echocardiography," *Echo Research and Practice*, vol. 8, no. 1, pp. G19–G59, 2021.

[7] P. Lancellotti, J. Magne, R. Dulgheru et al., "Outcomes of patients with asymptomatic aortic stenosis followed up in heart valve clinics," *JAMA Cardiology*, vol. 3, no. 11, pp. 1060–1068, 2018.

[8] Project Documents, Heart Valve Disease Presenting in Adults: Investigation and Management, Guidance, NICE. https://www.nice.org.uk/guidance/indevelopment/gid-ng10122/documents.

[9] J. Magne, B. Cosyns, B. A. Popescu et al., "Distribution and prognostic significance of left ventricular global longitudinal strain in asymptomatic significant aortic stenosis," *Journal of the American College of Cardiology: Cardiovascular Imaging*, vol. 12, no. 1, pp. 84–92, 2019.

[10] K. Kusunose, A. Goodman, R. Parikh et al., "Incremental prognostic value of left ventricular global longitudinal strain in patients with aortic stenosis and preserved ejection fraction," *Circulation: Cardiovascular Imaging*, vol. 7, no. 6, pp. 938–945, 2014.

[11] T. Podlesnikar, V. Delgado, and J. J. Bax, "Cardiovascular magnetic resonance imaging to assess myocardial fibrosis in valvular heart disease," *The International Journal of Cardiovascular Imaging*, vol. 34, no. 1, pp. 97–112, 2018.

[12] T. Onishi, S. K. Saha, A. Delgado-Montero et al., "Global longitudinal strain and global circumferential strain by speckle-tracking echocardiography and feature-tracking cardiac magnetic resonance imaging: comparison with left ventricular ejection fraction," *Journal of the American Society of Echocardiography*, vol. 28, no. 5, pp. 587–596, 2015.

[13] T. A. Musa, A. Uddin, P. P. Swoboda et al., "Myocardial strain and symptom severity in severe aortic stenosis: insights from cardiovascular magnetic resonance," *Quantitative Imaging in Medicine and Surgery*, vol. 7, no. 1, pp. 38–47, 2017.

[14] J. Erley, D. Genovese, N. Tapaskar et al., "Echocardiography and cardiovascular magnetic resonance based evaluation of myocardial strain and relationship with late gadolinium enhancement," *Journal of Cardiovascular Magnetic Resonance: Official Journal of the Society for Cardiovascular Magnetic Resonance*, vol. 21, pp. 46–11, 2019.

[15] M. R. Dweck, N. A. Boon, and D. E. Newby, "Calcific aortic stenosis," *Journal of the American College of Cardiology*, vol. 60, no. 19, pp. 1854–1863, 2012.

[16] S. Hein, E. Arnon, S. Kostin et al., "Progression from compensated hypertrophy to failure in the pressure-overloaded human heart," *Circulation*, vol. 107, no. 7, pp. 984–991, 2003.

[17] T. A. Treibel, B. López, A. González et al., "Reappraising myocardial fibrosis in severe aortic stenosis: an invasive and non-invasive study in 133 patients," *European Heart Journal*, vol. 39, no. 8, pp. 699–709, 2018.

[18] C. W. L. Chin, R. J. Everett, J. Kwiecinski et al., "Myocardial fibrosis and cardiac decompensation in aortic stenosis," *Journal of the American College of Cardiology: Cardiovascular Imaging*, vol. 10, no. 11, pp. 1320–1333, 2017.

[19] R. Bing, J. L. Cavalcante, R. J. Everett, M.-A. Clavel, D. E. Newby, and M. R. Dweck, "Imaging and impact of myocardial fibrosis in aortic stenosis," *Journal of the American College of Cardiology: Cardiovascular Imaging*, vol. 12, no. 2, pp. 283–296, 2019.

[20] T. A. Musa, T. A. Treibel, V. S. Vassiliou et al., "Myocardial scar and mortality in severe aortic stenosis," *Circulation*, vol. 138, no. 18, pp. 1935–1947, 2018.

[21] T. A. Treibel, R. Kozor, R. Schofield et al., "Reverse myocardial remodeling following valve replacement in patients with aortic stenosis," *Journal of the American College of Cardiology*, vol. 71, no. 8, pp. 860–871, 2018.

[22] R. J. Everett, T. A. Treibel, M. Fukui et al., "Extracellular myocardial volume in patients with aortic stenosis," *Journal of the American College of Cardiology*, vol. 75, no. 3, pp. 304–316, 2020.

[23] B. R. Lindman, "Management of asymptomatic severe aortic stenosis: evolving concepts in timing of valve replacement," *Journal of the American College of Cardiology: Cardiovascular Imaging*, vol. 13, pp. 481–493, 2020.

[24] G. T. Archer, A. Elhawaz, N. Barker et al., "Validation of four-dimensional flow cardiovascular magnetic resonance for aortic stenosis assessment," *Scientific Reports*, vol. 10, pp. 10569–10610, 2020.

[25] J. Garcia, A. J. Barker, and M. Markl, "The role of imaging of flow patterns by 4D flow MRI in aortic stenosis," *Journal of the American College of Cardiology: Cardiovascular Imaging*, vol. 12, no. 2, pp. 252–266, 2019.

[26] P. Lancellotti, C. Tribouilloy, A. Hagendorff et al., "Recommendations for the echocardiographic assessment of native valvular regurgitation: an executive summary from the European Association of Cardiovascular Imaging," *European Heart Journal-Cardiovascular Imaging*, vol. 14, no. 7, pp. 611–644, 2013.

[27] S. Robinson, L. Ring, D. X. Augustine et al., "The assessment of mitral valve disease: a guideline from the British Society of Echocardiography," *Echo Research and Practice*, vol. 8, no. 1, pp. G87–G136, 2021.

[28] P. Garg, A. J. Swift, L. Zhong et al., "Assessment of mitral valve regurgitation by cardiovascular magnetic resonance imaging," *Nature Reviews Cardiology*, vol. 17, no. 5, pp. 298–312, 2020.

[29] G. S. Gulsin, A. Singh, and G. P. McCann, "Cardiovascular magnetic resonance in the evaluation of heart valve disease," *BMC Medical Imaging*, vol. 17, pp. 67–14, 2017.

[30] S. Myerson, "Heart valve disease: investigation by cardiovascular magnetic resonance," *Journal of Cardiovascular Magnetic Resonance*, vol. 14, pp. 1–23, 2012.

[31] S. Uretsky, E. Argulian, J. Narula, and S. D. Wolff, "Use of cardiac magnetic resonance imaging in assessing mitral regurgitation," *Journal of the American College of Cardiology*, vol. 71, no. 5, pp. 547–563, 2018.

[32] N. C. Edwards, W. E. Moody, M. Yuan et al., "Quantification of left ventricular interstitial fibrosis in asymptomatic chronic primary degenerative mitral regurgitation," *Circulation: Cardiovascular Imaging*, vol. 7, no. 6, pp. 946–953, 2014.

[33] B. Liu, D. A. H. Neil, M. Premchand, M. Bhabra, and R. Patel, "Myocardial fibrosis in asymptomatic and symptomatic chronic severe primary mitral regurgitation and relationship

to tissue characterisation and left ventricular function on cardiovascular magnetic resonance," *Journal of Cardiovascular Magnetic Resonance : Official Journal of the Society for Cardiovascular Magnetic Resonance*, vol. 22, no. 1, pp. 86–12, 2020.

[34] D. Kitkungvan, E. Y. Yang, K. C. El Tallawi et al., "Extracellular volume in primary mitral regurgitation," *Journal of the American College of Cardiology: Cardiovascular Imaging*, vol. 14, no. 6, pp. 1146–1160, 2021.

[35] A.-L. Constant Dit Beaufils, O. Huttin, A. Jobbe-Duval et al., "Replacement myocardial fibrosis in patients with mitral valve prolapse," *Circulation*, vol. 143, no. 18, pp. 1763–1774, 2021.

[36] C. Basso, M. Perazzolo Marra, S. Rizzo et al., "Arrhythmic mitral valve prolapse and sudden cardiac death," *Circulation*, vol. 132, no. 7, pp. 556–566, 2015.

[37] L. A. Dejgaard, E. T. Skjølsvik, Ø. H. Lie et al., "The mitral annulus disjunction arrhythmic syndrome," *Journal of the American College of Cardiology*, vol. 72, no. 14, pp. 1600–1609, 2018.

[38] D. Kitkungvan, F. Nabi, R. J. Kim et al., "Myocardial fibrosis in patients with primary mitral regurgitation with and without prolapse," *Journal of the American College of Cardiology*, vol. 72, no. 8, pp. 823–834, 2018.

[39] J. F. Velu, A. Hirsch, S. M. Boekholdt et al., "Myocardial fibrosis predicts adverse outcome after MitraClip implantation," *Catheterization and Cardiovascular Interventions*, vol. 93, no. 6, pp. 1146–1149, 2019.

[40] A. P.-W. Lee, C.-N. Jin, Y. Fan, R. H. L. Wong, M. J. Underwood, and S. Wan, "Functional implication of mitral annular disjunction in mitral valve prolapse," *Journal of the American College of Cardiology: Cardiovascular Imaging*, vol. 10, no. 12, pp. 1424–1433, 2017.

Hindawi
Cardiology Research and Practice
Volume 2022, Article ID 6401180, 12 pages
https://doi.org/10.1155/2022/6401180

Research Article

Prospective Longitudinal Characterization of the Relationship between Diabetes and Cardiac Structural and Functional Changes

Amrit Chowdhary,[1] Nicholas Jex,[1] Sharmaine Thirunavukarasu,[1] Amanda MacCannell,[2] Natalie Haywood,[2] Altaf Almutairi,[1] Lavanya Athithan,[3] Manali Jain,[1] Thomas Craven,[1] Arka Das,[1] Noor Sharrack,[1] Christopher E. D. Saunderson,[1] Anshuman Sengupta,[4] Lee Roberts,[2] Peter Swoboda,[1] Richard Cubbon,[1] Klaus Witte,[2] John Greenwood,[1] Sven Plein,[1] and Eylem Levelt[1]

[1]*University of Leeds, Multidisciplinary Cardiovascular Research Centre and Biomedical Imaging Science Department, Leeds Institute of Cardiovascular and Metabolic Medicine, Leeds LS29JT, UK*
[2]*University of Leeds, Discovery and Translational Science Department, Leeds Institute of Cardiovascular and Metabolic Medicine, Leeds LS29JT, UK*
[3]*National Institute for Health Research Biomedical Research Centre—Department of Cardiovascular Sciences, University of Leicester, Glenfield Hospital, Groby Road, Leicester LE3 9QP, UK*
[4]*Department of Cardiology, Leeds Teaching Hospitals NHS Trust, Great George Street, Leeds LS13EX, UK*

Correspondence should be addressed to Eylem Levelt; e.levelt@leeds.ac.uk

Received 2 August 2021; Accepted 19 January 2022; Published 8 February 2022

Academic Editor: George Bazoukis

Objectives. In a cohort of type 2 diabetic (T2D) patients who underwent baseline cardiac magnetic resonance (CMR) and biomarker testing, during a median follow-up of 6 years, we aimed to determine longitudinal changes in the phenotypic expression of heart disease in diabetes, report clinical outcomes, and compare baseline clinical characteristics and CMR findings of patients who experienced major adverse cardiovascular events (MACE) to those remaining MACE free. *Background*. T2D increases the risk of heart failure (HF) and cardiovascular mortality. The long-term impact of T2D on cardiac phenotype in the absence of cardiovascular disease and other clinical events is unknown. *Methods*. Patients with T2D ($n = 100$) with no history of cardiovascular disease or hypertension were recruited at baseline. Biventricular volumes, function, and myocardial extracellular volume fraction (ECV) were assessed by CMR, and blood biomarkers were taken. Follow-up CMR was repeated in those without interim clinical events after 6 years. *Results*. Follow-up was successful in 83 participants. Of those, 29 experienced cardiovascular/clinical events (36%). Of the remaining 59, 32 patients who experienced no events received follow-up CMR. In this cohort, despite no significant changes in blood pressure, weight, or glycated hemoglobin, significant reductions in biventricular end-diastolic volumes and ejection fractions occurred over time. The mean ECV was unchanged. Baseline plasma high-sensitivity cardiac troponin T (hs-cTnT) was significantly associated with a change in left ventricular (LV) ejection fraction. Patients who experienced MACE had higher LV mass and greater LV concentricity than those who remained event free. *Conclusions*. T2D results in reductions in biventricular size and systolic function over time even in the absence of cardiovascular/clinical events.

1. Introduction

Cardiovascular disease represents the primary cause of death in type 2 diabetic patients (T2D) [1]. Although T2D is recognized as a strong risk factor for atherosclerosis-related events, heart failure (HF) is the commonest initial presentation of cardiovascular disease in T2D [1–3]. The risk of developing HF is increased 2.4-fold in men and 5-fold in women with T2D compared with age-matched controls [4], and the combination of T2D and HF is associated with a 4- to 6-fold higher mortality [5, 6]. The early detection of adverse subclinical myocardial structural and functional alterations associated with progressive myocardial dysfunction might offer the opportunity of early initiation of disease-modifying pharmacological therapies prior to the onset of overt HF [7].

Cardiac magnetic resonance imaging (CMR) is the reference standard for the assessment of cardiac volumes, mass, and function [8]. Using CMR, patients with T2D have been extensively phenotyped with a nuanced description of disease burden [9, 10]. However, to our knowledge no CMR study to date has examined longitudinal changes in biventricular structure and function in patients with T2D with no prior cardiovascular disease.

In this longitudinal observational study, we tested the hypothesis that T2D would be associated with a progressive decline in biventricular systolic function even in a cohort of diabetic patients with no prior cardiovascular disease or interim major adverse cardiovascular events (MACE) during the follow-up period. We also sought to report clinical outcomes and compare demographic, clinical, and biochemical variables, and CMR and plasma biomarkers measured at baseline between those patients who experienced MACE and those who remained free of MACE during the follow-up period.

2. Methods

Using CMR at two time points baseline visit and end of the study, we performed a prospective longitudinal study in a cohort of ethnically diverse, asymptomatic patients with T2D with no history or evidence on examination of cardiovascular disease. Participants who remained asymptomatic and free of MACE or any other new clinical comorbidity were invited for a second CMR scan after 6 years.

2.1. Participants. Recruitment was performed from primary care health centers in Leeds, the United Kingdom. One hundred participants with T2D were recruited at baseline [11]. The results of this initial study have been previously published [11, 12]. For this study, all surviving T2D participants who could be contacted and remained eligible were offered a follow-up research visit for a repeat CMR scan.

2.2. Inclusion and Exclusion Criteria. Asymptomatic adult patients with a diagnosis of T2D (diagnosed according to the World Health Organization criteria) [13] with the ability to provide informed written consent were recruited at baseline. Patients were excluded if they had a previous diagnosis of cardiovascular disease (previous cardiac surgery, angioplasty, myocardial infarction, angina, moderate or above valvular heart disease, and atrial fibrillation(AF)), hypertension (resting systolic blood pressure (BP) >140 mmHg and diastolic BP >90 mmHg on 24-hour ambulatory BP monitoring), contraindications to CMR, ischemic changes in 12-lead electrocardiogram (ECG), renal impairment (estimated glomerular filtration rate (eGFR) below 30 mL/min/1.73 m^2), or if they were using insulin. After 6 years, surviving participants who remained asymptomatic, with no MACE, other diabetic complications, or important comorbidity (such as inflammatory disease or malignancy) were invited for a second CMR study.

2.3. Baseline Clinical Assessment. At baseline and at the follow-up visit, height and weight were recorded and body mass index (BMI) was calculated. A fasting blood sample was taken from each participant at baseline for assessments of full blood count (FBC), eGFR, fasting glucose, glycated hemoglobin (HbA1c), high-sensitivity cardiac troponin T (hs-cTnT), and N-terminal prohormone B-type natriuretic peptide (NT-proBNP) levels. All participants underwent resting ECG, and all had 24-hour BP monitoring at baseline to exclude undiagnosed hypertension [11]. At the follow-up study visit, brachial BP was recorded as an average of 3 supine measures taken over 10 minutes (Dinamap 1846 SX, Critikon Corp), a fasting blood sample was obtained for repeated assessments of FBC, eGFR, glucose, HbA1c, and lipids, and a resting ECG was recorded.

2.4. Cardiac Magnetic Resonance Imaging. Imaging was performed on a 3.0 Tesla magnetic resonance system both at baseline and at year 6 CMR study visit. The baseline CMR protocol has been previously described [11]. Follow-up scans were performed using a matching imaging protocol.

Images for biventricular and left atrial (LA) volumes and function were acquired using a steady-state free precession (SSFP) sequence with breath holding at end expiration in multiple orientations (Figure 1). Adenosine stress myocardial perfusion CMR was performed to rule out significant epicardial coronary artery stenosis [14]. Pharmacological stress was achieved with adenosine infusion at 140 mcg/kg/min for a minimum of 3 mins, and an intravenous bolus of 0.075 mmol/kg gadobutrol (Gadovist®, Bayer Pharma, Berlin, Germany) was administered for each stress and rest perfusion imaging sequence. Visual analysis of the perfusion images was performed by one reporter (EL, with >8 years of CMR experience and level 3 CMR accreditation). Ischemia was defined as a territory with a perfusion defect during stress [14]. Late gadolinium enhancement (LGE) imaging was performed in matching LV short-axis planes >8 minutes after contrast administration to exclude the presence of previous silent myocardial infarction or regional fibrosis.

All image analyses were performed off-line by AC (with 2 years of CMR experience) in a blinded fashion, and all scan contours were subsequently reviewed by EL

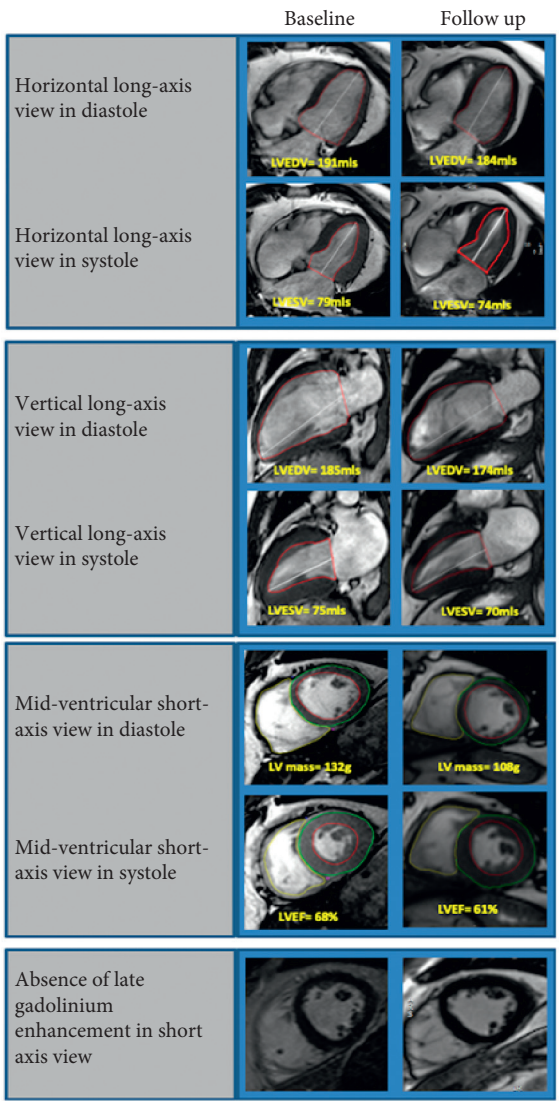

Figure 1: Representative examples of CMR imaging. Representative examples of cine images (horizontal long axis, vertical long axis, and mid-ventricular short axis in diastole and systole) and late gadolinium enhancement imaging (mid-ventricular short axis) in patients with T2D at baseline and follow-up.

using cvi42 software (Circle Cardiovascular Imaging, Calgary, Canada). Baseline and follow-up images were analyzed in a random order after the second visit by investigators blinded to any other data. Biventricular volumes and ejection fraction (EF) were obtained from contouring the endocardial and epicardial borders in diastole and systole on the SSFP short-axis stacks. The LA volume and EF were calculated using the biplane area-length method in the horizontal and vertical long axes as previously described [8]. Using cvi42 Tissue Tracking software, global longitudinal strain (GLS), and a marker of diastolic function, LV diastolic strain measurements were performed from balanced SSFP short-axis and 2-chamber and 4-chamber long-axis cine images, to calculate circumferential peak early diastolic strain rate (PEDSR) and longitudinal PEDSR [10].

2.5. Statistical Analysis. Statistical analysis was performed using SPSS (IBM SPSS statistics, version 26.0). Categorical data were compared with Pearson's chi-square test. Continuous variables were checked for normality using the Shapiro-Wilk test and are presented as mean ± SD. Comparisons of CMR data between baseline and follow-up were performed with a two-tailed paired *t*-test. Bivariate correlations were performed using Pearson's correlation coefficient. The relationships of change in left ventricular ejection fraction (LVEF) and right ventricular ejection fraction (RVEF) (ΔLVEF and ΔRVEF, respectively) with age, BMI, HBA_1c, fasting glucose, resting BP and heart rate (HR), NT-proBNP, and hs-cTnT were analyzed using multiple logistic regression. A p-value of ≤0.05 was considered statistically significant.

2.6. Ethical Considerations. The study was approved by the National Research Ethics Committee (Ref: 13/YH/0098), and informed written consent was obtained from each participant. The follow-up assessment was given additional ethical approval (Ref: 18/YH/0168). Participants were asked to sign a second consent form for the follow-up scan.

3. Results

3.1. Participant Characteristics and Clinical Outcomes. Clinical outcomes of the baseline cohort were determined after a median follow-up of 6.3 years (interquartile range (IQR): 6.05–6.53 years) using electronic health records systems, and symptom status was determined by phone assessments (Figure 1). Demographics, clinical, and biochemical data are shown in Table 1. Of the hundred participants with T2D recruited at baseline (82 men, mean age 61 ± 11 years, median diabetic duration 4.1 years (IQR: 1.4–7 years), 17 participants were uncontactable (Figure 2). The healthcare records of the remaining 83 participants revealed that 5 participants (6%) had died during the follow-up period (one due to acute coronary syndrome (ACS)), 8 participants (9.6%) had survived an ACS, 3 participants (3.8%) had a cerebrovascular accident, 6 participants (7.7%) developed a malignancy, 1 participant (1.3%) had a permanent pacemaker implanted for a high-grade atrioventricular block, and 1 participant (1.3%) developed significant renal dysfunction (Figure 2). These participants were not invited back for a follow-up CMR scan. Of the remaining 59 participants (76%) with T2D who remained free of MACE invited for a repeat CMR scan, 16 participants declined, and a further 6 participants were unable to attend for their research visit due to the coronavirus pandemic (Figure 2). Hence, 37 participants completed a second CMR scan. Of these, 5 were found to have suffered a silent MI as evidenced by subendocardial hyperenhancement on LGE and were excluded from further analysis leaving a study population of 32 participants. About 25% of the original study population had suffered a major adverse cardiovascular event (MI, angina, revascularization, stroke, and cardiovascular mortality) during the 6-year follow-up period (Figure 3) with an overall clinical event rate of 35%.

Table 1: Clinical and biochemical characteristics.

Variable	Baseline total participants ($n = 100$)	Follow-up ($n = 32$)	P value
Age, years	61 ± 11	64 ± 11	0.2
BMI, kg/m^2	29 ± 4	27 ± 4	0.02*
Male, *n* (%)	82 (82)	29 (91)	0.2
Diabetes duration, years	5.0 ± 4.4	10.9 ± 1.3	0.0001*
Smoking, *n* (%)	6 (6)	2 (6)	0.9
Heart rate, bpm	71 ± 12	68 ± 12	0.2
Systolic blood pressure, mmHg	131 ± 15	129 ± 16	0.5
Diastolic blood pressure, mmHg	73 ± 9	74 ± 7	0.6
Plasma fasting glucose, mmol/L	9.9 ± 4.1	9.4 ± 3.8	0.5
Glycated hemoglobin, mmol/mol	63 ± 20	64 ± 18	0.7
Total cholesterol, mmol/L	4.4 ± 1.1	4.5 ± 1.2	0.7
HDL, mmol/L	1.19 ± 0.35	1.36 ± 0.38	0.03*
LDL, mmol/L	2.60 ± 0.98	2.59 ± 1.21	0.9
Medications, *n* (%)			
Metformin	87 (87)	22 (69)	0.01*
Sulfonylurea	33 (33)	13 (40)	0.4
Aspirin	18 (18)	9 (28)	0.2
Statin	69 (69)	23 (72)	0.7
ACEI	0 (0)	13 (40)	0.001*
ARB	0 (0)	3 (9)	0.0001*

Values are mean ± standard deviations or percentages. *signifies $P \leq 0.05$. *n*-numbers; BMI-body mass index; kg-kilogram; m-meter; bpm-beats per minute; mmHg-millimeters of mercury; mmol-millimoles; L-liters; mol-moles; HDL-high-density lipoprotein; LDL-low-density lipoprotein; ACEI-angiotensin-converting enzyme inhibitor; ARB-angiotensin receptor blocker.

3.2. Baseline to Follow-Up Demographics and Medical Therapy. In the 32 patients comprising this study cohort, 29 were men, the mean age was 64 ± 9 years, and median diabetic duration was 11.9 years (IQR: 11.8–12.3 years). There were no significant differences in resting HR and BP, glycemic control, or BMI between the baseline and follow-up measurements (Table 2). Glucose-lowering treatment had been altered for the majority of patients between baseline and follow-up. While the proportion of patients on a biguanide reduced from 88% to 69% ($p = 0.01$), the proportion taking a sodium-glucose cotransporter-2 (SGLT2) inhibitor increased from none to 12% ($p = 0.03$). The number of participants on sulfonylureas, thiazolidinediones, gliptins, aspirin, or statins did not significantly change during the follow-up period.

None of the patients were on an angiotensin-converting enzyme inhibitor (ACEI) or an angiotensin receptor blocker (ARB) therapy at baseline as per recruitment criteria of the initial study [11], whereas 13 participants (41%) were receiving this therapy at the time of follow-up visit (Table 2).

3.3. Cardiac Geometry, Function, and Myocardial Scarring. The CMR results of the 32 participants at baseline and follow-up are shown in Table 3. At follow-up, there was a reduction in cardiac size with reduced biventricular end-diastolic volumes (Figures 4(a) and 4(b)) and a deterioration of biventricular systolic function (mean LVEF 60 ± 7% vs. 55 ± 8%, $p = 0.0001$; mean RVEF 55 ± 5% vs. 51 ± 7%, $p = 0.003$) (Figures 4(c) and 4(d)) with reductions in stroke volumes. In keeping with the reduction in cardiac size, the LV mass and mass index were reduced at follow-up compared with baseline ($p = 0.01$ and $p = 0.04$, respectively). There was no change in LV PEDSR over time (Figures 4(e) and 4(f)). Consistent with the changes in LVEF, GLS was numerically reduced from baseline over time; however, this trend did not reach statistical significance. In keeping with the reductions in biventricular volumes, LA volumes were also decreased, but there was no change in LA function over time.

Mean change in LVEF was the same in those taking and those not taking renin-angiotensin-aldosterone blocking agents.

The presence of new mid-wall fibrosis in a nonischemic pattern was detected in only one patient at follow-up. There were no changes in mean ECV between baseline and follow-up ($p = 0.3$).

3.4. Comparison of CMR Features, Plasma Biomarkers, and Biochemistry at Baseline between Patients Who Experienced Cardiovascular Events and Those Who Remained Asymptomatic. There were no differences in baseline hs-cTnT and NT-proBNP biomarker levels or clinical and biochemical variables at baseline in participants who experienced MACE (angina, myocardial infarction, revascularization, cerebrovascular accident, and cardiovascular mortality) compared to those who did not (Table 4). However, patients who experienced MACE during the follow-up period had higher LV mass, LV mass indexed to body surface area, and a higher LV mass-to-LV EDV ratio indicating a greater concentric remodeling of the LV at baseline compared to those remaining asymptomatic and event free during the follow-up (Table 5).

3.5. Associations of the Change in Myocardial Function and Baseline Variables. There were no associations between changes in cardiac function and the baseline clinical

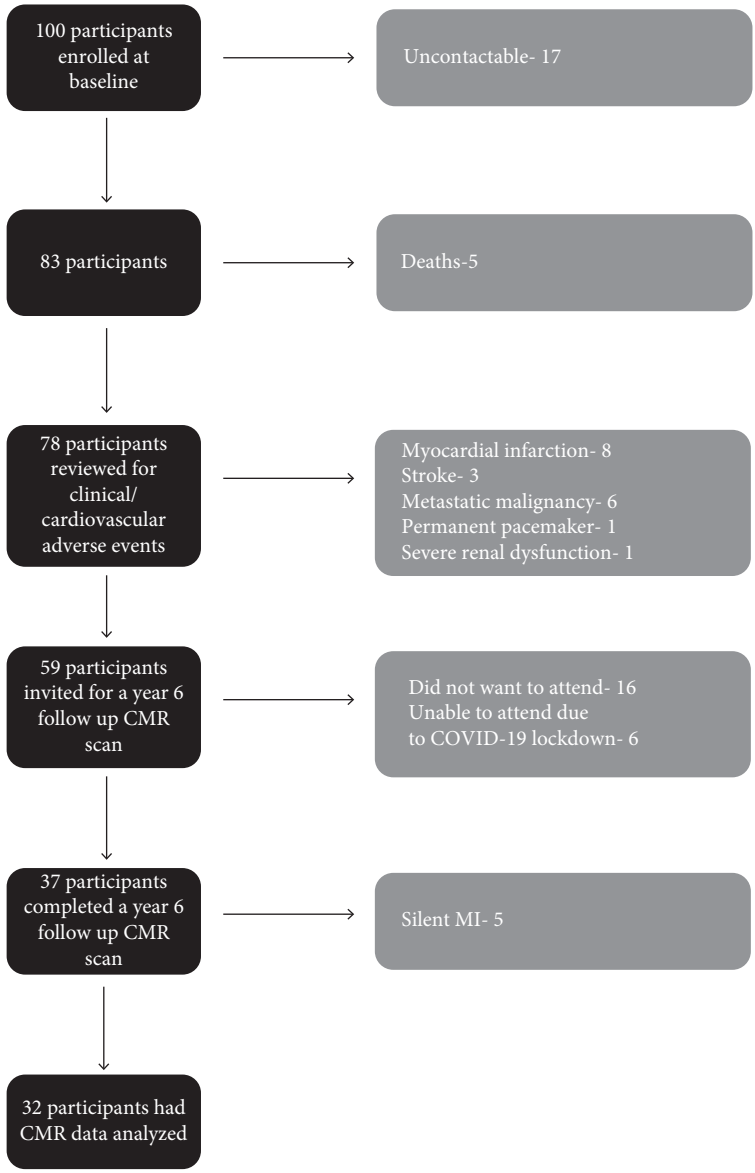

Figure 2: Recruitment flowchart. Recruitment flowchart demonstrating recruitment and follow-up pathway for the participants (CMR-cardiac magnetic resonance; COVID-19-coronavirus disease; MI-myocardial infarction).

variables. Although there were also no associations between laboratory variables of glucose management or NT-proBNP, there was a significant correlation between the change in LVEF and baseline plasma hs-cTnT ($R = -0.44$, $p = 0.01$). There was no such association for change in RVEF.

4. Discussion

Despite the epidemiologically established link between T2D and congestive cardiac failure [2], longitudinal cardiac structural and functional changes in asymptomatic patients with T2D who remain free of cardiovascular events have not been explored before. In a cohort of ethnically diverse, asymptomatic patients with T2D with no history of prior cardiovascular disease, this study has shown for the first time that T2D is associated with clinically relevant adverse changes in biventricular function at follow-up after 6 years even in the absence of cardiovascular events, cardiac ischemia, or other predisposing factors such as hypertension. The present data have also shown that baseline glucose control seems to have no effect, although plasma hs-cTnT does predict the magnitude of the subsequent change in LVEF. Finally, underscoring the prognostic relevance of changes in LV mass and LV geometry in diabetes, this study has also shown higher LV mass and greater LV concentric remodeling at baseline in patients who experienced MACE during the follow-up compared to those who remained asymptomatic and event free. There were no other significant differences in clinical or biochemical variables between the two groups, suggesting that the adverse cardiovascular events in T2D are not limited to patients with poor glycemic, BP, or weight control.

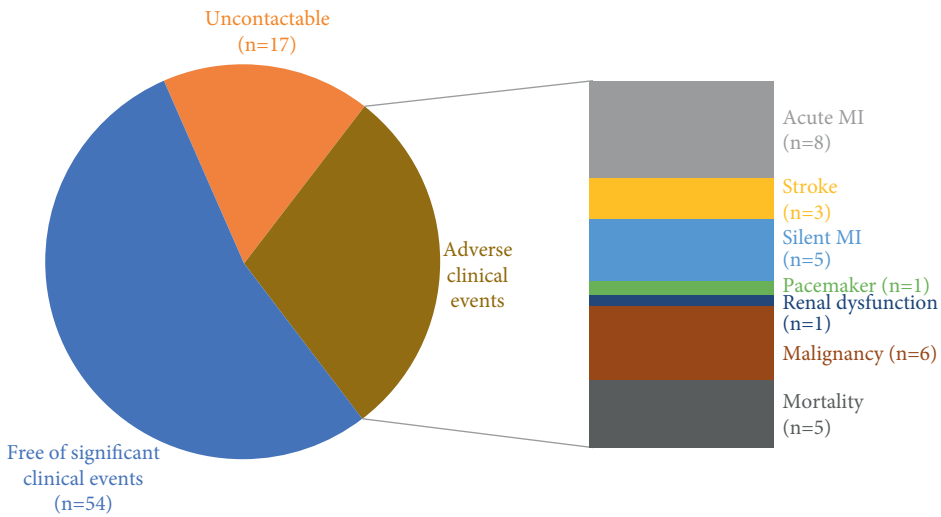

Figure 3: Major adverse cardiovascular event rates. The major adverse cardiovascular event rate (MI, angina, revascularization, CVA, and death) during the 6-year follow-up period, including the patients with a silent MI, amounted to 25% in this study with an overall clinical event rate of 35%.

Table 2: Clinical and biochemical characteristics of the participants who had baseline and year 6 follow-up CMR scans.

Variable	Baseline ($n = 32$)	Follow-up ($n = 32$)	P value
Age, years	58 ± 11	64 ± 11	0.03*
BMI, kg/m^2	28 ± 4	27 ± 4	0.1
Male, n (%)	29 (91)	29 (91)	1.0
Smoker, n (%)	1 (3)	2(6)	0.6
Diabetes duration, years	5.1 ± 1.2	10.9 ± 1.3	0.0001*
Heart rate, bpm	72 ± 13	68 ± 12	0.3
Systolic blood pressure, mmHg	131 ± 16	129 ± 16	0.7
Diastolic blood pressure, mmHg	73 ± 10	74 ± 7	0.4
Plasma fasting glucose, mmol/L	8.5 ± 3.5	9.4 ± 3.8	0.3
Glycated hemoglobin, mmol/mol	61 ± 15	64 ± 18	0.13
hs-cTnT, ng/ml	7.35 ± 5.14	—	
Total cholesterol, mmol/L	4.5 ± 1.3	4.5 ± 1.2	1.0
HDL, mmol/L	1.24 ± 0.31	1.36 ± 0.38	0.2
LDL, mmol/L	2.86 ± 1.19	2.59 ± 1.21	0.4
Medications n (%)			
Metformin, n (%)	28 (88)	22 (69)	0.01*
Sulfonylurea, n (%)	12 (38)	13 (40)	0.3
Gliptin, n (%)	3 (9)	7 (22)	0.1
Thiazolidinediones, n (%)	0	2 (6)	0.1
SGLT2 inhibitors, n (%)	0	4 (12)	0.03*
Aspirin, n (%)	7 (22)	9 (28)	0.1
Statin, n (%)	22 (69)	23 (72)	0.3
ACEI, n (%)	0 (0)	13 (40)	0.0001*
ARB, n (%)	0 (0)	3 (9)	0.08

Values are mean ± standard deviations or percentages. *signifies $P \leq 0.05$. CMR-cardiovascular magnetic resonance imaging; n-numbers; BMI-body mass index; kg-kilogram; m-meter; bpm-beats per minute; mmHg-millimeters of mercury; mmol-millimoles; L-liters; mol-moles; hs-cTnT-high-sensitivity cardiac troponin-T; ng-nanograms; HDL-high-density lipoprotein; LDL-low-density lipoprotein; SGLT2-sodium glucose cotransporter 2; ACEI-angiotensin-converting enzyme inhibitor; ARB-angiotensin receptor blocker.

4.1. Longitudinal Morphological Alterations in Type 2 Diabetes. Our results show that cardiac size and mass decrease over time in patients with T2D, while biventricular function deteriorates. In contrast to our findings in patients with T2D, in healthy aging LVEF remains static or increases over time as shown by multiple studies [15–19].

In this study, in 30% of the patients on the year 6 CMR scan, LVEF levels dropped below the normal range (<50%) despite the asymptomatic status of these patients [20]. Supporting our findings, multiple studies showed that even in asymptomatic individuals with T2D, there is a high prevalence of LV systolic and diastolic dysfunction [10, 21]. The American Heart Association has classified

Table 3: CMR findings.

Variable	Baseline ($n = 32$)	Follow-up ($n = 32$)	P value
LV end-diastolic volume (ml)	159 ± 29	145 ± 22	0.005*
LV end-diastolic volume index (ml/m^2)	78 ± 12	73 ± 10	0.02*
LV end-systolic volume (ml)	64 ± 16	65 ± 19	0.5
LV end-systolic volume index (ml/m^2)	31 ± 7	33 ± 9	0.3
LV stroke volume (ml)	95 ± 20	80 ± 14	0.001*
LV ejection fraction (%)	60 ± 7	55 ± 8	0.0001*
ΔLVEF (%)		−(5.66 ± 4.38)	
LV mass (gm)	102 ± 17	94 ± 16	0.01*
LV mass index (gm/m^2)	51 ± 8	47 ± 8	0.04*
LV mass to LV end-diastolic volume (gm/ml)	0.65 ± 0.12	0.66 ± 0.14	0.8
Global longitudinal strain (%, negative)	13.06 ± 2.05	11.74 ± 2.54	0.8
Peak diastolic circumferential strain rate (1/s)	0.98 ± 0.28	1.04 ± 0.23	0.4
Peak diastolic longitudinal strain rate (1/s)	0.86 ± 0.19	0.69 ± 0.17	0.1
RV end-diastolic volume (ml)	166 ± 33	142 ± 25	0.03*
RV end-diastolic volume index (ml/m^2)	82 ± 14	71 ± 12	0.0001*
RV end-systolic volume (ml)	76 ± 18	70 ± 16	0.05*
RV end-systolic volume index (ml/m^2)	37 ± 8	35 ± 8	0.1
RV stroke volume (ml)	91 ± 20	72 ± 15	<0.0001*
RV ejection fraction (%)	55 ± 5	51 ± 7	0.003*
ΔRVEF (%)		−(6.69 ± 4.15)	
LA maximum volume (ml)	88 ± 17	67 ± 21	0.0001*
LA ejection fraction (%)	58 ± 6	56 ± 9	0.4
Extracellular volume (%)	24.96 ± 3.02	24.10 ± 2.66	0.3

Values are mean±standard deviations or percentages. *signifies $P \leq 0.05$. CMR-cardiac magnetic resonance imaging; n-numbers; LV-left ventricle; ml-milliliters; m-meter; ΔLVEF-change in LV ejection fraction; gm-grams; s-seconds; RV-right ventricle; ΔRVEF-change in RV ejection fraction; LA-left atrium.

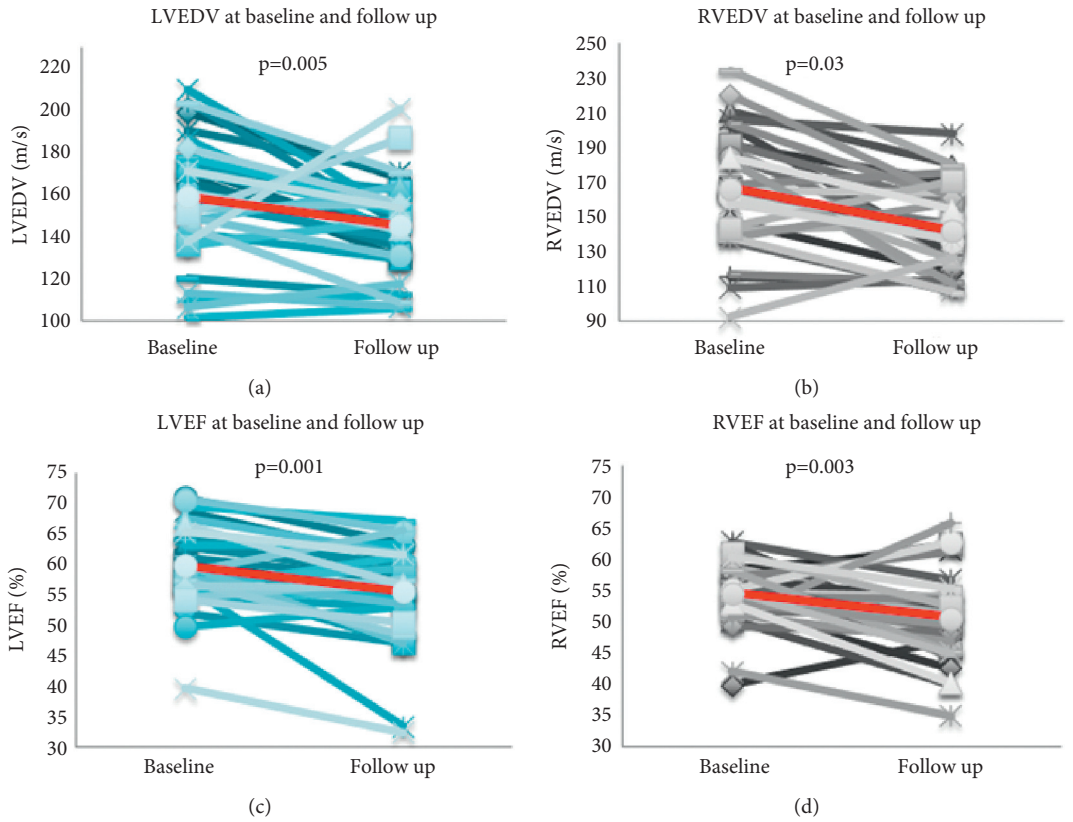

Figure 4: Continued.

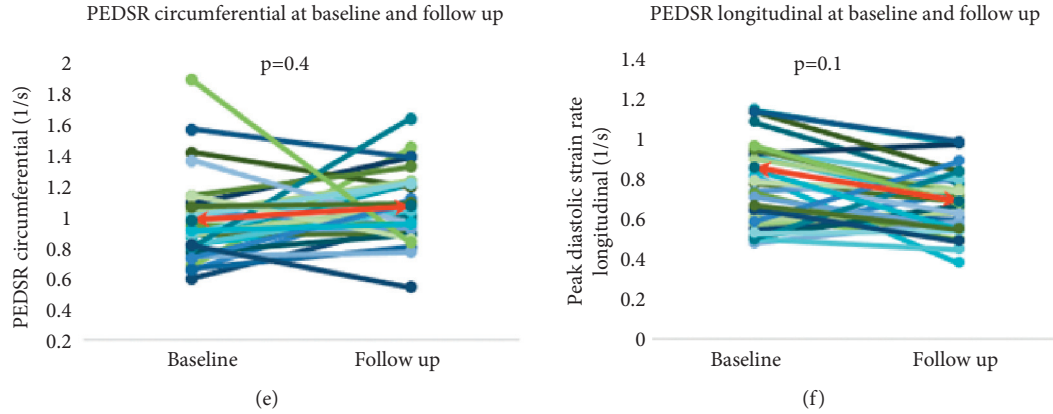

Figure 4: Comparison of imaging parameters at baseline and follow-up. Comparison between the left ventricular end-diastolic volume (LVEDV), right ventricular end-diastolic volume (RVEDV), left ventricular ejection fraction (LVEF), right ventricular ejection fraction (RVEF), peak diastolic strain rate (PEDSR) circumferential and PEDSR longitudinal at baseline, and year 6 follow-up scans (line in red indicates mean values for each variable).

Table 4: Clinical and biochemical characteristics at baseline of the participants with and without MACE (angina, myocardial infarction, revascularization, and cerebrovascular accident) at follow-up.

Variable	No MACE ($n = 65$)	MACE ($n = 18$)	P value
Age, years	66 ± 11	65 ± 9	0.7
BMI (baseline), kg/m^2	29 ± 4	28 ± 3	0.3
Male, %	55 (85)	17 (94)	0.2
Diabetes duration, years	9.9 ± 4.6	10.6 ± 3.8	0.6
Smoker, *n* (%)	6 (10)	6 (33)	0.01*
Systolic blood pressure, mmHg	131 ± 15	132 ± 14	0.8
Diastolic blood pressure, mmHg	72 ± 9	74 ± 9	0.4
Glycated hemoglobin, mmol/mol	62 ± 21	71 ± 20	0.1
Troponin T, ng/L	7.6 ± 5.8	7.0 ± 3.6	0.7
NT-proBNP, pg/ml	72 ± 129	39 ± 42	0.3
Total cholesterol, mmol/L	4.3 ± 1.1	4.6 ± 1.3	0.3
LDL, mmol/L	2.6 ± 0.9	2.7 ± 1.6	0.7
Medications, *n* (%)			
Metformin, *n* (%)	57 (88)	15 (83)	0.6
Sulfonylurea, *n* (%)	21 (32)	6 (33)	0.9
Gliptins, *n* (%)	7 (11)	4 (22)	0.2
Thiazolidinediones, *n* (%)	0 (0)	0 (0)	—
SGLT2 inhibitors, *n* (%)	0 (0)	0 (0)	—
Aspirin, *n* (%)	15 (23)	3 (17)	0.6
Statin, *n* (%)	47 (72)	13 (72)	0.9
ACE-I, *n* (%)	0 (0)	0 (0)	—
ARB, *n* (%)	0 (0)	0 (0)	—
Beta-blockers, *n* (%)	3 (4)	1 (5)	0.9
Calcium channel blockers, *n* (%)	6 (8)	3 (17)	0.4

Values are mean ± standard deviations or percentages. *signifies $P \leq 0.05$. MACE-major adverse cardiovascular events; n-numbers; BMI-body mass index; kg-kilograms; m-meters; mmHg-millimeters of mercury; mmol-millimoles, mol-moles; ng-nanograms; L-liters; NT-pro BNP-N-terminal prohormone B-type natriuretic peptide; pg-picograms; ml-milliliters; LDL-low-density lipoprotein; SGLT2-sodium-glucose cotransporter 2; ACE-I-angiotensin-converting enzyme inhibitor; ARB-angiotensin receptor blocker.

asymptomatic individuals with impaired cardiac function as having stage B HF [22]. These patients remain at risk for significant cardiovascular morbidity and mortality and experience a 5-fold increase in the risk of subsequent symptomatic HF development [23]. As stage B HF is a precursor to clinical HF, earlier identification of the cardiovascular manifestations of stage B HF may permit earlier diagnosis and treatment of patients at higher risk.

4.2. Relationship of Glycemic Control, Blood Pressure Control, Body Weight Changes, and Longitudinal Cardiac Functional Changes in Type 2 Diabetes. There were no changes in mean HbA1c, systolic and diastolic BP, resting HR, or BMI at follow-up. Moreover, we detected no relationship between the baseline systolic or diastolic BP, HR, BMI, HBA1c, and glucose levels with the change in LVEF and RVEF over time (ΔLVEF and ΔRVEF, respectively). This lack of

Table 5: CMR findings at baseline of the participants with and without MACE (angina, myocardial infarction, revascularization, and cerebrovascular accident) at follow-up.

	No MACE ($n = 65$)	MACE ($n = 18$)	P value
LV end-diastolic volume (ml)	146 ± 35	147 ± 35	0.9
LV end-diastolic volume index (ml/m^2)	73 ± 15	72 ± 14	0.8
LV end-systolic volume (ml)	59 ± 21	58 ± 22	0.9
LV end-systolic volume index (ml/m^2)	29 ± 9	28 ± 9	0.9
LV stroke volume (ml)	87 ± 20	89 ± 16	0.7
LV ejection fraction (%)	60 ± 7	61 ± 6	0.6
LV mass (gm)	102 ± 23	116 ± 25	0.02*
LV mass index (gm/m^2)	51 ± 9	57 ± 10	0.01*
LV mass to LV end-diastolic volume (gm/ml)	0.72 ± 0.13	0.79 ± 0.15	0.05*
RV end-diastolic volume (ml)	151 ± 37	147 ± 31	0.6
RV end-diastolic volume index (ml/m^2)	76 ± 17	72 ± 14	0.3
RV end-systolic volume (ml)	68 ± 21	67 ± 17	0.8
RV end-systolic volume index (ml/m^2)	34 ± 10	33 ± 7	0.7
RV stroke volume (ml)	83 ± 19	80 ± 19	0.5
RV ejection fraction (%)	55 ± 5	54 ± 7	0.5

Values are mean± standard deviations or percentages. *signifies $P \leq 0.05$. CMR-cardiovascular magnetic resonance; MACE-major adverse cardiovascular events; LV-left ventricle; ml-milliliters, m-meter; gm-grams; RV-right ventricle.

association between glycemic control and cardiac functional decline supports the notion that there are more central mechanisms to HF pathophysiology in diabetes than glycemic control. While a few studies demonstrated a positive impact of metabolic control on ventricular function [24, 25], most previous studies failed to demonstrate any favorable changes in cardiac function despite improvements in glycemic control [26, 27]. Interestingly, we have not detected any significant changes in the diastolic function in this cohort despite the aging process. This is likely to be a consequence of the normotensive status of the cohort at baseline with no significant changes in systolic or diastolic BP assessments over time despite the aging process.

4.3. Relationship of Plasma Biomarkers (High-Sensitivity Cardiac Troponin T and N Terminal Pro B-type Natriuretic Peptide) and Longitudinal Cardiac Functional Changes in Type 2 Diabetes. High-sensitivity cardiac troponin isoforms are unique to the cardiac myocyte and are objective, quantifiable, and sensitive biomarkers for detecting cardiac injury [28]. They are predictors of cardiovascular morbidity and mortality risk in population-based studies besides their role as the cornerstone for the diagnosis of acute myocardial infarction [29]. We show in this study for the first time that there is a significant association between the plasma hs-cTnT measured at baseline with change in LVEF over time, highlighting a potentially important role for hs-cTnT as a biomarker for assessing HF risk in patients with T2D. A recent study has shown that lifestyle factors, such as smoking, diet, and physical activity, are associated with changes in high-sensitivity cardiac troponin levels, suggesting that lifestyle modifications may be able to affect changes in troponin and be beneficial in reducing mortality risk. As an easily obtainable plasma biomarker, hs-cTnT may be of great assistance in the incremental risk stratification of patients with T2D into high-risk and low-risk subgroups [28].

Our study does not suggest a similar role for NT-proBNP in asymptomatic patients with T2D with no known cardiovascular disease. A previous diabetic study did, however, demonstrate an independent correlation of NT-proBNP with the short-term prognosis of cardiovascular events [30]. The discrepancy between the two studies might have resulted from the distinct populations investigated. While Huelsmann et al. [30] have not excluded symptomatic patients, patients with ischemic heart disease, AF, or other significant cardiovascular diseases, in order to better characterize the occult heart disease in diabetes we have excluded these comorbidities and symptomatic patients.

4.4. Left Ventricular Geometry and Major Adverse Cardiovascular Events in Type 2 Diabetes. LV mass is a strong and independent predictor of subsequent cardiovascular events, including myocardial infarction, HF, and mortality [31]. While the precise underlying mechanism of LV hypertrophy and concentric LV remodeling in the absence of significant hypertension remains unclear, it has been suggested that T2D induces LV mass enlargement through metabolic, and not hemodynamic pathways [32]. Supporting this, a recent study has shown that treatment with selective SGLT2 inhibitor empagliflozin was associated with significant reductions in LV mass, which may account in part for the beneficial cardiovascular outcomes of empagliflozin [33].

5. Study Limitations

The present data are in a modest number of patients, recruited to a single study site. The study was not powered to assess the potential association of the treatments and the CMR findings with regression analysis. However, the longitudinal nature of the study allowed paired analysis of images that, to minimize bias, were randomized in time and by subject. Moreover, the image data of a random sample of subjects were evaluated by two investigators to demonstrate good inter- and intraobserver reproducibility.

Another limitation is the small number of female participants as only a smaller proportion agreed to return for a second scan. While diabetes has been consistently found to be a stronger risk factor for heart disease in women compared to men [2], in this study we show that biventricular reductions in systolic function occur over time even in a predominantly male population.

6. Conclusions

Even in the absence of overt clinical CAD, significant valvular disease, uncontrolled hypertension, or change in BMI, T2D resulted in a significant reduction in cardiac size and biventricular systolic function over time. Plasma hs-cTnT measured at baseline was associated with the magnitude of change in LV systolic function suggesting that hs-cTnT could play a role in identifying patients with T2D at higher risk for heart failure. Patients who experienced MACE during the follow-up exhibited higher LV mass and greater LV concentric remodeling at baseline compared to those who remained asymptomatic and event free.

Abbreviations List

ACEI:	Angiotensin-converting enzyme inhibitor
ARB:	Angiotensin receptor blocker
AF:	Atrial fibrillation
BMI:	Body mass index
BP:	Blood pressure
CAD:	Coronary artery disease
CMR:	Cardiovascular magnetic resonance imaging
ECG:	Electrocardiogram
ECV:	Extracellular volume fraction
EF:	Ejection fraction
eGFR:	Estimated glomerular filtration rate
HBA1c:	Glycated hemoglobin
HDL:	High-density lipoprotein
HF:	Heart failure
hs-cTnT:	High-sensitivity cardiac troponin T
IQR:	Interquartile range
LA:	Left atrial
LGE:	Late gadolinium enhancement
LV:	Left ventricular
LVEDV:	Left ventricular end-diastolic volume
LVEF:	Left ventricular ejection fraction
MACE:	Major adverse cardiovascular events
NT-proBNP:	N-terminal prohormone B-type natriuretic peptide
PEDSR:	Peak early diastolic strain rate
RVEF:	Right ventricular ejection fraction
SGLT2:	Sodium-glucose cotransporter-2
SSFP:	Steady-state free precession
T2D:	Type 2 diabetes.

Data Availability

Data can be made available on request through e-mail to the corresponding author.

Additional Points

Clinical Perspectives. Competency in Medical Knowledge: in the absence of overt clinical coronary artery disease, uncontrolled hypertension, change in BMI, or HbA1c, T2D results in significant reductions in cardiac size and biventricular systolic function over time. There is a significant correlation of the change in cardiac function with baseline plasma hs-cTnT. Plasma hs-cTnT could, therefore, potentially serve as a screening tool to identify patients with T2D at higher heart failure risk. Translational Outlook 1: larger studies are needed to further delineate the relationship between plasma hs-cTnT with the risk of developing cardiac dysfunction in patients with T2D. As an easily obtainable plasma biomarker, hs-cTnT may be of use in the incremental risk stratification of patients with T2D into high- and low-risk subgroups and to translate prognostic projections into individualized management plans to address the excess heart failure risk in diabetes. Translational Outlook 2: the data from this study suggest that patients with T2D with higher LV mass and LV concentric remodeling might be at a higher risk of MACE. Aggressively targeting risk factors in patients with T2D with higher LV mass and/or LV concentric remodeling might lead to improved cardiovascular outcomes.

Disclosure

This research project has been presented in the form of an abstract at the British Cardiovascular Society Virtual Annual Conference "Cardiology and the Environment" 7–10 June 2021.

Conflicts of Interest

The authors declare no conflicts of interest.

Authors' Contributions

AC contributed to subject recruitment and data acquisition, analysis, and interpretation; drafting of manuscript; and revisions. NJ and ST contributed to data analysis, data interpretation, and manuscript revision. AA contributed to data acquisition and data analysis. PS contributed to data acquisition, data interpretation, and manuscript revision. AC, AM NH, LA, MJ, TC, NS, AD, CEDS, AS, LR, RC, KW, and JG contributed to data interpretation and manuscript revision. SP contributed to study conception and design, data interpretation, drafting of manuscript and revisions, and study supervision. EL contributed to study conception and design, data acquisition, analysis and interpretation, drafting of manuscript, revisions, and study supervision.

Acknowledgments

The studies were supported by the British Heart Foundation (RG.DOBI.107805) and the Wellcome Trust (207726/Z/17/Z). AC was funded by the British Heart Foundation on a Clinical Research Training Fellowship (FS/CRTF/20/24003).

EL was funded by the Wellcome Trust Clinical Career Development Fellowship (221690/Z/20/Z)

References

[1] WHO, *Fact Sheet No 310; the Top 10 Causes of Death*, World Health Organization, Geneva, Switzerland, 2014.

[2] W. B. Kannel and D. L. McGee, "Diabetes and cardiovascular disease: the framingham study," *JAMA*, vol. 241, no. 19, pp. 2035–2038, 1979.

[3] A. D. Shah, C. Langenberg, E. Rapsomaniki et al., "Type 2 diabetes and incidence of cardiovascular diseases: a cohort study in 1·9 million people," *The Lancet Diabetes & Endocrinology*, vol. 3, no. 2, pp. 105–113, 2015.

[4] M. J. Garcia, P. M. McNamara, T. Gordon, and W. B. Kannell, "Morbidity and mortality in diabetics in the framingham population. Sixteen year follow-up study," *Diabetes*, vol. 23, no. 2, pp. 105–111, 1974.

[5] P. M. Okin, R. B. Devereux, K. E. Harris et al., "In-treatment resolution or absence of electrocardiographic left ventricular hypertrophy is associated with decreased incidence of new-onset diabetes mellitus in hypertensive patients," *Hypertension*, vol. 50, no. 5, pp. 984–990, 2007.

[6] B. M. Brenner, M. E. Cooper, D. de Zeeuw et al., "Effects of losartan on renal and cardiovascular outcomes in patients with type 2 diabetes and nephropathy," *New England Journal of Medicine*, vol. 345, no. 12, pp. 861–869, 2001.

[7] J. Hippisley-Cox and C. Coupland, "Diabetes treatments and risk of heart failure, cardiovascular disease, and all cause mortality: cohort study in primary care," *BMJ*, vol. 354, 2016.

[8] L. E. Hudsmith, S. E. Petersen, D. J. Tyler et al., "Determination of cardiac volumes and mass with FLASH and SSFP cine sequences at 1.5 vs. 3 Tesla: a validation study," *Journal of Magnetic Resonance Imaging*, vol. 24, no. 2, pp. 312–318, 2006.

[9] E. Levelt, M. Mahmod, S. K. Piechnik et al., "Relationship between left ventricular structural and metabolic remodeling in type 2 diabetes," *Diabetes*, vol. 65, no. 1, pp. 44–52, 2016.

[10] G. S. Gulsin, D. J. Swarbrick, W. H. Hunt et al., "Relation of aortic stiffness to left ventricular remodeling in younger adults with type 2 diabetes," *Diabetes*, vol. 67, no. 7, pp. 1395–1400, 2018.

[11] P. P. Swoboda, A. K. McDiarmid, B. Erhayiem et al., "Diabetes mellitus, microalbuminuria, and subclinical cardiac disease: identification and monitoring of individuals at risk of heart failure," *Journal of the American Heart Association*, vol. 6, Article ID e005539, 2017.

[12] P. A. Swoboda, B. Erhayiem, R. Kan et al., "Cardiovascular magnetic resonance measures of aortic stiffness in asymptomatic patients with type 2 diabetes: association with glycaemic control and clinical outcomes," *Cardiovascular Diabetology*, vol. 17, 2018.

[13] K. G. M. M. Alberti and P. Z. Zimmet, "Definition, diagnosis and classification of diabetes mellitus and its complications. Part 1: diagnosis and classification of diabetes mellitus. Provisional report of a WHO consultation," *Diabetic Medicine*, vol. 15, no. 7, pp. 539–553, 1998.

[14] P. Kellman, M. S. Hansen, S. Nielles-Vallespin et al., "Myocardial perfusion cardiovascular magnetic resonance: optimized dual sequence and reconstruction for quantification," *Journal of Cardiovascular Magnetic Resonance*, vol. 19, no. 1, p. 43, 2017.

[15] S. P. Schulman, E. G. Lakatta, J. L. Fleg et al., "Age-related decline in left ventricular filling at rest and exercise," *The American Journal of Physiology*, vol. 263, pp. H1932–H1938, 1992.

[16] F. F. Gong, J. M. Coller, M. McGrady et al., "Age-related longitudinal change in cardiac structure and function in adults at increased cardiovascular risk," *ESC Heart Failure*, vol. 7, no. 3, pp. 1344–1361, 2020.

[17] S. Cheng, V. R. Fernandes, D. A. Bluemke, R. L. McClelland, R. A. Kronmal, and J. A. Lima, "Age-related left ventricular remodeling and associated risk for cardiovascular outcomes: the multi-ethnic study of atherosclerosis," *Circulation: Cardiovascular Imaging*, vol. 2, no. 3, pp. 191–198, 2009.

[18] C. Gebhard, B. E. Stähli, C. E. Gebhard et al., "Age- and gender-dependent left ventricular remodeling," *Echocardiography*, vol. 30, no. 10, pp. 1143–1150, 2013.

[19] S. Kou, L. Caballero, R. Dulgheru et al., "Echocardiographic reference ranges for normal cardiac chamber size: results from the NORRE study," *European Heart Journal Cardiovascular Imaging*, vol. 15, no. 6, pp. 680–90, 2014.

[20] N. Kawel-Boehm, A. Maceira, E. R. Valsangiacomo-Buechel et al., "Normal values for cardiovascular magnetic resonance in adults and children," *Journal of Cardiovascular Magnetic Resonance*, vol. 17, no. 1, p. 29, 2015.

[21] J. K. Boyer, S. Thanigaraj, K. B. Schechtman, and J. E. Pérez, "Prevalence of ventricular diastolic dysfunction in asymptomatic, normotensive patients with diabetes mellitus," *The American Journal of Cardiology*, vol. 93, no. 7, pp. 870–875, 2004.

[22] L. R. Goldberg and M. Jessup, "Stage B heart failure," *Circulation*, vol. 113, no. 24, pp. 2851–2860, 2006.

[23] T. J. Wang, J. C. Evans, E. J. Benjamin, D. Levy, E. C. LeRoy, and R. S. Vasan, "Natural history of asymptomatic left ventricular systolic dysfunction in the community," *Circulation*, vol. 108, no. 8, pp. 977–982, 2003.

[24] M. Leung, V. W. Wong, M. Hudson, and D. Y. Leung, "Impact of improved glycemic control on cardiac function in type 2 diabetes mellitus," *Circulation: Cardiovascular Imaging*, vol. 9, Article ID e003643, 2016.

[25] H. von Bibra, A. Hansen, V. Dounis, T. Bystedt, K. Malmberg, and L. Rydén, "Augmented metabolic control improves myocardial diastolic function and perfusion in patients with non-insulin dependent diabetes," *Heart*, vol. 90, no. 12, pp. 1483-1484, 2004.

[26] K. K. Naka, K. Pappas, K. Papathanassiou et al., "Lack of effects of pioglitazone on cardiac function in patients with type 2 diabetes and evidence of left ventricular diastolic dysfunction: a tissue doppler imaging study," *Cardiovascular Diabetology*, vol. 9, p. 57, 2010.

[27] C. Jarnert, L. Landstedt-Hallin, K. Malmberg et al., "A randomized trial of the impact of strict glycaemic control on myocardial diastolic function and perfusion reserve: a report from the DADD (diabetes mellitus and diastolic dysfunction) study," *European Journal of Heart Failure*, vol. 11, no. 1, pp. 39–47, 2009.

[28] M. Gori, D. K. Gupta, B. Claggett et al., "Natriuretic peptide and high-sensitivity troponin for cardiovascular risk prediction in diabetes: the atherosclerosis risk in communities (ARIC) study," *Diabetes Care*, vol. 39, no. 5, pp. 677–685, 2016.

[29] X. Jia, W. Sun, R. C. Hoogeveen et al., "High-sensitivity troponin I and incident coronary events, stroke, heart failure hospitalization, and mortality in the ARIC study," *Circulation*, vol. 139, no. 23, pp. 2642–2653, 2019.

[30] M. Huelsmann, S. Neuhold, G. Strunk et al., "NT-proBNP has a high negative predictive value to rule-out short-term

cardiovascular events in patients with diabetes mellitus," *European Heart Journal*, vol. 29, no. 18, pp. 2259–2264, 2008.

[31] B. A. Vakili, P. M. Okin, and R. B. Devereux, "Prognostic implications of left ventricular hypertrophy," *American Heart Journal*, vol. 141, no. 3, pp. 334–341, 2001.

[32] J. P. Seferovic, M. Tesic, P. M. Seferovic et al., "Increased left ventricular mass index is present in patients with type 2 diabetes without ischemic heart disease," *Scientific Reports*, vol. 8, no. 1, p. 926, 2018.

[33] S. Verma, C. D. Mazer, A. T. Yan et al., "Effect of empagliflozin on left ventricular mass in patients with type 2 diabetes mellitus and coronary artery disease," *Circulation*, vol. 140, no. 21, pp. 1693–1702, 2019.

Hindawi
Cardiology Research and Practice
Volume 2021, Article ID 2045493, 8 pages
https://doi.org/10.1155/2021/2045493

Research Article

The Auxiliary Role of Cardiac Magnetic Resonance Feature-Tracking Parameters in the Differentiation between Cardiac Amyloidosis and Constrictive Pericarditis

Sanaz Asadian,[1] **Mahta Farzin**,[2] **Faezeh Tabesh**,[1] **Nahid Rezaeian**,[1] **Hooman Bakhshandeh**,[1] **Leila Hosseini**,[3] **Yaser Tolouei tabar**,[1] **and Mohammad Mehdi Hemmati Komasi**[2]

[1]*Rajaie Cardiovascular Medical and Research Center, Iran University of Medical Sciences, Tehran, Iran*
[2]*Iran University of Medical Sciences, Tehran, Iran*
[3]*North Khorasan University of Medical Sciences, Bojnurd, Iran*

Correspondence should be addressed to Nahid Rezaeian; nahid6069@yahoo.com

Received 11 August 2021; Revised 30 September 2021; Accepted 18 October 2021; Published 23 October 2021

Academic Editor: George Bazoukis

Objectives. Cardiac amyloidosis (CA) and constrictive pericarditis (CP) are described as the differential diagnoses of restrictive hemodynamic alterations of the heart. We aimed to explain cardiac magnetic resonance (CMR) imaging findings (especially feature tracking (FT)) of CA and CP cases and compare them with healthy controls. Moreover, we evaluated the role of biventricular FT parameters in differentiating CA from CP. *Methods*. Thirty-eight patients who underwent CMR between February 2016 and January 2018 with the ultimate diagnosis of CA (19 patients) or CP (19 patients) were enrolled. We included biopsy-proven light-chain amyloidosis patients. The data of 28 healthy controls were utilized for comparison. The patients were followed up for 8–23 months to register mortality and their surveillance. All CMR morphological and functional data, including FT parameters, were recorded and analyzed. *Results*. Of only 13/19 (68.4%) CA patients who had the follow-up data, 11/13 (84.6%) died. One of The CP patients (5.3%) expired during the follow-up. Significant between-group differences were noted concerning the biventricular ejection fraction as well as global longitudinal, circumferential, and radial strain values ($Ps < 0.001$). The left ventricular (LV) global longitudinal strain (GLS) ≤10% was detected in 13/19 (68.4%) of the CA and 1/19 (5.3%) of CP cases ($P < 0.001$). A significant difference between the mean value of the LVGLS and LV global circumferential strain (GCS) of the basal LV level compared to the mid and apical levels was observed ($Ps < 0.001$) in the CA patients. The differences between the mean LVGLS and the GCS measures of the mid and apical LV levels were not significant ($P = 1$ and $P = 0.06$, respectively). *Conclusions*. In our study, CA and CP severely disrupted ventricular strains. Biventricular GLS was meaningfully lower in the CA subjects. Therefore, strain analysis, especially in the longitudinal direction, could be helpful to differentiate CA from CP.

1. Introduction

Cardiomyopathies, which are commonly classified based on structural and hemodynamic criteria, are subdivided into dilated, hypertrophic, restrictive (RCM), arrhythmogenic, infiltrative, and ischemic types [1]. RCM is an uncommon type of cardiomyopathy resulting in myocardial stiffness and impaired ventricular filling [2]. Its pathophysiologic basis may be hereditary, acquired, or a combination of both.

One of the chief causes of RCM is cardiac amyloidosis (CA). Amyloidosis is a multisystem disorder in which an unstable and misfolded protein (amyloid) aggregates in different organs [1]. The 2 main types of amyloidosis that affect the heart are light-chain and transthyretin amyloidosis. Amyloid infiltration of the heart results in the thickening of the myocardium and diastolic dysfunction, which ultimately leads to heart failure. The prognosis is largely determined by the occurrence and extent of myocardial involvement [3–6].

A traditional well-known differential diagnosis for CA is constrictive pericarditis (CP). Cardiac surgeries and inflammatory/infectious processes are among the most common causes of CP. Both CA and CP present insidiously and have many imaging features in common [7]. The distinction between these 2 conditions is critical because CP is a curable disease with cardiac surgery, whereas the therapeutic options for CA are more challenging [8].

Cardiac magnetic resonance (CMR) imaging can assist in the differentiation of CA from CP [2, 8]. Utilizing its tissue-characterization capability consisting of late gadolinium enhancement (LGE) study, CMR may play a fundamental role in the diagnosis and treatment guidance in CA. Moreover, it can limit the use of endomyocardial biopsy [9]. The tissue-characterization property of the CMR is helpful in the diagnosis of CP by demonstrating the thickening, edema, and enhancement of the pericardium. The conflict occurs in CP cases without the typical morphological imaging findings which hemodynamically mimic CA [10–12].

Recently developed CMR methods, consisting of mapping techniques and feature tracking (FT), contribute to the diagnosis of variable cardiomyopathies. Noncontrast T1 mapping is a highly accurate tool for the detection of the CA (especially AL subtype) with even more sensitivity comparing with the LGE images. Increased myocardial T1 value may be an indicator of amyloid deposition [13].

FT-CMR method has diagnostic potential in many cardiac disorders such as the different types of cardiomyopathies. This technique is contrast-free and is valuable in patients with the limitation in the administration of the gadolinium-based agents [14–18].

Speckle-tracking echocardiographic studies have demonstrated that strain values help differentiate between CA and CP. Patients with CP have markedly abnormal circumferential deformation with relative sparing of longitudinal strains, whereas CA is associated with abnormal longitudinal mechanics [8]. FT-CMR is a postprocessing technique that is widely used to assess global and regional myocardial function; however, there are scarce data on the role of FT-CMR in differentiating CP from CA [19].

In this study, we investigated CMR characteristics in 2 groups of CA and CP patients. We also compared the 2 groups with healthy controls. Ultimately, we determined FT-CMR capability in differentiating these 2 disorders.

2. Methods

2.1. Study Population. This retrospective study enrolled all patients who were referred to the imaging department of Rajaie Cardiovascular Medical and Research Center for CMR between February 2016 and January 2018 who were ultimately diagnosed with CA or CP. Nineteen patients with CA and 19 cases of CP were included. Moreover, the CMR data of 28 healthy controls with no signs or symptoms of a cardiac disease without any cardiovascular risk factors were utilized for comparison. Written informed consent was obtained from all the participants and in the case of death from their families. The study was approved by the Ethics Committee of Iran University of Medical Sciences.

All the CA patients had highly suspicious clinical and echocardiographic findings in addition to histologically proven (positive Congo red staining of endomyocardial, abdominal fat, renal, rectal, or bone marrow biopsies) amyloid light-chain amyloidosis. Moreover, CMR findings were characteristics of CA [20]. All our CP patients had typical imaging findings of the disease and underwent pericardiectomy during the follow-up, which confirmed the diagnosis.

All patients suffering from significant arrhythmia, undesirable CMR image quality, or inappropriate cine images for FT analysis were excluded. The follow-up continued for 8–23 months.

2.2. Cardiac Magnetic Resonance Imaging Protocol. A 1.5 T MRI machine (MAGNETOM Avanto, Siemens Healthcare, Erlangen, Germany) utilizing a vendor-supplied body surface coil was used to perform CMR studies. After axial, coronal, and sagittal localizer images were obtained, 2-, 3-, and 4-chamber, as well as short-axis cine steady-state free precession (SSFP) images, were acquired (slice thickness = 8 mm, field of view = 300 mm, no interslice gap; repetition time/echo time = 3–4/1.2 ms, imaging matrix = 156 × 192, voxel size = 1.9 × 1.6 × 7 mm, and "reported" repetition time (TR)≈31.5 ms) (Figure 1). Axial, coronal, and sagittal T1-weighted images were taken for all the CP patients to assess the pericardial thickness. The LGE sequence was obtained 10–15 minutes after the injection of 0.15 mmol/kg of Dotarem (gadoterate meglumine, Guerbet, Roissy CdG, France) in the same views as the functional images. LGE images were acquired using 2D phase-sensitive inversion recovery (PSIR) Turbo FLASH sequences (slice thickness = 8 mm, TR = 700 ms, time to echo (TE) = 5.4 ms, and flip angle = 25°).

The TI scout sequence was taken at the mid-ventricular level in the short-axis plane (slice thickness = 8 mm, TR = 20 ms, TE = 1.2 ms, flip angle = 50°, and produced with 20 ms increments from 85 to 805 ms). The inversion time applied for the LGE image was the time to the complete nulling of the myocardial signal at the TI scout sequence. LGE sequences were performed 10 minutes after TI scout image.

2.3. Image Interpretation

2.3.1. Blood Pool/Myocardial Nulling. On the TI scout sequence, the normal order of nulling is as follows: first, the contrast containing blood pool nulls, followed by the myocardium and the spleen. The nulling pattern was considered abnormal whenever the mentioned order was deranged [21].

2.3.2. LGE Assessment. The LGE pattern was divided into no enhancement, subendocardial, and transmural based on the visually assessed enhancement characteristics of our CA patients (Figure 2).

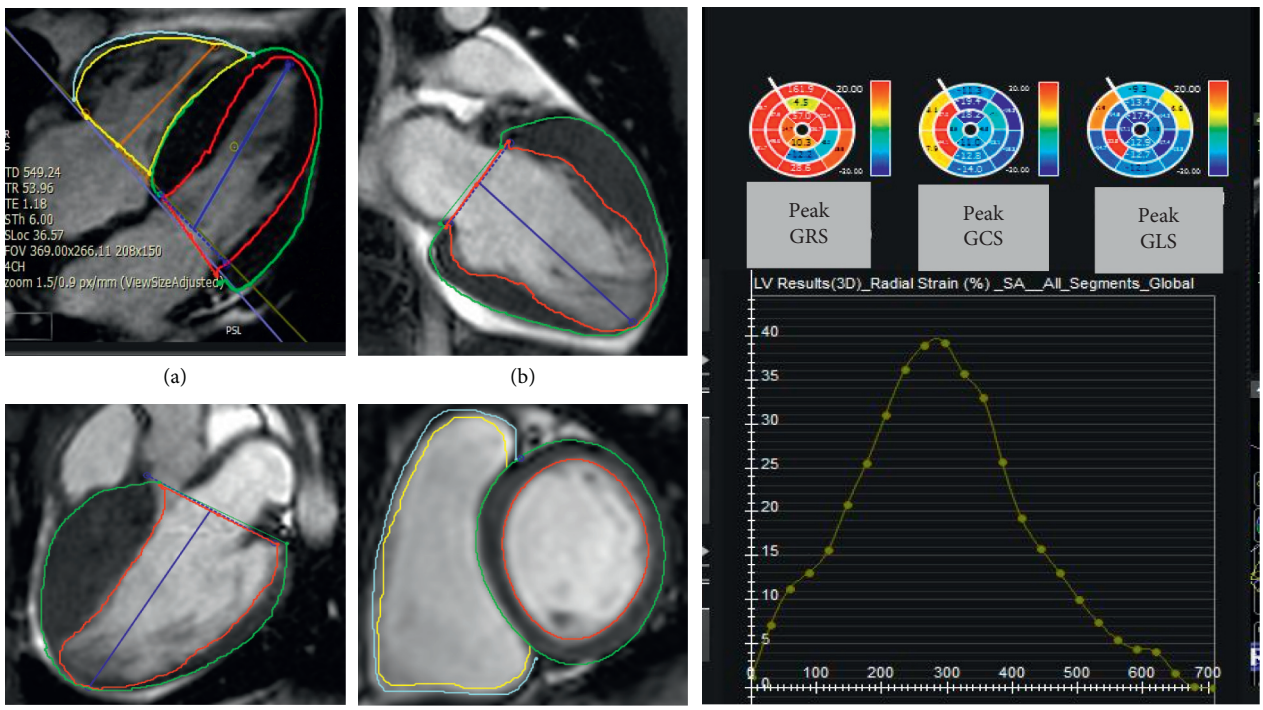

Figure 1: TheCMR feature tracking method for the analysis of myocardial strain. (a–d) Four-, two-, and three-chamber as well as short-axis cine functional images with defined endocardial and epicardial borders for strain analysis by feature-tracking cardiac magnetic resonance method. (e) Bull's eye plot depicts peak segmental longitudinal, circumferential, and radial strain values.

2.3.3. Myocardial Deformation Analysis. The strain values were calculated utilizing the cvi42 (Circle Cardiovascular Imaging, Calgary, Alberta, Canada) version 5.6.2 (634). The endocardial and epicardial borders of both ventricles were delineated manually at the end-diastolic frame in 2-, 3-, 4-chamber views and all short-axis stacks for the left ventricle (LV) as well as 4-chamber and short-axis images for the right ventricle (RV). Three-dimensional LV and 2D RV strain values were extracted after the propagation of the contours during the entire cardiac cycle. For both ventricles, the absolute values of the global longitudinal strain (GLS), the global circumferential strain (GCS), and the global radial strain (GRS) were assessed. Furthermore, in CA patients, GLS was evaluated in the LV basal, mid, and apical levels (Figure 3). All the patients were stable hemodynamically with euvolemic status during the CMR examination.

2.3.4. Other Assessments. Left and right atrial (LA and RA) areas, the LV mass index, and the interatrial septal thickness were measured in the 4-chamber view at the end of cardiac systole. The presence of any pericardial or pleural effusion, as well as ascites, was registered. The measurements were done by an expert cardiologist with 5.5 years of experience in the field of cardiac imaging, who was blinded to the study subjects' data.

2.4. Follow-Up. All the patients were followed up by medical file reviewing and telephone interviews for 8–23 months to assess the mortality rate. The cardiovascular events were collected by an independent cardiologist blinded to the patient's data and FT values.

2.5. Statistical Analysis. The analyses were performed utilizing SPSS software, version 22.00. Normally distributed continuous variables were described as the mean ± the standard deviation (SD), while categorical variables were expressed as frequencies and percentages. The Kolmogorov–Smirnov test was utilized for the evaluation of the normality of the distribution of the numerical variables. The χ^2 test was applied to compare the ratio of the patients with LVGLS ≤10% in the CA and CP groups. For the comparison of the variables between our 3 study groups, the ANOVA test was employed. To modulate the effect of age between nonmatched groups, the analysis of covariance (ANCOVA) test was applied. Then, the post hoc Bonferroni test was utilized to reveal between-group differences. Moreover, a 2-independent sample *t*-test was applied for the intergroup comparisons of quantitative variables. A repeated-measures ANOVA test was performed to evaluate the differences between 3D LV strains at basal, mid, and apical levels in the CA subjects. A cutoff value of 0.05 was considered for the *P* value to mention statistically significant results.

3. Results

The study population consisted of 66 subjects: 19 patients with CA (68.4% male, mean age = 57 ± 10 y), 19 cases with CP (73.7% male, mean age = 51 ± 17.5 y), and 28 healthy controls (50% male, mean age = 31 ± 4 y). Table 1

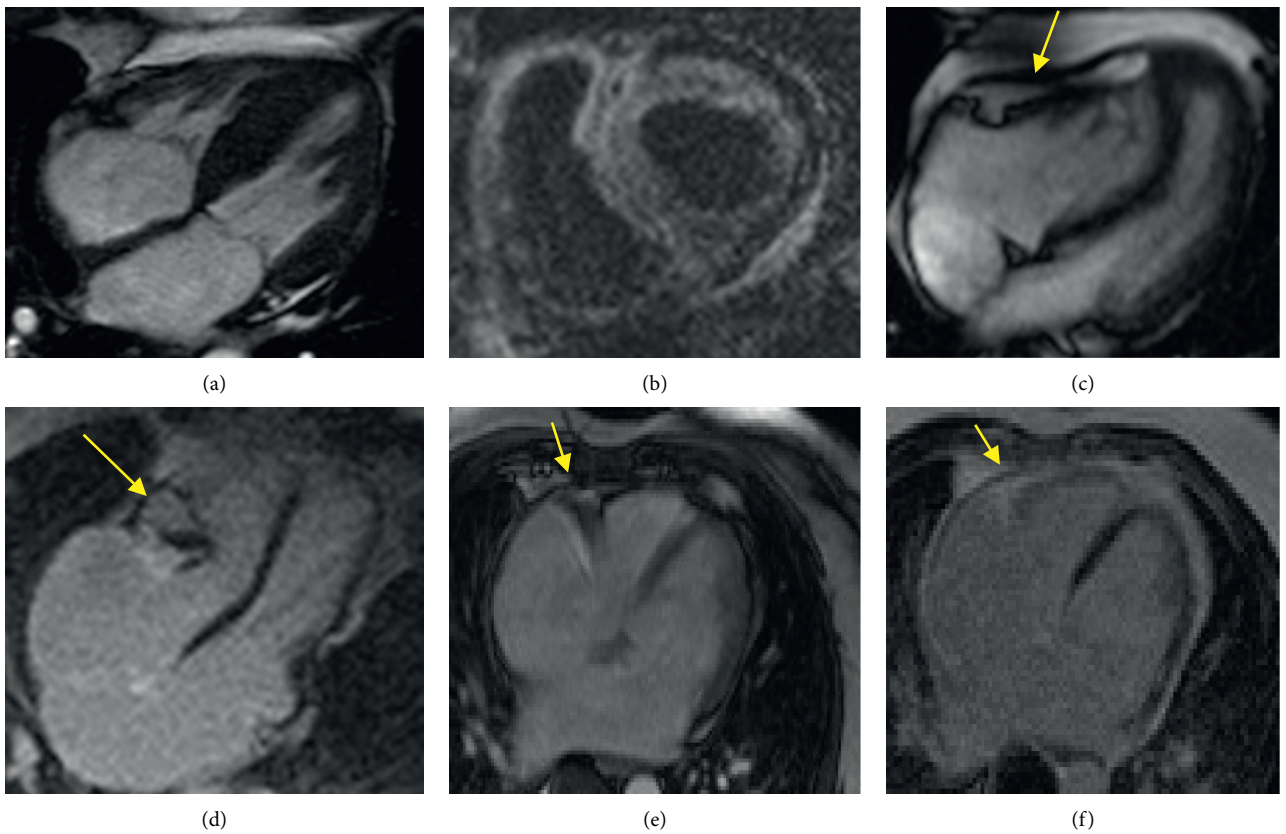

Figure 2: CMR findings in a patient with CA and CP. (a) Four-chamber cine function shows LV hypertrophy and thickened IAS in a CA patient. (b) Short-axis LGE depicts transmural LV and RV GD enhancement in CA. (c) Four-chamber cine function shows pericardial thickening (yellow arrow) in a CP patient. (d) LGE image in four-chamber view shows significant localized pericardial thickening and calcification (yellow arrow). (e, f) Localizer and LGE images of a 49-year-old woman with a history of shortness of breath and palpitations from three months ago. The patient had restrictive physiology on echocardiography. For further evaluation, CMR was performed, which showed restrictive physiology with normal pericardial thickness (arrow), and notably, a moderate reduction in the strain values (GLS: −14.01%), which was more in favor of CP. Hemodynamic finding in invasive angiography was an indicator of constriction. Finally, CP with normal pericardial thickness was confirmed during surgery.

demonstrates the demographic and CMR values of the study population.

The LV myocardial fibrosis pattern was predominantly transmural in 15/19 (78.9%), predominantly subendocardial in 2/19 (10.5%), and mixed transmural and subendocardial in 2/19 (10.5%) of the CA group.

Only 13/19 (68.4%) CA patients had the follow-up. The mortality rate was 11/13 (84.6%). One of the CP patients (5.3%) died during the follow-up.

Significant differences were found in the mean values of the interatrial septal thickness, the LV mass index, and the biatrial areas between the CA and the healthy controls (all $Ps < 0.001$).

The one-way ANOVA and ANCOVA tests revealed significant differences between our 3 study groups concerning the LV ejection fraction (EF) (F [2, 63] = 42.75, $P < 0.001$), EF (F [2, 63] = 26.24, $P < 0.001$), LVGLS (F [2, 63] = 105.52, $P < 0.001$), LVGCS (F [2, 63] = 42.06, $P < 0.001$), LVGRS (F [2, 63] = 30.76, $P < 0.001$), RVGLS (F [2,63] = 16.49, $P < 0.001$), RVGCS (F [2, 63] = 63.96, $P < 0.001$), and RVGRS (F [2,63] = 46.99, $P < 0.001$).

The results of the post hoc Bonferroni test to reveal between-group differences are demonstrated in Table 2.

LVGLS ≤10% was detected in 13/19 (68.4%) of the CA group and 1/19 (5.3%) of the CP group. The difference between these groups considering LVGLS ≤10% was significant ($P < 0.001$).

A significant difference in the mean value of the LVGLS of the basal LV level compared with mid and apical levels was detected (mean differences = −7.54 and −7.11; $Ps < 0.001$) in the CA population. The differences between the mean LVGLS measures of the mid and apical LV levels were not significant (mean difference = 0.42; $P = 1.00$). Similarly, the LVGCS value at the basal ventricular level was significantly lower than that at the mid and apical levels. The mean differences were −5.56 and −3.98, respectively ($Ps < 0.001$). The difference between the mean GCS value of the mid and apical LV levels was not meaningful (mean difference = 1.57; $P = 0.06$). The comparison of the mean GRS value between the 3 LV levels demonstrated a significant difference between the radial strain measures of the apical and basal as well as mid-ventricular levels (mean

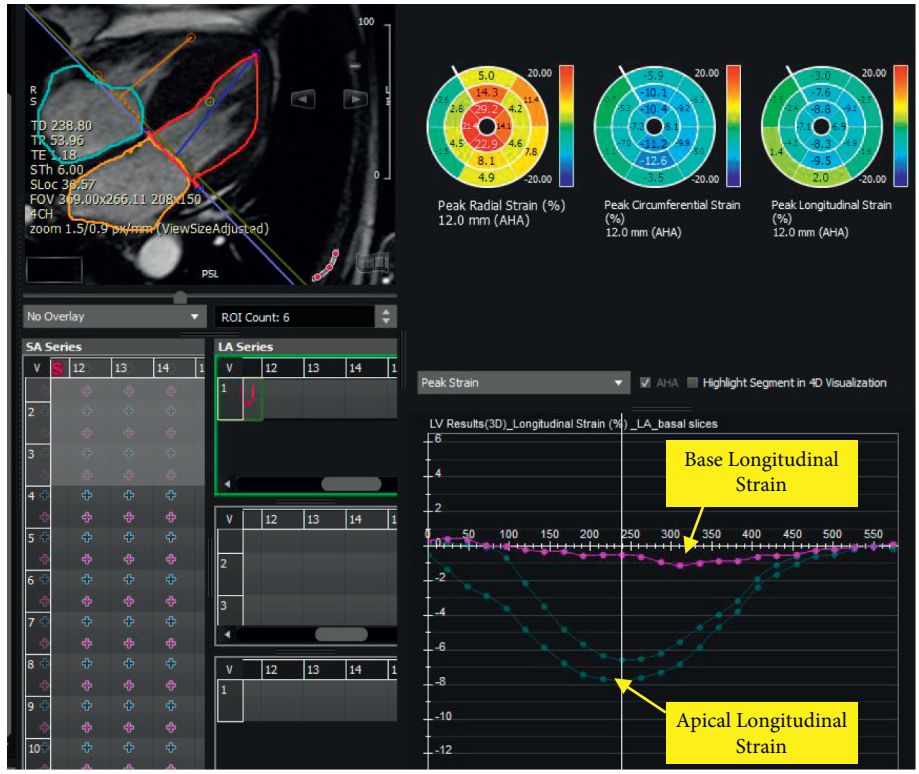

Figure 3: LV longitudinal strain in base, mid, and apical levels in a patient with CA depicts apical sparing with the significant reduction of strain value in the basal level. LV: left ventricle; CA: cardiac amyloidosis.

Table 1: Demographic and CMR parameters of the study population.

Variable	Age (mean ± SD)	Gender (male) %	
CA	57 ± 10	68.4%	
CP	51 ± 17	73.7%	
Control	32 ± 4	50%	
Study group	CA	CP	Control
Frequency (n)	19	19	28
CMR parameter	Mean ± SD	Mean ± SD	Mean ± SD
LVGLS%	8 ± 3	13 ± 2.7	18 ± 1.4
LVGCS%	10.5 ± 3.79	15 ± 3.2	18.7 ± 2.18
LVGRS%	17.5 ± 8.89	31 ± 12.3	40 ± 7.8
RVGLS%	14.6 ± 5.70	19.4 ± 5.90	23.6 ± 4.48
RVGCS%	9.9 ± 2.92	9.2 ± 4.00	17.7 ± 1.79
RVGRS%	16 ± 5.3	14.2 ± 5.96	31.1 ± 7.75
LVEF%	38 ± 11.9	52.5 ± 6.63	58 ± 2.7
LVEDVI (ml)	82.5 ± 33.99	64.3 ± 17.76	79.9 ± 2.94
LVESVI (ml)	52.6 ± 32.94	29.9 ± 6.64	34.5 ± 2.82
RVEF%	39 ± 12.0	47 ± 7.8	56 ± 2.2
RVEDVI (ml)	70.9 ± 25.40	71.2 ± 20.08	63.6 ± 3.00
RVESVI (ml)	43.3 ± 18.25	36.8 ± 12.27	28.8 ± 2.29
IAS thickness	5.8 ± 1.53	1.4 ± 0.2	1.4 ± 0.19
LV mass index	92.8 ± 25.81	57 ± 10.2	54.9 ± 8.57
LA area (cm^2)	27.4 ± 7.24	24 ± 3.4	18 ± 1.7
RA area (cm^2)	25.3 ± 4.10	18 ± 2.3	16.8 ± 1.60

CA: cardiac amyloidosis, CP: constrictive pericarditis, LV: left ventricle, RV: right ventricle, EF: ejection fraction, GLS: global longitudinal strain, GCS: global circumferential strain, GRS: global radial strain, CI: confidence interval, EDVI: end-diastolic volume index, ESVI: end-systolic volume index, IAS: interatrial septum, LA: left atrium, and RA: right atrium.

Table 2: The results of the post hoc Bonferroni test.

Dependent variables	Group 1	Group 2	Mean difference (95% CI)	P value
LVEF	Normal	CA	20.01 (14.64–25.38)	<0.001
	Normal	CP	5.70 (0.34–11.07)	0.03
	CP	CA	14.30 (20.16–8.45)	<0.001
RVEF	Normal	CA	16.46 (10.84–22.08)	<0.001
	Normal	CP	8.20 (2.58–13.82)	0.002
	CP	CA	8.26 (2.13–14.39)	0.005
LVGLS	Normal	CA	10.00 (8.30–11.71)	<0.001
	Normal	CP	5.05 (3.35–6.76)	<0.001
	CP	CA	4.95 (3.09–6.81)	<0.001
LVGCS	Normal	CA	8.19 (6.00–10.39)	<0.001
	Normal	CP	3.44 (1.25–5.64)	0.001
	CP	CA	4.75 (2.35–7.15)	<0.001
LVGRS	Normal	CA	22.28 (15.30–29.28)	<0.001
	Normal	CP	9.24 (2.26–16.25)	0.005
	CP	CA	13.04 (5.41–20.67)	<0.001
RVGLS	Normal	CA	8.98 (5.13–12.84)	<0.001
	Normal	CP	4.22 (0.37–8.08)	0.02
	CP	CA	4.76 (0.55–8.97)	0.02
RVGCS	Normal	CA	7.80 (5.69–9.92)	<0.001
	Normal	CP	8.46 (6.35–10.58)	<0.001
	CP	CA	−0.65 (−2.97–1.65)	1.00
RVGRS	Normal	CA	15.09 (10.25–19.95)	<0.001
	Normal	CP	16.83 (11.98–21.69)	<0.001
	CP	CA	−1.73 (−7.03–3.56)	1.00

CA: cardiac amyloidosis, CP: constrictive pericarditis, LV: left ventricle, RV: right ventricle, EF: ejection fraction, GLS: global longitudinal strain, GCS: global circumferential strain, GRS: global radial strain, and CI: confidence interval.

differences = 18.87 and 17.47; $Ps < 0.001$). The difference in the mean GRS value between the basal and mid-LV levels was not significant (mean difference = −1.40; $P = 0.14$).

4. Discussion

The 2 traditionally mentioned together differential diagnoses with restrictive cardiac hemodynamic manifestations are CA and CP. Several clinical and imaging criteria have been described for the precise diagnosis and differentiation of these conditions [7, 8]. In the present investigation, we compared CMR features between 3 groups: CA, CP, and healthy controls. The main findings of our study were as follows:

(1) All biventricular strain values were severely impaired in the CA and CP groups compared with the healthy controls.

(2) The incidence of LVGLS ≤10% in the CA group was significantly higher than that of the CP group.

(3) Compared with the patients with CP, LV strains were significantly reduced in the CA group. Among the RV strains, only RVGLS was meaningfully different between the 2 categories of patients.

(4) In the CA group, LVGLS and GCS were significantly decreased at the basal level by comparison with the mid and apical parts. Moreover, LVGRS was diminished at both basal and mid-ventricular levels compared with the apex.

(5) In our research, with a mean follow-up of 15.5 months, the mortality rate was 84.6% in the subjects with CA and 5.3% in those with CP.

Distinguishing between CA and CP is a challenging but vital process that affects patient survival [8]. The therapeutic options are revolutionized for CA, especially if diagnosed early. Moreover, CP is a curable disease by pericardiectomy, and the sooner the diagnosis of CA and CP is established, the better the outcome is [7, 22–24].

Detecting and classifying myocardial dysfunction in patients with CA before obvious clinical symptoms of heart failure are needed to find CA patients who benefit from autologous stem cell transplantation and high-dose chemotherapy to improve prognosis [7, 8, 22, 25, 26]. Strain analysis can successfully detect subtle functional impairments associated with several diseases such as CA and CP. In addition to conventional diagnostic methods, the ventricular strain measurement may be a beneficial diagnostic aid in differentiating between these 2 conditions (Figures 2(e) and 2(f)).

We analyzed myocardial FT parameters in 3 groups of patients: CA, CP, and healthy controls. Compared with the healthy control group, biventricular strain values, comprising GLS, GCS, and GRS, were severely impaired in both CA and CP groups.

Bhatti et al. showed that LVGLS was affected earlier than radial and circumferential strain in 46 patients with multiple myeloma with suspected CA [27]. They included a subgroup of patients with multiple myeloma who still had normal LV

wall thickness with biopsy-proven CA, indicating early stages of the disease, while we examined patients with relatively advanced CA and apparent cardiac involvement in our CMR study. It seems that in the advanced stages of CA, all ventricular strains are severely reduced. We suppose that further studies on groups of amyloidosis patients concerning cardiac involvement severity may be of great interest.

The main finding of our study was that all global LV strain values demonstrated a meaningful decline in the CA group by in comparison with the CP group. Previous studies have revealed abnormal circumferential deformation, torsion, and untwisting velocity in CP accompanied by preserved GLS [28, 29]. We found that 68% (13/19) of the subjects with CA had LVGLS ≤10%, while only 5% (1/19) of the cases with CP showed the stated finding ($P < 0.001$). Therefore, it is logical to consider LVGLS as a powerful marker for differentiating between these disease classes. A previous study demonstrated that abnormal LV deformation was related to coronary microvascular dysfunction, which has a more prominent impact on the longitudinal function of the heart. Additionally, there is a link between impaired GLS and worse outcomes in patients with amyloid light chain and thus may help to predict prognosis in CA patients [22].

In our investigation, RVGCS and RVGRS impairment was similar between the CA and CP groups, while RVGLS was significantly lower in the CA patients compared with the CP subjects. In other words, only RVGLS had a significant difference in the CA group by comparison with the CP group. In CA patients, RV involvement happens in more advanced stages of the disease. Similar to our results, in another study, impaired RV-free wall longitudinal strain in patients with CA was reported [30]. We postulated that CP patients might have preserved RVGLS compared with CA cases and that it could be utilized as a CMR marker. Nonetheless, more research is needed in this regard.

We also demonstrated LV apical sparing in strain values in the subgroup of patients with CA. In previous investigations, similar to our current work, the pattern of LV apical sparing in strain values was also observed in cases with CA. The preservation of LV apical longitudinal strain in CA may be related to low amyloid deposition in this region compared with the base, and it is a sensitive and specific marker in CA patients [29]. Interestingly, Moñivas Palomero et al. described an apical sparing pattern in the RV as previously described in the LV [30]. Singh et al. mentioned that the accuracy of apical sparing in strain values for the diagnosis of amyloid light chain was reduced in patients with chronic kidney disease [31].

In our investigation, as in previous works, the prognosis of patients with CA was much worse than that of patients with CP. Approximately, 85% of our cases with CA died within an average of 15.5 months, indicating the importance of the early diagnosis of these patients. On the other hand, the early diagnosis of patients with CP is of utmost importance because, with timely surgical intervention, most patients survive and return to routine daily life.

4.1. Limitations. The major limitation of our study was its relatively small sample size within each group of CP and CA, precluding the extraction of a cutoff for strain values to differentiate between these categories of disease. Novel parametric mapping was not included in our study, and planning research with the inclusion of mapping techniques is helpful. Designing studies in the early stages of the disease is essential. Moreover, evaluation of the inter and intraobserver variability was not part of our study.

5. Conclusion

FT-CMR is a novel noninvasive method to detect insidious myocardial disorders. In the present study, cardiac deformation parameters were declined significantly in both groups of CA and CP compared with healthy controls. Biventricular GLS was meaningfully reduced in CA subjects. Strain analysis, especially in the longitudinal direction, is an auxiliary finding to differentiate CA from CP subjects.

Data Availability

The datasets generated during the current research are available from the corresponding author on reasonable request.

Conflicts of Interest

The authors declare that they have no conflicts of interest.

Authors' Contributions

Dr. MF collected the data. Dr. FT, YT, MHK, and Dr. LH prepared the primary draft. Dr. HB contributed in data analysis. Dr. NR and Dr. SA participated in data gathering as well as writing the paper.

References

[1] W. J. McKenna, B. J. Maron, and G. Thiene, "Classification, epidemiology, and global burden of cardiomyopathies," *Circulation Research*, vol. 121, no. 7, pp. 722–730, 2017.

[2] G. Habib, C. Bucciarelli-Ducci, A. L. P. Caforio et al., "Multimodality imaging in restrictive cardiomyopathies: an EACVI expert consensus document in collaboration with the "working group on myocardial and pericardial diseases" of the European society of cardiology endorsed by the Indian academy of echocardiography," *European Heart Journal-Cardiovascular Imaging*, vol. 18, no. 10, pp. 1090–1121, 2017.

[3] D. Eisenberg and M. Jucker, "The amyloid state of proteins in human diseases," *Cell*, vol. 148, no. 6, pp. 1188–1203, 2012.

[4] M. Skinner, J. J. Anderson, R. Simms et al., "Treatment of 100 patients with primary amyloidosis: a randomized trial of melphalan, prednisone, and colchicine versus colchicine only," *The American Journal of Medicine*, vol. 100, no. 3, pp. 290–298, 1996.

[5] R. H. Falk, R. L. Comenzo, and M. Skinner, "The systemic amyloidoses," *New England Journal of Medicine*, vol. 337, no. 13, pp. 898–909, 1997.

[6] C. Rapezzi, G. Merlini, C. C. Quarta et al., "Systemic cardiac amyloidoses," *Circulation*, vol. 120, no. 13, pp. 1203–1212, 2009.

[7] M. J. Garcia, "Constrictive pericarditis versus restrictive cardiomyopathy?" *Journal of the American College of Cardiology*, vol. 67, no. 17, pp. 2061–2076, 2016.

[8] J. B. Geske, N. S. Anavekar, R. A. Nishimura, J. K. Oh, and B. J. Gersh, "Differentiation of constriction and restriction," *Journal of the American College of Cardiology*, vol. 68, no. 21, pp. 2329–2347, 2016.

[9] N. Galea, G. Polizzi, M. Gatti, G. Cundari, M. Figuera, and R. Faletti, "Cardiovascular magnetic resonance (CMR) in restrictive cardiomyopathies," *La Radiologia Medica*, vol. 127, pp. 1–15, 2020.

[10] J. M. Czum, A. M. Silas, and M. C. Althoen, "Evaluation of the pericardium with CT and MR," *International Scholarly Research Notices*, vol. 2014, Article ID 174908, 2014.

[11] C. C. Quarta, S. D. Solomon, I. Uraizee et al., "Left ventricular structure and function in transthyretin-related versus light-chain cardiac amyloidosis," *Circulation*, vol. 129, no. 18, pp. 1840–1849, 2014.

[12] M. Fontana, S. Pica, P. Reant et al., "Prognostic value of late gadolinium enhancement cardiovascular magnetic resonance in cardiac amyloidosis," *Circulation*, vol. 132, no. 16, pp. 1570–1579, 2015.

[13] T. D. Karamitsos, S. K. Piechnik, S. M. Banypersad et al., "Noncontrast T1 mapping for the diagnosis of cardiac amyloidosis," *Journal of the American College of Cardiology: Cardiovascular Imaging*, vol. 6, no. 4, pp. 488–497, 2013.

[14] F. Jafari, A. M. Safaei, L. Hosseini et al., "The role of cardiac magnetic resonance imaging in the detection and monitoring of cardiotoxicity in patients with breast cancer after treatment: a comprehensive review," *Heart Failure Reviews*, vol. 26, no. 3, pp. 679–697, 2021.

[15] M. Sharifian, N. Rezaeian, S. Asadian et al., "Efficacy of novel noncontrast cardiac magnetic resonance methods in indicating fibrosis in hypertrophic cardiomyopathy," *Cardiology Research and Practice*, vol. 2021, Article ID 9931136, 2021.

[16] A. M. Safaei, T. M. Kamangar, S. Asadian et al., "Detection of the early cardiotoxic effects of doxorubicin-containing chemotherapy regimens in patients with breast cancer through novel cardiac magnetic resonance imaging: a short-term follow-up," *Journal of Clinical Imaging Science*, vol. 11, no. 33, 2021.

[17] N. Rezaeian, M. A. Mohtasham, A. J. Khaleel, N. Parnianfard, K. Kasani, and R. Golshan, "Comparison of global strain values of myocardium in beta-thalassemia major patients with iron load using specific feature tracking in cardiac magnetic resonance imaging," *The International Journal of Cardiovascular Imaging*, vol. 36, no. 7, pp. 1343–1349, 2020.

[18] S. Asadian, N. Rezaeian, L. Hosseini, Y. Tolouei tabar, M. M. H. Komasi, and L. Shayan, "How does iron deposition modify the myocardium? a feature-tracking cardiac magnetic resonance study," *The International Journal of Cardiovascular Imaging*, pp. 1–9, 2021.

[19] Z. U. Rahman, P. Sethi, G. Murtaza et al., "Feature tracking cardiac magnetic resonance imaging: a review of a novel non-invasive cardiac imaging technique," *World Journal of Cardiology*, vol. 9, no. 4, p. 312, 2017.

[20] M. A. Gertz, R. Comenzo, R. H. Falk et al., "Definition of organ involvement and treatment response in immunoglobulin light chain amyloidosis (AL): a consensus opinion from the 10th international symposium on amyloid and amyloidosis," *American Journal of Hematology*, vol. 79, no. 4, pp. 319–328, 2005.

[21] T. Pandey, K. Jambhekar, R. Shaikh, S. Lensing, and S. Viswamitra, "Utility of the inversion scout sequence (TI scout) in diagnosing myocardial amyloid infiltration," *The International Journal of Cardiovascular Imaging*, vol. 29, no. 1, pp. 103–112, 2013.

[22] R. Li, Z.-G. Yang, H.-Y. Xu et al., "Myocardial deformation in cardiac amyloid light-chain amyloidosis: assessed with 3T cardiovascular magnetic resonance feature tracking," *Scientific Reports*, vol. 7, no. 1, pp. 1–9, 2017.

[23] C. Lei, X. Zhu, D. H. Hsi et al., "Predictors of cardiac involvement and survival in patients with primary systemic light-chain amyloidosis: roles of the clinical, chemical, and 3-D speckle tracking echocardiography parameters," *BMC Cardiovascular Disorders*, vol. 21, no. 1, pp. 43–11, 2021.

[24] A. V. Macedo, P. V. Schwartzmann, B. M. De Gusmão, M. D. De Melo, and O. R. Coelho-Filho, "Advances in the treatment of cardiac amyloidosis," *Current Treatment Options in Oncology*, vol. 21, no. 5, pp. 1–8, 2020.

[25] M. Bergman, J. Vitrai, and H. Salman, "Constrictive pericarditis: a reminder of a not so rare disease," *European Journal of Internal Medicine*, vol. 17, no. 7, pp. 457–464, 2006.

[26] J. Ternacle, D. Bodez, A. Guellich et al., "Causes and consequences of longitudinal LV dysfunction assessed by 2D strain echocardiography in cardiac amyloidosis," *Journal of the American College of Cardiology: Cardiovascular Imaging*, vol. 9, no. 2, pp. 126–138, 2016.

[27] S. Bhatti, S. Vallurupalli, S. Ambach, A. Z. Magier, A. Hakeem, and W. Mazur, "Determination of strain pattern in patients with cardiac amyloidosis secondary to multiple myeloma: a feature tracking study," *Journal of Cardiovascular Magnetic Resonance*, vol. 18, no. 1, pp. 1-2, 2016.

[28] P. P. Sengupta, V. K. Krishnamoorthy, W. P. Abhayaratna et al., "Disparate patterns of left ventricular mechanics differentiate constrictive pericarditis from restrictive cardiomyopathy," *Journal of the American College of Cardiology: Cardiovascular imaging*, vol. 1, no. 1, pp. 29–38, 2008.

[29] J. Gil, L. Abreu, H. Antunes et al., "Apical sparing of longitudinal strain in speckle-tracking echocardiography," *Netherlands Heart Journal*, vol. 26, no. 12, p. 635, 2018.

[30] V. Moñivas Palomero, A. Durante-Lopez, M. T. Sanabria et al., "Role of right ventricular strain measured by two-dimensional echocardiography in the diagnosis of cardiac amyloidosis," *Journal of the American Society of Echocardiography*, vol. 32, no. 7, pp. 845–853, 2019.

[31] V. Singh, P. Soman, and S. Malhotra, "Reduced diagnostic accuracy of apical-sparing strain abnormality for cardiac amyloidosis in patients with chronic kidney disease," *Journal of the American Society of Echocardiography*, vol. 33, no. 7, pp. 913–916, 2020.

Hindawi
Cardiology Research and Practice
Volume 2021, Article ID 9927533, 11 pages
https://doi.org/10.1155/2021/9927533

Review Article

The Role of SGLT2 Inhibitors in Heart Failure: A Systematic Review and Meta-Analysis

Vasiliki Tsampasian,[1] **Ranu Baral**,[1] **Rahul Chattopadhyay**,[2,3] **Maciej Debski**,[1] **Shruti S Joshi**,[4] **Johannes Reinhold**,[1,3] **Marc R Dweck**,[4] **Pankaj Garg**,[1,3] **and Vassilios S Vassiliou**[1,3]

[1]*Department of Cardiology, Norfolk and Norwich University Hospitals, Norwich, UK*
[2]*Department of Cardiology, Cambridge University Hospitals, Cambridge, UK*
[3]*Norwich Medical School, University of East Anglia, Norwich, UK*
[4]*University of Edinburgh/British Heart Foundation Centre for Cardiovascular Science, Edinburgh, UK*

Correspondence should be addressed to Vasiliki Tsampasian; tsampasian@doctors.org.uk and Vassilios S Vassiliou; v.vassiliou@uea.ac.uk

Received 15 March 2021; Accepted 13 August 2021; Published 20 August 2021

Academic Editor: Andrea Rossi

Aims. Recent randomised controlled trials (RCTs) have shown a significant prognostic benefit of sodium-glucose cotransporter 2 (SGLT2) inhibitors in the cardiovascular (CV) profile of patients with diabetes. This systematic review and meta-analysis aim to provide a concise evaluation of all the available evidence for the use of these agents in patients with heart failure (HF) regardless of their baseline diabetes status. *Methods and Results*. PubMed, Web of Science, and Cochrane library databases were systematically searched from inception until November 20th 2020. Eight studies consisting of 13,275 patients were included in the meta-analysis. For the total population, SGLT2 inhibitors reduced the risk of all-cause mortality (HR: 0.83; 95% CI: 0.75–0.91; I^2 0%), hospitalisation for HF (HR: 0.68; 95% CI: 0.61–0.75; I^2: 0%), CV death (HR: 0.82; 95% CI: 0.74–0.92; I^2: 0%), and hospitalisation for HF or CV death (HR: 0.72; 95% CI: 0.66–0.78; I^2: 0%). Subgroup analyses of the total population according to the diabetes status showed that SGLT2 inhibitors significantly reduced the risk of hospitalisation for HF (HR: 0.68; 95% CI: 0.61, 0.75; I^2: 0%), as well as the risk of hospitalisation for HF or CV death (HR: 0.72; 95% CI: 0.66, 078; I^2: 0%) and CV death (HR: 0.82; 95% CI: 0.74, 0.91; I^2: 0%). *Conclusions*. The results of this meta-analysis confirm the growing evidence in the literature of the favourable profile of SGLT2 inhibitors in cardiovascular outcomes and mortality in patients with heart failure regardless of the baseline diabetes status. This systematic review has been registered with PROSPERO (CRD42021224777).

1. Introduction

Over the recent years, large randomised controlled trials have demonstrated that sodium-glucose cotransporter 2 (SGLT2) inhibitors improve cardiovascular outcomes irrespective of diabetes, including risk of hospitalisation for heart failure (HHF), cardiovascular death, and all-cause mortality [1–4]. Being a glucose-lowering medication, SGLT2 inhibitors proved to have a significant role in reducing major adverse cardiovascular outcomes and hospitalisation for heart failure initially in patients with diabetes. The magnitude of their impact has been subsequently shown to be potentially independent—or, at least, separated—from their glucose-lowering value with a few hypotheses behind the exact mechanisms of their actions [5, 6]. The rapid accumulation of such evidence showing their favourable impact has triggered further research exploring their potential on cardiovascular outcomes and mortality in larger cohorts, not necessarily limited to diabetic populations. In response to this, two large randomised controlled studies investigated the impact of SGLT2 inhibitors in heart failure patients, with the cohort being comprised of patients with and without diabetes [7, 8].

With an increasing number of trials reporting on SGLT2 inhibitors in patients with and without diabetes, the goal of this systematic review and meta-analysis is to provide a concise evaluation of all the available evidence so far and analyse the data from the existing studies that focus on patients with heart failure, so as to better comprehend the clinical implications of the use of SGLT2 inhibitors. Additionally, we *a priori* planned to analyse the existing evidence depending on the diabetic status with the goal to determine the efficacy of SGLT2 both in the diabetic population and in heart failure patients without diabetes.

2. Methods

This is a systematic review and meta-analysis conducted and reported according to the Preferred Reporting Items for Systematic Reviews and Meta-Analysis (PRISMA) guidelines. It has been submitted and registered with PROSPERO (registration number: CRD42021224777).

2.1. Search Strategy. PubMed, Web of Science, and Cochrane library databases were systematically searched from inception until November 20th 2020. The key terms used for the search were ("SGLT2" *or* "Sodium-glucose cotransporter-2 inhibitors" or "canagliflozin" or "dapagliflozin" or "empagliflozin" or "ertugliflozin") and "heart failure."

2.2. Study Selection. After removing duplicates, all the remaining studies were screened at the title/abstract level. Our inclusion criteria were as follows:

(1) Observational or randomised controlled studies comparing SGLT2 inhibitors with placebo
(2) Included adults (>18 years old)
(3) Included patients diagnosed with heart failure, either with prespecified echocardiographic parameters (ejection fraction) or investigator-reported
(4) Assessed mortality or clinical outcomes in patients with heart failure taking SGLT2 inhibitors
(5) Studies which include imaging or blood biomarker parameters as outcomes that were included in the systematic review but not the meta-analysis

The selected studies underwent full-text screening. This process was performed by 3 independent investigators (R. C., M. D., and V. T.). Any conflicts were resolved by discussion, after which consensus was achieved. The study selection process is depicted in Figure 1 in Supplementary Materials.

2.3. Data Extraction. Two investigators (V. T. and R. B.) independently extracted the data from the selected studies using prespecified collection forms. The data extracted included type and characteristics of the study, number of patients on each group, number of diabetic and nondiabetic patients (where applicable), hazard ratios and confidence intervals for hospitalisation for heart failure (HHF), cardiovascular (CV) mortality, and all-cause mortality. The main outcomes of interest were all-cause mortality, CV mortality, and HHF. In studies that included both HF and non-HF patients, the data for the HF group with reduced ejection fraction was extracted from the prespecified subgroup analysis given in the respective study. Additionally, wherever possible, the outcomes were evaluated in subgroup analyses that included (1) patients with diabetes and (2) patients without diabetes.

2.4. Data Analysis. The hazard ratios and 95% CI that were given in each study were used for the meta-analysis. A random-effects model with inverse-variance weights was used to combine the effect measures from all studies on a logarithmic scale. Wherever possible, subgroup analysis in diabetic versus nondiabetic patients was performed. Statistical heterogeneity was assessed using the I^2 statistic. The statistical analyses were conducted using the Review Manager (RevMan) software (version 5.3. Copenhagen: The Nordic Cochrane Centre, The Cochrane Collaboration, 2014). The statistical significance was defined as $p < 0.05$. The between-study variance component was estimated using the DerSimonian and Laird method, which is the default approach of the software used for this meta-analysis [9].

3. Results

Out of the 86 studies that underwent full-text evaluation, a total of 8 studies including 13,275 participants were included. A total of 6,877 of these participants were in the SGLT2 group, while 6,398 were in the placebo group. Dapagliflozin was used in three Randomised Control Trials (RCT), empagliflozin in two RCTs, and canagliflozin, sotagliflozin, and ertugliflozin were used in one RCT each. Some three studies included patients with and without diabetes, two of which provided hazard ratios for cardiovascular and mortality outcomes that were used in the statistical analyses [7, 8]. The nondiabetic cohort is comprised of 4,576 patients, out of which 2,284 were in the SGLT2 group and 2,292 were in the placebo group. While the majority of the studies had prespecified left ventricular ejection fraction (LVEF) in their inclusion criteria, two studies had "investigator reported HF" with no prerequisite for EF for inclusion in the study, while one required specific NT-proBNP level along with previous hospitalisation for HF. Three studies included patients with EF ≤ 40%, two studies included patients with EF ≤ 45% and EF > 45%, one study reports a median baseline EF of 35% and two studies did not have prespecified baseline ejection fraction of the heart failure population in their inclusion criteria. The two studies (DECLARE-TIMI 58 & VERTIS CV) that have included patients with both EF ≤ 45% and EF > 45% have provided separate hazard ratios for the two groups. In order to maintain a more homogeneous group of baseline characteristics, the hazard ratios given for the group with the EF < 45% were used in the meta-analyses of the efficacy endpoints for the total population examined in our review

and in the subgroup analysis according to the baseline diabetes status. However, a further subgroup analysis was performed to examine the impact of SGLT2 inhibitors in patients with EF ≤ 45% compared with their impact in patients with EF > 45%. Table 1 summarises the characteristics of all the studies included in the meta-analysis with the available number of cardiovascular events provided from each study, while Supplementary Table 1 summarises the cardiovascular outcomes for patients with and without diabetes from the studies that investigated these cohorts separately. Cochrane collaboration's tool was used for assessment of risk of bias to assess the randomised controlled studies (Supplementary Table 2).

3.1. Efficacy Endpoints. In the analyses that included all the participants (regardless of diabetes status), the use of SGLT2 inhibitors was associated with significantly reduced risk of all-cause mortality (HR = 0.83, 95% CI, 0.75–0.91; I^2 0%) (Figure 1), hospitalisation for heart failure (HHF) (HR = 0.68, 95% CI, 0.61–0.75; I^2 0%) (Figure 2), CV death (HR = 0.82, 95% CI, 0.74–0.92; I^2 0%) (Figure 3), and hospitalisation for heart failure or CV death (HR = 0.72, 95% CI, 0.66–0.78; I^2 0%) (Figure 4) compared with placebo. Subgroup analysis of the total population according to the diabetes status showed that SGLT2 inhibitors significantly reduced the risk of HHF both in patients with and without diabetes (HR = 0.68, 95% CI: 0.60–0.76; I^2 0% and HR = 0.69, 95% CI: 0.56–0.84; I^2 0%, respectively) (Figure 5), as well as the risk of HHF or CV death (HR = 0.70, 95% CI: 0.64–0.77; I^2 0% and HR = 0.75, 95% CI: 0.66–0.87; I^2 0%, respectively) (Figure 6). The favourable impact of SGLT2 inhibitors on the outcome of CV death alone was significant in the participants with diabetes although it did not reach the level of statistical significance in the participants without diabetes (Figure 7). Additionally, subgroup analysis according to baseline EF was performed from the data available from the two studies (DECLARE-TIMI 58 & VERTIS CV) that stratified patients according to this. SGLT2 inhibitors did not have a significant impact on all-cause mortality (HR = 0.88, 95% CI: 0.67–1.14; I^2 45%) (Supplementary Figure 2) or cardiovascular death (HR = 0.95, 95% CI: 0.63–1.44; I^2 65%) (Supplementary Figure 3) with no significant differences between the two groups. However, SGLT2 inhibitors significantly reduced the risk of hospitalisation for heart failure or CV death (HR 0.78, 95% CI: 0.65–0.94; I^2 9%) with more pronounced effect on the group of heart failure with reduced ejection fraction, whereas in participants with EF > 45%, the favourable impact of SGLT2 inhibitors did not reach the level of statistical significance (Supplementary material Figure 4).

Funnel plots for unadjusted all-cause mortality (Supplementary Figure 5) and hospitalisation for heart failure (Supplementary Figure 6) were used to assess publication bias with no evidence of significant publication bias.

3.2. The Impact of SGLT2 on LV Function and BNP. A relatively small number of studies have been published so far investigating the impact of SGLT2 inhibitors on LV function and dimensions as assessed by imaging parameters, biomarkers (NT-proBNP or BNP), exercise capacity, symptom improvement, and quality of life in patients with heart failure. Table 2 summarises these studies along with their main characteristics and outcomes of interest.

EMPA-TROPISM is the only study so far investigating the effect of SGLT2 exclusively in nondiabetic patients [10]. Comprised of 84 participants, it showed that empagliflozin had a significantly positive impact on LV function and remodelling as well as on the quality of life compared to placebo. On the other hand, the EMPIRE-HF study, which included 190 diabetic and nondiabetic patients, did not show significant differences between empagliflozin and placebo in any of the endpoints investigated (NT-proBNP, activity level and quality of life/symptomatic improvement) 3 months after initiation of the treatment [11]. While this RCT did not study LV function or volumes by any means of imaging, it is notable that the follow-up period was relatively short (3 months), which differentiates it from the rest of the studies. Apart from the relatively short follow-up period, the participants of this study were patients with a relatively milder phenotype of heart failure with better baseline status and functional capacity and lower baseline NT-proBNP levels [11].

LV function was assessed by echocardiography in some of the studies and by CMR in others. From the echocardiographic studies, it was noted that SGLT2 inhibitors did have a positive impact on diastolic function. In two of the three studies, the majority of the patients had HF with preserved ejection fraction [12, 13], while the third study included a small number of patients (twelve) with advanced/drug refractory heart failure [14]. Even in this small cohort with advanced disease, there was an improvement in the E/e' ratio; however, this did not reach the level of statistical significance (p value given as 0.06).

From the studies that utilised CMR, it may be argued that SGLT2 favours cardiac remodelling and improvement in LV volumes; however, results are not consistent. More specifically, the LV end-diastolic volume (LVEDV) was assessed with the use of CMR in three RCTs: SUGAR-DM-HF, EMPA-TROPISM, and REFORM [10, 15, 16]. SUGAR-DM-HF and EMPA-TROPISM included a combined number of 189 patients and demonstrated a significant improvement of the LVEDV in the SGLT2 arm compared to placebo [10, 15]. Remarkably, this positive effect was also noted in the nondiabetic cohort that the EMPA-TROPISM study included [10]. The REFORM study included 56 patients in total, and after 12 months of follow-up, the investigators did not find significant differences in the LV volumes between the SGLT2 and placebo groups [16]. It should be noted that the patient cohort consisted of diabetic patients with mild HF symptoms on modest doses of loop diuretics. Nevertheless, in the same study, a significant reduction in the diuretic requirements was noted in the SGLT2 group.

The evidence regarding BNP/NT-proBNP is somewhat inconsistent, with some of the studies showing improvement [13–15] and others demonstrating no substantial changes between the two groups [12, 17]. This could be explained by

Table 1: Characteristics of studies included in the meta-analysis.

Trial	SGLT2	Definition of HF at baseline	Diabetes status of participants	Number of participants		HHF events		CV death		All-cause mortality		CV death or HF	
				SGLT2	Placebo	SGLT2	Placebo	SGLT2	Placebo	SGLT2	Placebo	SGLT2	Placebo
Emperor-reduced	Empagliflozin	EF ≤ 40%	DM + non-DM	1863	1867	388	553	187	202	249	266	361	462
Soloist-WHF	Sotagliflozin	Previous hospitalisation for HF and BNP > 150pg/ml (>450pg/ml for AF) (reported median EF 35%)	DM	608	614	194	297	51	58	65	76	245	355
Vertis-CV‡	Ertugliflozin	EF ≤ 45%‡	DM	319	159	—	—	42	21	54	27	62	38
		EF > 45%		680	327			47	21	63	30	68	35
Empareg	Empagliflozin	Investigator reported HF	DM	462	244	48	30	38	27	56	35	75	49
Declare-Timi 58 (HF)⁇	Dapagliflozin	EF ≤ 45%	DM	318	353	41	63	25	47	38	68	59	95
		EF > 45%						54	38	84	81	92	99
Dapa-HF	Dapagliflozin	EF ≤ 40%	DM + non-DM	2373	2371	231	318	227	273	276	329	382	495
Define-HF	Dapagliflozin	EF ≤ 40%	DM + non-DM	131	132	12	13	—	—	—	—	—	—
CanvasS	Canagliflozin	Investigator reported HF	DM	803	658	—	—	—	—	—	—	—	—

‡Only the group with EF <45% and known history of HF was analysed in the total population analysis and in the subgroup analysis according to baseline diabetes status. ⁇The subgroup of HF with reduced ejection fraction was analysed in the total population analysis and in the subgroup analysis according to baseline diabetes status.

Study or Subgroup	log[Hazard Ratio]	SE	SGL T2 Total	Placebo Total	Weight	Hazard Ratio IV, Random, 95% CI
CANVAS	-0.3567	0.1616	803	658	9.1%	0.70 [0.51, 0.96]
DAPA-HF	-0.1863	0.0797	2373	2371	37.6%	0.83 [0.71, 0.97]
DECLARE-TIMI 58	-0.5276	0.1983	318	353	6.1%	0.59 [0.40, 0.87]
EMPAREG	-0.2357	0.2134	462	244	5.2%	0.79 [0.52, 1.20]
EMPEROR-REDUCED	-0.0834	0.0908	1863	1867	29.0%	0.92 [0.77, 1.10]
SOLOIST-WHF	-0.1985	0.168	608	614	8.5%	0.82 [0.59, 1.14]
VERTIS CV	-0.0408	0.2314	319	159	4.5%	0.96 [0.61, 1.51]
Total (95% CI)			**6746**	**6266**	**100.0%**	**0.83 [0.75, 0.91]**

Heterogeneity: $Tau^2 = 0.00$; $Chi^2 = 5.81$, df = 6 (P = 0.45); $I^2 = 0\%$
Test for overall effect: Z = 3.89 (P = 0.0001)

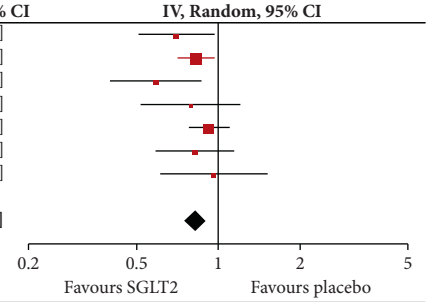

Figure 1: Effect of SGLT2 inhibitors versus placebo on all-cause mortality for the total population.

Study or Subgroup	log[Hazard Ratio]	SE	SGL T2 Total	Placebo Total	Weight	Hazard Ratio IV, Random, 95% CI
CANVAS	-0.6733	0.2221	803	658	5.6%	0.51 [0.33, 0.79]
DAPA-HF	-0.3567	0.0872	2373	2371	36.2%	0.70 [0.59, 0.83]
DECLARE-TIMI 58	-0.4463	0.2029	318	353	6.7%	0.64 [0.43, 0.95]
DEFINE-HF	-0.1744	0.4323	131	132	1.5%	0.84 [0.36, 1.96]
EMPAREG	-0.2877	0.2277	462	244	5.3%	0.75 [0.48, 1.17]
EMPEROR-REDUCED	-0.3567	0.0959	1863	1867	29.9%	0.70 [0.58, 0.84]
SOLOIST-WHF	-0.4463	0.1363	608	614	14.8%	0.64 [0.49, 0.84]
Total (95% CI)			**6558**	**6239**	**100.0%**	**0.68 [0.61, 0.75]**

Heterogeneity: $Tau^2 = 0.00$; $Chi^2 = 2.59$, df = 6 (P = 0.86); $I^2 = 0\%$
Test for overall effect: Z = 7.38 (P < 0.0001)

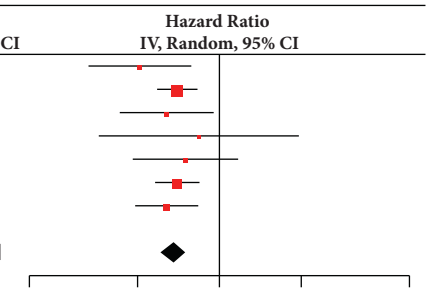

Figure 2: Effect of SGLT2 inhibitors versus placebo on hospitalisation for heart failure for the total population.

Study or Subgroup	log[Hazard Ratio]	SE	SGL T2 Total	Placebo Total	Weight	Hazard Ratio IV, Random, 95% CI
CANVAS	-0.3285	0.1759	803	658	9.9%	0.72 [0.51, 1.02]
DAPA-HF	-0.1985	0.0881	2373	2371	39.4%	0.82 [0.69, 0.97]
DECLARE-TIMI 58	-0.5978	0.2454	318	353	5.1%	0.55 [0.34, 0.89]
EMPAREG	-0.3425	0.2559	462	244	4.7%	0.71 [0.43, 1.17]
EMPEROR-REDUCED	-0.0834	0.1042	1863	1867	28.1%	0.92 [0.75, 1.13]
SOLOIST-WHF	-0.1744	0.189	608	614	8.6%	0.84 [0.58, 1.22]
VERTIS CV	-0.0408	0.266	319	159	4.3%	0.96 [0.57, 1.62]
Total (95% CI)			**6746**	**6266**	**100.0%**	**0.82 [0.74, 0.92]**

Heterogeneity: $Tau^2 = 0.00$; $Chi^2 = 5.10$, df = 6 (P = 0.53); $I^2 = 0\%$
Test for overall effect: Z = 3.56 (P = 0.0004)

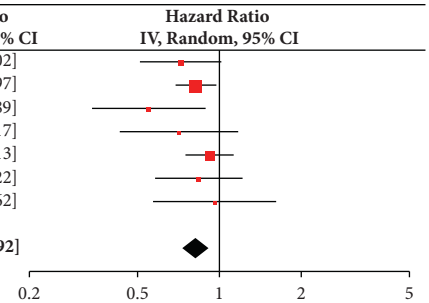

Figure 3: Effect of SGLT2 inhibitors versus placebo on cardiovascular death for the total population.

Study or Subgroup	log[Hazard Ratio]	SE	SGL T2 Total	Placebo Total	Weight	Hazard Ratio IV, Random, 95% CI
CANVAS	-0.4943	0.144	803	658	8.4%	0.61 [0.46, 0.81]
DAPA-HF	-0.2877	0.073	2373	2371	32.7%	0.75 [0.65, 0.87]
DECLARE-TIMI 58	-0.478	0.1635	318	353	6.5%	0.62 [0.45, 0.85]
EMPAREG	-0.3285	0.186	462	244	5.0%	0.72 [0.50, 1.04]
EMPEROR-REDUCED	-0.2877	0.073	1863	1867	32.7%	0.75 [0.65, 0.87]
SOLOIST-WHF	-0.4005	0.1293	608	614	10.4%	0.67 [0.52, 0.86]
VERTIS CV	-0.2744	0.2035	319	159	4.2%	0.76 [0.51, 1.13]
Total (95% CI)			**6746**	**6266**	**100.0%**	**0.72 [0.66, 0.78]**

Heterogeneity: $Tau^2 = 0.00$; $Chi^2 = 3.16$, df = 6 (P = 0.79); $I^2 = 0\%$
Test for overall effect: Z = 7.92 (P < 0.00001)

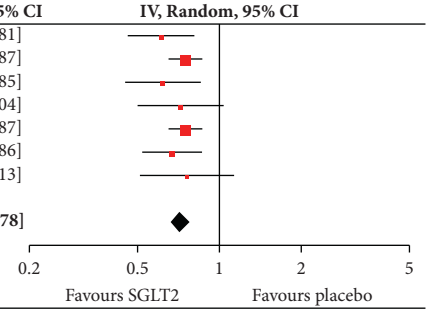

Figure 4: Effect of SGLT2 inhibitors versus placebo on hospitalisation for heart failure or cardiovascular death for the total population.

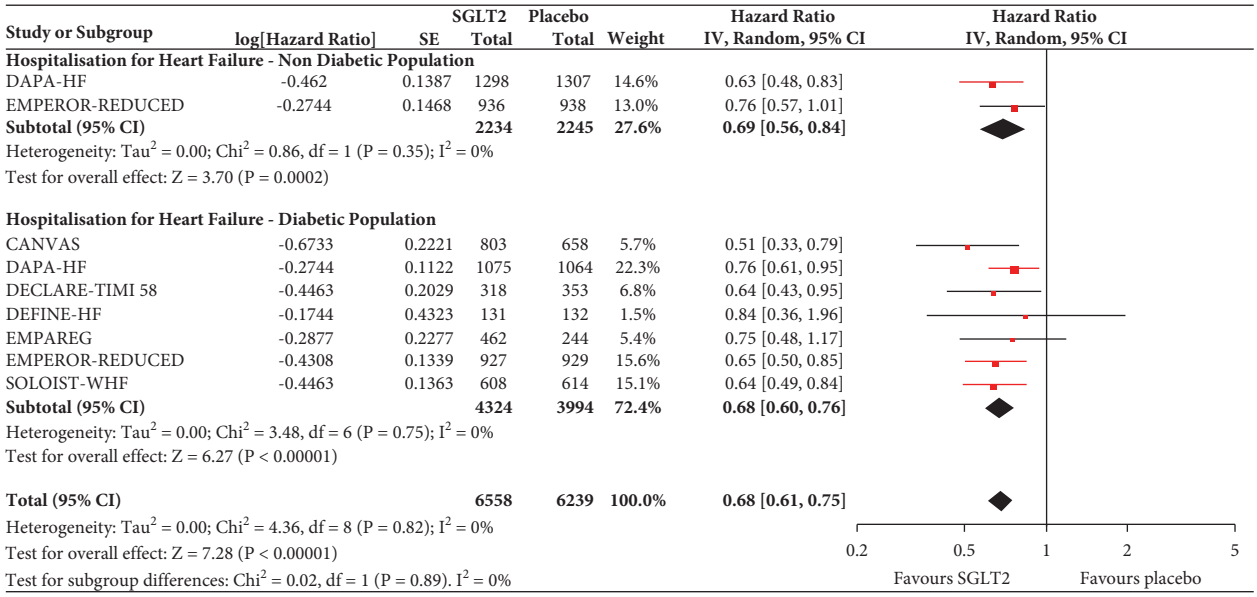

Figure 5: Subgroup analysis of the treatment effect SGLT2 inhibitors on hospitalisation for heart failure depending on baseline diabetes status.

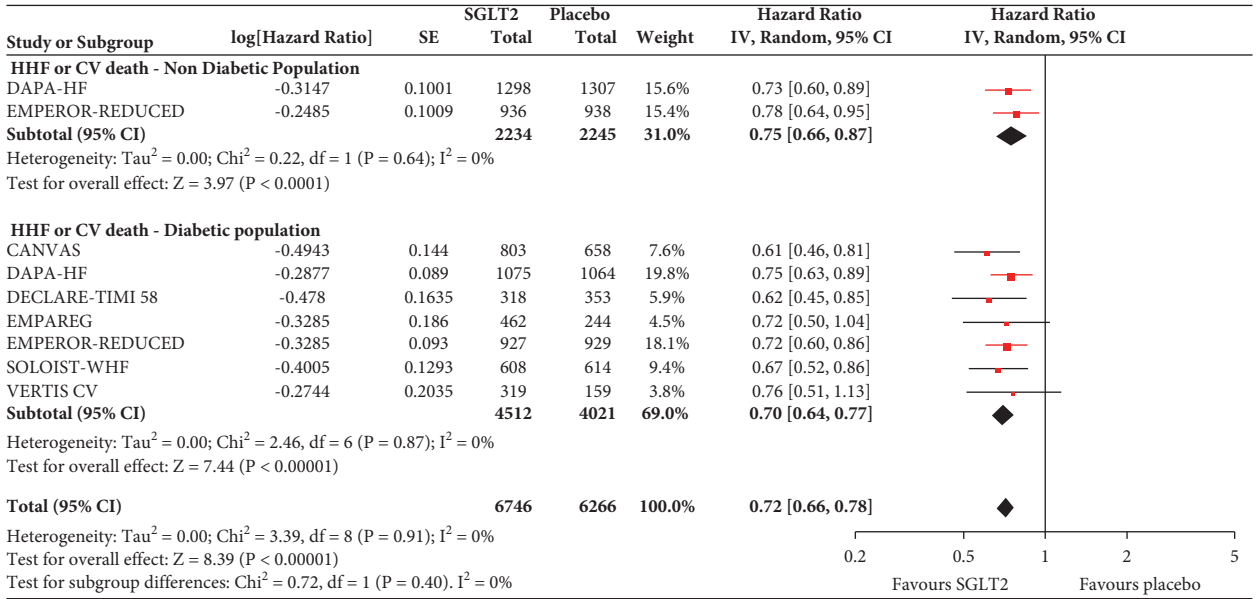

Figure 6: Subgroup analysis of the treatment effect SGLT2 inhibitors on hospitalisation for heart failure or cardiovascular death depending on baseline diabetes status.

the discrepancies in the baseline characteristics of the participants in addition to the different follow-up periods and methodology in each study.

Despite the fact that each of the aforementioned studies comprised a relatively small number of patients and investigated LV function and parameters by different imaging modalities (echocardiography or CMR), it can be argued that even in this heterogeneous group, there is a general trend towards improvement of diastolic function and LV volumes in the SGLT2 group, even if these did not always reach the level of statistical significance. Further research with large randomised controlled trials would be beneficial in portraying the impact of SGLT2 inhibitors on LV function, tissue characterisation, and cardiac remodelling.

4. Discussion

The present meta-analysis, the largest to date, shows that the use of SGLT2 inhibitors is associated with reduction in the risk of hospitalisation for heart failure, cardiovascular death, and all-cause mortality in patients with heart failure primarily with reduced ejection fraction. In subgroup analyses

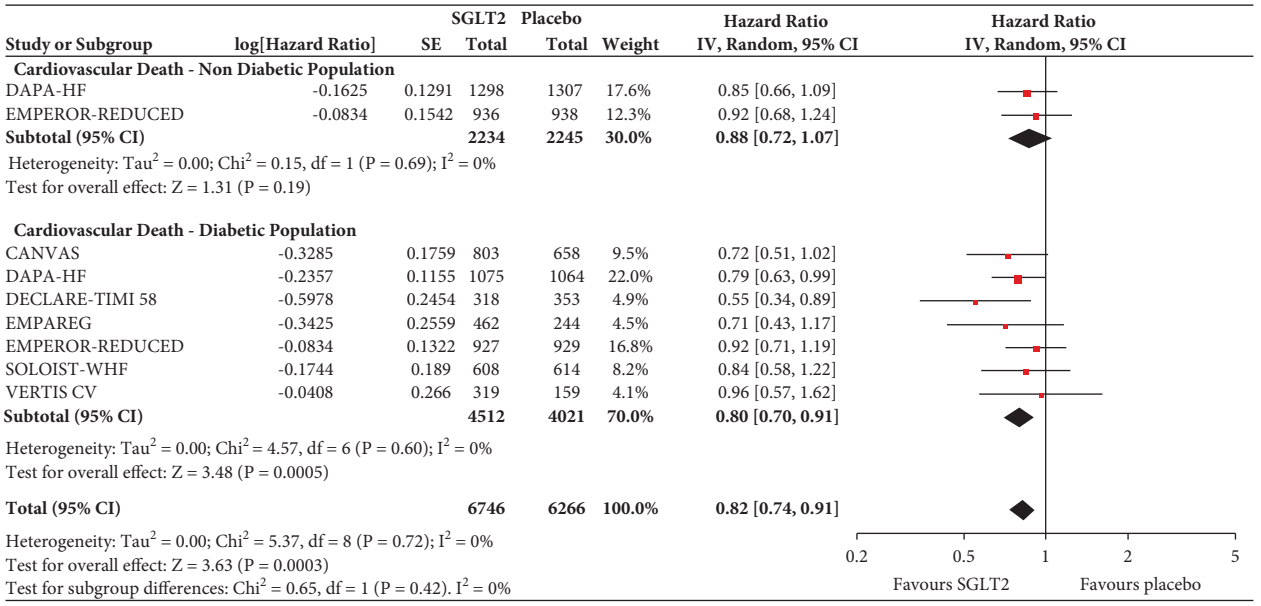

Figure 7: Subgroup analysis of the treatment effect SGLT2 inhibitors on cardiovascular death depending on baseline diabetes status.

Table 2: Review of studies on SGLT2 and LV function.

Study (authors and name of trial where applicable)	Study design	Number of participants	Baseline HF status	Diabetes status of participants	Follow-up period	Study endpoints	Outcomes
Lee et al. Sugar-DM-HF	RCT (empagliflozin versus placebo)	105	EF ≤ 40%	DM prediabetes	9 months	Primary: difference in change of LVESVi & GLS Secondary: difference in change of LVEF, LVEDVi, NT-proBNP, 6MWT, KCCQ-TSS (all imaging parameters assessed by CMR)	Significant improvement in LVESVi, LVEDVi, NT-proBNP in the empagliflozin group compared to placebo. No difference in GLS, LVEF, 6MWT, and KCCQ-TSS between the groups.
Jensen et al. Empire-HF	RCT (empagliflozin versus placebo)	190	EF ≤ 40%	DM Non-DM	3 months	Primary: difference in change of NT-proBNP Secondary: daily activity level, KCCQ-OSS	No differences noted between the groups in the change of NT-proBNP, daily activity level or KCCQ-OSS
Santos-Gallego et al. Empa-tropism	RCT (empagliflozin versus placebo)	84	EF < 50%	Non-DM	6 months	Primary: difference in change of LVEDV and LVESV Secondary: difference in change in peak VO2 (assessed by CPET), LVM, LVEF, 6MWT, and KCCQ-12 (all imaging parameters assessed by CMR)	Significant improvement of all the study endpoints (primary and secondary) in the empagliflozin group
Singh et al. REFORM	RCT (dapagliflozin versus placebo)	56	EF < 45%	DM	12 months	Primary: difference in change of LVESV Secondary: LVEDV, LVMi, and LVEF (all imaging parameters assessed by CMR)	No differences between the groups in the change of LVESV, LVEDV, LVMi, and LVEF

Table 2: Continued.

Study (authors and name of trial where applicable)	Study design	Number of participants	Baseline HF status	Diabetes status of participants	Follow-up period	Study endpoints	Outcomes
Tanaka et al.	Prospective multicentre study (dapagliflozin)	53	HFpEF and HFrEF (majority HFpEF)	DM	6 months	Primary: diastolic function (E/e'), GLS Secondary: LVEDV, LVESV, LVEF, LVMi, LAVi, and BNP (all imaging parameters assessed by 2D echocardiography)	Dapagliflozin was associated with improvement in diastolic function (E/e') and GLS as well as LAVi. No significant changes in the rest of the parameters studied in the 6-month follow-up period
Seo et al.	Retrospective study (empagliflozin, canagliflozin, dapagliflozin)	12	Advanced/ drug-refractory HF	DM	6 months	NYHA class, BNP, LVEDV, LVEF, E/e', TRPG (all imaging parameters assessed by 2D echocardiography)	Improvement was noted in NYHA class, LVEDV, TRPG, and BNP levels 6 months after initiation of the SGLT2. No changes in the rest of the parameters studied in the 6-month follow-up period
Sezai et al. Canossa	Prospective controlled trial (canagliflozin)	35	HFpEF and HFrEF (majority HFpEF)	DM	12 months	Primary: changes of subcutaneous, visceral, and total fat areas (determined by computed tomography) Secondary: ANP, BNP, LVEF, LVMi, diastolic function (E/e') (amongst others) (all imaging parameters assessed by 2D echocardiography)	All fat areas significantly decreased after 12 months treatment with SGLT2. ANP, BNP, LVEF, LVMi, and E/e' also significantly improved

RCT, randomised controlled trial; HFpEF, heart failure with preserved ejection fraction; HFrEF, heart failure with reduced ejection fraction; EF, ejection fraction; DM, diabetes mellitus; LVESVi, left ventricular end systolic volume indexed; LVEDVi, left ventricular end-diastolic volume indexed; GLS, global longitudinal strain; LVEF, left ventricular ejection fraction; LVMI, left ventricular mass indexed; LAVi, left atrial volume indexed; 6MWT, 6-minute walk test; KCCQ-TSS, Kansas City Cardiomyopathy Questionnaire Total Symptom Score; KCCQ-OSS, Kansas City Cardiomyopathy Questionnaire Overall Summary Score; CPET, cardiopulmonary exercise test; E/E', ratio of early diastolic peak velocity of Doppler transmitral flow to early diastolic mitral annular velocity; TRPG, pressure gradient of tricuspid regurgitation; ANP, atrial natriuretic peptide; BNP, brain natriuretic peptide.

stratified by the presence of diabetes, it is demonstrated that SGLT2 inhibitors provide consistent benefit on cardiovascular outcomes regardless of the baseline diabetes status.

Our data are in agreement with previous evidence that supports the prognostic value of SGLT2 in cardiovascular outcomes and mortality. Crucially, our findings highlight the importance of this drug group in the patients with heart failure regardless of diabetes status, revealing in this way that the potential therapeutic benefit in this population cohort could be invaluable.

4.1. Current Evidence and Recommendations. Previous large RCTs have shown remarkable benefits of SGLT2 specifically in cardiovascular outcomes in the diabetic population [18–20]. These results drew the attention to one or more potentially unrevealed thus far cardioprotective mechanisms of SGLT2 inhibitors that make it unique in the world of oral antidiabetic medications. Interestingly, the impact of SGLT2 inhibitors on cardiovascular outcomes does not seem to be directly related with their glucose-lowering efficacy [5]. Since there are now accumulating evidence supporting that the cardioprotective mechanisms are not associated with the glycemic control, the focus has been shifted to using these agents to patients regardless of their baseline diabetes status. Previous studies that have investigated the effect of SGLT2 inhibitors in nondiabetic cohorts have so far demonstrated positive results [7, 8, 10, 21]. The rapidly accumulating evidence of the substantial favourable impact of these agents on risk reduction in hospitalisation for heart failure and

cardiovascular death has led in their inclusion in the latest recommendations for the management of patients with heart failure [22]. Notably, given the results of DAPA-HF and EMPEROR-Reduced trials, dapagliflozin and empagliflozin are now recommended in symptomatic patients with HF and reduced EF on optimal treatment, regardless of the presence of diabetes [7, 8, 22].

4.2. Potential Mechanisms of Action. While the exact pathophysiological process remains to be fully understood, there are several hypotheses that investigate the cardiometabolic profile of these agents. Some of the benefits observed most notably particularly in the HF population could be explained by the natriuresis and osmotic diuresis that these agents promote [5, 23]. This, subsequently, results in improvement of the left ventricular loading conditions by a reduction in the preload. While one may argue that this is a feature of all the commonly used diuretics, it has been noted that SGLT2 inhibitors do not reduce the intravascular volume as much as the common diuretics but instead target rather selectively the interstitial fluid, with a greater reduction in the extracellular fluid and no major impact on organ perfusion [24, 25]. Interestingly, in a small study by Griffin et al., it was demonstrated that empagliflozin resulted in natriuresis which was independent of the glucose load, indicating a direct natriuretic effect distinct from the osmotic diuresis [26]. Additionally, in contrast with the loop diuretics, SGLT2 inhibitors promote uricosuria and can reverse diuretic-induced hyperuricaemia, another contributing factor to their cardiovascular protective effects [27].

SGLT2 inhibitors have also been shown to reduce the blood pressure without increasing the heart rate and therefore improve the myocardial workload [28]. The pathophysiology behind this mechanism is not delineated yet; nevertheless, there is data to suggest that reduction in arterial stiffness and improvement on vascular resistance may play a significant role [5, 6, 28].

The action of SGLT2 inhibitors on a cellular level is surprising as they induce a state that mimics starvation [29]. As a result, there is activation of signaling pathways that involve important enzymes such as the sirtuin 1 (SIRT1) and the adenosine monophosphate-activated protein kinase (AMPK), both of which attenuate oxidative stress and inflammation and promote oxidation of fatty acids resulting in ketonaemia [29, 30]. Additionally, the activation of SIRT1 leads to stimulation of erythropoietin synthesis and erythrocytosis, which has been found to be one of the factors contributing to the significant cardiovascular benefits of SGLT2 inhibitors [31, 32].

Furthermore, SGLT2 inhibitors improve insulin sensitivity and glycemic control. With reduced requirements in insulin, SGLT2 inhibitors promote weight loss which also contributes to lower blood pressure [33]. While it could be argued that these effects are reflected on the improvement of diastolic function and filling pressure parameters noted in the echocardiographic studies investigating the impact of these agents on LV function, further research on this matter is required to prove this hypothesis.

Another promising emerging feature of SGLT2 inhibitors is their antifibrotic impact on the heart [34, 35]. Preclinical research data have demonstrated that empagliflozin directly attenuates cardiac myofibroblast activity and collagen remodelling [34], while dapagliflozin also diminishes the process of myocardial fibrosis after myocardial infarction [35]. It will be of great clinical interest to assess if these research data are in accordance with findings from CMR studies focusing on the left ventricular tissue characterisation.

Undoubtedly, CMR holds an important role in the assessment of LV function, and it can provide invaluable information about the impact of the SGLT2 inhibitors on left ventricular function and remodelling. Recently, the EMPA-HEART CardioLink-6 randomised placebo-controlled trial thoroughly investigated data from 74 patients with diabetes type 2 with coronary artery disease that underwent a comprehensive CMR study [36]. It demonstrated a significant reduction in myocardial extracellular compartment volume (ECV), indexed extracellular compartment volume (iECV), and indexed LV mass (LVMi) after 6 months of treatment with empagliflozin compared with placebo. In the same study, tissue remodelling biomarkers were also measured at baseline and at 6 months, with no significant difference found between the SGLT2 and placebo groups. It has to be noted however that this study was not powered to detect differences in these and that in this patient cohort the baseline levels of these biomarkers were actually in the normal range. Therefore, further studies, including ideally patients with heart failure, are required to obtain detailed information that could provide a new perspective in the mechanism of action of SGLT2 inhibitors on the diseased myocardium.

Independently of the mode of action, our meta-analysis conclusively confirms that SGLT2 inhibitors have a beneficial effect in patients with HF independently of the diabetes status, reducing mortality by 17%, and hospitalisation for heart failure by almost a third, supporting the need for increased utilisation in patients with reduced LVEF.

5. Limitations

This study has potential limitations that should be considered. Firstly, not all the randomised controlled trials have published the necessary subgroup data for all the endpoints. Therefore, some of these trials were not included in the analysis of individual endpoints. Secondly, in this meta-analysis we included RCTs that performed subgroup analysis depending on the HF status, regardless of their definition of HF. While most of the studies gave prespecified EF in their inclusion criteria, some studies had "investigator-reported HF." Additionally, in order to maintain homogeneity, the data published for the cohort with the reduced EF were used in the meta-analyses of the efficacy endpoints for the total population, as this cohort represents the vast majority of the participants in the RCTs analysed in this meta-analysis. We performed subgroup analysis of the main endpoints according to the EF, when these data were provided. Whereas the level of heterogeneity for the analyses of the

endpoints for the total population was insignificant as assessed by I^2 of 0%, there was moderate to substantial heterogeneity in the subgroup analyses of endpoints according to EF as evidenced by an I^2 that ranged between 9% and 65%. It has to be acknowledged that the subgroup analysis of endpoints according to baseline EF was comprised of only two studies and a small number of individuals, and this could be one of the reasons for the higher level of heterogeneity. Finally, we acknowledge that assessment of publication bias with the use of funnel plots is less reliable when the meta-analysis is comprised of less than ten studies in total.

6. Conclusion

It is without a doubt that SGLT2 inhibitors provide prognostic benefit in patients with heart failure, regardless of the exact mechanism of action. The recent large RCTs have shown that this positive impact is expanded in patients without diabetes. This systematic review and meta-analysis provide robust summative evidence of the effectiveness of these agents in patients with heart failure regardless of the diabetes status. Our results also suggest that they are likely to be more effective in patients with reduced LVEF. Data on their mechanism is limited with imaging studies performed to date providing conflicting information. Further studies are needed to better understand their mechanisms of action and their long-term impact on LV function and biomarkers as well as the heart failure phenotype that will benefit most from them. Nevertheless, given the unique pathophysiological profile of SGLT2 inhibitors and their significant benefit in cardiovascular profile, they have an invaluable role in the management of patients with heart failure. The role of CMR is critical in facilitating volumes and tissue characterisation, and it will take a prominent role in future research studies.

Data Availability

Previously reported data were used to support this meta-analysis. These prior studies (and datasets) are cited at relevant places within the text as references.

Consent

No consent is required.

Disclosure

This is a meta-analysis of already published data.

Conflicts of Interest

The authors declare that they have no conflicts of interest.

Acknowledgments

MRD was supported by the British Heart Foundation (FS/14/78/31020) and is the recipient of a Sir Jules Thorn Award for Biomedical Research Award 2015 (15/JTA). SJ was supported by the British Heart Foundation (FS/CRTF/20/24087).

Supplementary Materials

Supplementary Table 1. Characteristics of the studies included in the meta-analysis that have outcomes for the patients with and without diabetes. *Supplementary Table 2.* Cochrane Collaboration's tool for assessing risk of bias in randomised controlled trials. *Supplementary Figure 1.* PRISMA flow diagram of the study selection progress. *Supplementary Figure 2.* Subgroup analysis of the treatment effect of SGLT2 inhibitors on all-cause mortality depending on baseline ejection fraction. *Supplementary Figure 3.* Subgroup analysis of the treatment effect SGLT2 inhibitors on cardiovascular death depending on baseline ejection fraction. *Supplementary Figure 4.* Subgroup analysis of the treatment effect SGLT2 inhibitors on risk of hospitalisation for heart failure (HHF) or cardiovascular death depending on baseline ejection fraction. *Supplementary Figure 5.* Funnel plot for unadjusted all-cause mortality demonstrating no evidence of significant publication bias. *Supplementary Figure 6.* Funnel plot for unadjusted risk of hospitalisation for heart failure demonstrating no evidence of significant publication bias. (*Supplementary Materials*)

References

[1] D. L. Bhatt, M. Szarek, P. G. Steg et al., "Sotagliflozin in patients with diabetes and recent worsening heart failure," *New England Journal of Medicine*, vol. 384, no. 2, pp. 117–128, 2021.

[2] E. T. Kato, M. G. Silverman, O. Mosenzon et al., "Effect of dapagliflozin on heart failure and mortality in type 2 diabetes mellitus," *Circulation*, vol. 139, no. 22, pp. 2528–2536, 2019.

[3] D. Fitchett, B. Zinman, C. Wanner et al., "Heart failure outcomes with empagliflozin in patients with type 2 diabetes at high cardiovascular risk: results of the EMPA-REG OUTCOMEtrial," *European Heart Journal*, vol. 37, no. 19, pp. 1526–1534, 2016.

[4] K. Rådholm, G. Figtree, V. Perkovic et al., "Canagliflozin and heart failure in type 2 diabetes mellitus," *Circulation*, vol. 138, no. 5, pp. 458–468, 2018.

[5] S. Verma and J. J. V. McMurray, "SGLT2 inhibitors and mechanisms of cardiovascular benefit: A state-of-the-art review," *Diabetologia*, vol. 61, no. 10, pp. 2108–2117, 2018.

[6] B. M. Bonora, A. Avogaro, and G. P. Fadini, "Extraglycemic effects of SGLT2 inhibitors: A review of the evidence," *Diabetes, Metabolic Syndrome and Obesity: Targets and Therapy*, vol. 13, pp. 161–174, 2020.

[7] S. D. Anker, J. Butler, G. Filippatos et al., "Effect of empagliflozin on cardiovascular and renal outcomes in patients with heart failure by baseline diabetes status," *Circulation*, vol. 143, no. 4, pp. 337–349, 2021.

[8] J. J. V. McMurray, S. D. Solomon, S. E Inzucchi et al., "Dapagliflozin in patients with heart failure and reduced ejection fraction," *New England Journal of Medicine*, vol. 381, pp. 1995–2008, 2019.

[9] A. A. Veroniki, D. Jackson, W. Viechtbauer et al., "Methods to estimate the between-study variance and its uncertainty in meta-analysis," *Research Synthesis Methods*, vol. 7, no. 1, pp. 55–79, 2016.

[10] C. G. Santos-Gallego, A. P. Vargas-Delgado, J. A. Requena et al., "Randomized trial of empagliflozin in non-diabetic patients with heart failure and reduced ejection fraction," *Journal of the American College of Cardiology*, vol. 77, no. 3, , 2020, https://linkinghub.elsevier.com/retrieve/pii/S0735109720377536.

[11] J. Jensen, M. Omar, C. Kistorp et al., "Twelve weeks of treatment with empagliflozin in patients with heart failure and reduced ejection fraction: A double-blinded, randomized, and placebo-controlled trial," *American Heart Journal*, vol. 228, pp. 47–56, 2020.

[12] H. Tanaka, F. Soga, K. Tatsumi et al., "Positive effect of dapagliflozin on left ventricular longitudinal function for type 2 diabetic mellitus patients with chronic heart failure," *Cardiovascular Diabetology*, vol. 19, no. 1, pp. 1–9, 2020.

[13] A. Sezai, H. Sekino, S. Unosawa, M. Taoka, S. Osaka, and M. Tanaka, "Canagliflozin for Japanese patients with chronic heart failure and type II diabetes," *Cardiovascular Diabetology*, vol. 18, no. 1, pp. 1–13, 2019.

[14] Y. Seo, M. Yamamoto, T. Machino-Ohtsuka, T. Ishizu, and K. Aonuma, "Effects and safety of sodium glucose cotransporter 2 inhibitors in diabetes patients with drug-refractory advanced heart failure," *Circulation Journal*, vol. 82, no. 7, pp. 1959–1962, 2018.

[15] M. M. Y. Lee, K. J. M. Brooksbank, K. Wetherall et al., "Effect of empagliflozin on left ventricular volumes in patients with type 2 diabetes, or prediabetes, and heart failure with reduced ejection fraction (SUGAR-DM-HF)," *Circulation*, vol. 143, no. 6, 2020.

[16] J. S. S. Singh, I. R. Mordi, K. Vickneson et al., "Dapagliflozin versus placebo on left ventricular remodeling in patients with diabetes and heart failure: the reform trial," *Diabetes Care*, vol. 43, no. 6, pp. 1356–1359, 2020.

[17] J. Jensen, M. Omar, C Kistorp et al., "Empagliflozin in heart failure patients with reduced ejection fraction: A randomized clinical trial (Empire HF)," *Trials*, vol. 20, pp. 374–4, 2019.

[18] B. Neal, V. Perkovic, K. W. Mahaffey et al., "Canagliflozin and cardiovascular and renal events in type 2 diabetes," *New England Journal of Medicine*, vol. 377, no. 7, pp. 644–657, 2017.

[19] B. Zinman, C. Wanner, J. M. Lachin et al., "Empagliflozin, cardiovascular outcomes, and mortality in type 2 diabetes," *New England Journal of Medicine*, vol. 373, no. 22, pp. 2117–2128, 2015.

[20] S. Verma, C. D. Mazer, A. T. Yan et al., "Effect of empagliflozin on left ventricular mass in patients with type 2 diabetes mellitus and coronary artery disease," *Circulation*, vol. 140, no. 21, pp. 1693–1702, 2019.

[21] M. E. Nassif, S. L. Windsor, F. Tang et al., "Dapagliflozin effects on biomarkers, symptoms, and functional status in patients with heart failure with reduced ejection fraction," *Circulation*, vol. 140, no. 18, pp. 1463–1476, 2019.

[22] P. M. Seferović, A. J. S. Coats, P Ponikowski et al., "European Society of Cardiology/Heart Failure Association position paper on the role and safety of new glucose-lowering drugs in patients with heart failure," *European Journal of Heart Failure*, vol. 22, pp. 196–213, 2020.

[23] C. S. P. Lam, C. Chandramouli, V. Ahooja, and S. Verma, "SGLT-2 inhibitors in heart failure: Current management, unmet needs, and therapeutic prospects," *Journal of the American Heart Association*, vol. 8, pp. e013389–12, 2019.

[24] K. M. Hallow, G. Helmlinger, P. J. Greasley, J. J. V. McMurray, and D. W. Boulton, "Why do SGLT2 inhibitors reduce heart failure hospitalization? A differential volume regulation hypothesis," *Diabetes, Obesity and Metabolism*, vol. 20, no. 3, pp. 479–487, 2018.

[25] K. Ohara, T. Masuda, M. Morinari et al., "The extracellular volume status predicts body fluid response to SGLT2 inhibitor dapagliflozin in diabetic kidney disease," *Diabetology & Metabolic Syndrome*, vol. 12, no. 1, pp. 1–9, 2020.

[26] M. Griffin, V. S. Rao, J. Ivey-Miranda et al., "Empagliflozin in heart failure," *Circulation*, vol. 142, no. 11, pp. 1028–1039, 2020.

[27] C. J. Bailey, "Uric acid and the cardio-renal effects of SGLT2 inhibitors," *Diabetes, Obesity and Metabolism*, vol. 21, no. 6, pp. 1291–1298, 2019.

[28] R. Chilton, I. Tikkanen, C. P. Cannon et al., "Effects of empagliflozin on blood pressure and markers of arterial stiffness and vascular resistance in patients with type 2 diabetes," *Diabetes, Obesity and Metabolism*, vol. 17, no. 12, pp. 1180–1193, 2015.

[29] M. Packer, "SGLT2 inhibitors produce cardiorenal benefits by promoting adaptive cellular reprogramming to induce a state of fasting mimicry: A paradigm shift in understanding their mechanism of action," *Diabetes Care*, vol. 43, no. 3, pp. 508–511, 2020.

[30] H. Zhou, S. Wang, P. Zhu, S. Hu, Y. Chen, and J. Ren, "Empagliflozin rescues diabetic myocardial microvascular injury via AMPK-mediated inhibition of mitochondrial fission," *Redox Biology*, vol. 15, pp. 335–346, 2018.

[31] S. E. Inzucchi, B. Zinman, D. Fitchett et al., "How does empagliflozin reduce cardiovascular mortality? Insights from a mediation analysis of the EMPA-REG OUTCOME trial," *Diabetes Care*, vol. 41, no. 2, pp. 356–363, 2018, http://care.diabetesjournals.org/lookup/suppl/http://www.diabetesjournals.org/content/diabetes-core-update-podcasts.

[32] J. Li, M. Woodward, V. Perkovic et al., "Mediators of the effects of canagliflozin on heart failure in patients with type 2 diabetes," *Journal of the American College of Cardiology: Heart Failure*, vol. 8, no. 1, pp. 57–66, 2020.

[33] H. J. L. Heerspink, B. A. Perkins, D. H. Fitchett, M. Husain, and D. Z. I. Cherney, "Sodium glucose cotransporter 2 inhibitors in the treatment of diabetes mellitus," *Circulation*, vol. 134, no. 10, pp. 752–772, 2016.

[34] S. Kang, S. Verma, A. F. Hassanabad et al., "Direct effects of empagliflozin on extracellular matrix remodelling in human cardiac myofibroblasts: Novel translational clues to explain EMPA-REG OUTCOME results," *Canadian Journal of Cardiology*, vol. 36, no. 4, pp. 543–553, 2020.

[35] T.-M. Lee, N.-C. Chang, and S.-Z. Lin, "Dapagliflozin, a selective SGLT2 Inhibitor, attenuated cardiac fibrosis by regulating the macrophage polarization via STAT3 signaling in infarcted rat hearts," *Free Radical Biology and Medicine*, vol. 104, pp. 298–310, 2017.

[36] T. Mason, O. R. Coelho-Filho, S. Verma et al., "Empagliflozin reduces myocardial extracellular volume in patients with type 2 diabetes and coronary artery disease," *JACC Cardiovasc Imaging*, vol. 14, no. 6, 2021.

Hindawi
Cardiology Research and Practice
Volume 2021, Article ID 9931136, 7 pages
https://doi.org/10.1155/2021/9931136

Research Article

Efficacy of Novel Noncontrast Cardiac Magnetic Resonance Methods in Indicating Fibrosis in Hypertrophic Cardiomyopathy

Maedeh Sharifian,[1] **Nahid Rezaeian**,[1] **Sanaz Asadian**,[1] **Ali Mohammadzadeh**,[1] **Ali Nahardani**,[1] **Kianosh Kasani**,[1] **Yaser Tolouei-tabar**,[1] **Ali Mohammad Farahmand**,[2] **and Leila Hosseini**[1]

[1]*Rajaie Cardiovascular Medical and Research Center, Iran University of Medical Sciences, Tehran, Iran*
[2]*Tehran University of Medical Sciences, Tehran, Iran*

Correspondence should be addressed to Sanaz Asadian; asadian_s@yahoo.com

Received 3 March 2021; Accepted 19 May 2021; Published 25 May 2021

Academic Editor: Gary Tse

Objective. In hypertrophic cardiomyopathy (HCM), myocardial fibrosis is routinely shown by late gadolinium enhancement (LGE) in cardiac magnetic resonance (CMR) imaging. We evaluated the efficacy of 2 novel contrast-free CMR methods, namely, diffusion-weighted imaging (DWI) and feature-tracking (FT) method, in detecting myocardial fibrosis. *Methods*. This cross-sectional study was conducted on 26 patients with HCM. Visual and quantitative comparisons were made between DWI and LGE images. Regional longitudinal, circumferential, and radial strains were compared between LGE-positive and LGE-negative segments. Moreover, global strains were compared between LGE-positive and LGE-negative patients as well as between patients with mild and marked LGE. *Results*. All 3 strains showed significant differences between LGE-positive and LGE-negative segments ($P < 0.001$). The regional longitudinal and circumferential strain parameters showed significant associations with LGE ($P < 0.001$), while regional circumferential strain was the only independent predictor of LGE in logistic regression models (OR: 1.140, 95% CI: 1.073 to 1.207, $P < 0.001$). A comparison of global strains between patients with LGE percentages of below 15% and above 15% demonstrated that global circumferential strain was the only parameter to show impairment in the group with marked myocardial fibrosis, with borderline significance ($P = 0.09$). A review of 212 segments demonstrated a qualitative visual agreement between DWI and LGE in 193 segments (91%). The mean apparent diffusion coefficient was comparable between LGE-positive and LGE-negative segments ($P = 0.51$). *Conclusions*. FT-CMR, especially regional circumferential strain, can reliably show fibrosis-containing segments in HCM. Further, DWI can function as an efficient qualitative method for the estimation of the fibrosis extent in HCM.

1. Introduction

Hypertrophic cardiomyopathy (HCM) is the most common genetic cardiac disorder with autosomal dominant inheritance and heterogeneous patterns of penetration and expression [1, 2]. The condition is characterized by left ventricular (LV) hypertrophy with no other probable causative etiologies. The clinical presentation varies from the absence of symptoms to exertional dyspnea, chest pain, syncope, and sudden cardiac death. In many cases, sudden cardiac death due to ventricular tachyarrhythmia is the first presentation [3]. Myocardial fibrosis occurs in more than half of this patient population [4] and is an underlying cause of ventricular tachyarrhythmia [5]. Cardiac magnetic resonance (CMR) imaging is able to detect the presence and extent of fibrosis manifested as areas of late gadolinium enhancement (LGE). Areas of LGE are compatible with fibrosis on histopathology [6]. The explanatory mechanism for LGE is the widening of extracellular spaces in fibrotic areas, which leads to the temporary distribution of gadolinium and relative hyperenhancement by comparison with adjacent healthy tissues [7]. The 2020 guidelines of the

American Heart Association/American College of Cardiology (AHA/ACC) for the diagnosis and management of HCM suggest LGE as a useful risk modifier for sudden cardiac death among patients in whom the risk is deemed borderline based on conventional risk stratification [8]. Nonetheless, the need for contrast injection limits the utilization of LGE in patients with contrast allergy and renal insufficiency, which explains why recent years have witnessed an increase in research on the usefulness of contrast-free techniques such as diffusion-weighted imaging (DWI), native T1, and extracellular volume (ECV) mapping.

The results of a study on infarcted swine hearts indicated comparable accuracy between DWI, LGE, and histology in detecting and delineating densely scarred areas, border zone areas, and healthy tissues [9]. A few small-scale studies have shown that not only can DWI depict fibrosis in HCM hearts but also its results exhibit a good correlation with LGE findings [10–12]. There have also been investigations suggesting the superiority of DWI over LGE owing to such probable advantages as the capability to show both diffuse scarring in the early stages of HCM [10, 12] and fibrotic areas that are not well visualized by LGE [12]. Additionally, the relatively novel technique of feature-tracking cardiac magnetic resonance (FT-CMR) has proven its efficaciousness in some cardiac disorders by assisting in diagnosis, risk stratification, and prognostication [13–18]. Since FT-CMR is a contrast-free method and is feasible through a post-processing analysis of routine cine images, it can act as a practical, available, and cost-beneficial method in the diagnosis of areas with myocardial fibrosis.

In the present study, we studied 26 patients with HCM to evaluate the efficacy of the 2 novel techniques of DWI and FT-CMR in demonstrating areas with myocardial fibrosis.

2. Methods

2.1. Study Population. The current investigation enrolled 30 consecutive patients with HCM who were referred to our center for CMR between July 2019 and December 2019. All these patients provided informed written consent for participation in the project. The study protocol was approved by the Medical Research Ethics Board of Iran University of Medical Sciences.

The exclusion criteria were a history of previous cardiac surgeries, including myectomy; contraindications for CMR such as severe contrast allergy, severe renal failure (glomerular filtration rate $<45\,\text{mL/min/1.73}\,\text{m}^2$), and the presence of cardiac devices such as internal cardioverter defibrillators and pacemakers; coronary artery disease; systemic hypertension; severe valvular disease; and systemic diseases affecting the myocardium such as amyloidosis.

2.2. Diagnostic Criteria of CMR. The present study recruited adult patients with a maximal end-diastolic LV wall thickness of 15 mm or greater in the absence of other etiologies for LV hypertrophy or 13 mm or greater in the presence of a positive family history or genetic test for HCM [8].

2.3. Cardiac Imaging Protocol. All the patients underwent a comprehensive study in keeping with a prespecific routine CMR imaging protocol using a 1.5 T MRI machine (MAGNETOM Avanto, Siemens Healthcare, Erlangen, Germany) and a vendor-supplied body surface coil. The imaging protocol consisted of the acquisition of 2-, 3-, and 4-chamber views, short-axis cine (functional) images, and LGE images 10 minutes after contrast injection. Also, breath-hold low *b*-value myocardial DWI spin-echo echo-planar imaging (EPI) sequences were performed on all the patients with an interactive ECG-gating regime to collect all signals at the freezing point of myocardial contraction (repetition time $= 90$ ms, echo time $= 54$ ms, flip angle $= 90^\circ$, pixel bandwidth $= 2220$ KHz, resolution $= 1.45 \times 1.45\,\text{mm}^2$, slice thickness $= 10$ mm, average $= 1$, $b = 0\,\text{s/mm}^2$, and $b = 100/150\,\text{s/mm}^2$).

2.4. Image Analysis

2.4.1. LGE Sequence Interpretation. The presence of LGE in each patient and each different segment was detected by an expert with more than 5 years of experience in cardiac imaging. With the aid of CVI42 software, the LGE percentage was calculated for each patient as the sum of hyperenhanced regions with +5SD signal intensity above the normal remote myocardium divided by the total LV myocardial mass, expressed as the percentage of the enhanced myocardial mass. The patients were classified into 2 groups: marked fibrosis (fibrosis percentage ≥15%) and mild fibrosis (fibrosis percentage <15%).

2.4.2. FT-CMR Analysis. Circle CVI's imaging platform, cvi42 (Calgary, Canada), was used to measure 3D longitudinal, circumferential, and radial strain parameters from cine images. First, brightness was adjusted to reach the optimal discrimination of the endocardium and blood pool. Next, endocardial and epicardial borders were defined on 3 long-axis views (2-, 3-, and 4- chamber views) and short-axis views (Figure 1). The next step saw the propagation of the contours before the calculation of regional strain values for the 16 AHA segments as well as the calculation of global strain values with the aid of the software. For ease, the absolute amounts of strain values were used.

2.4.3. DWI and Apparent Diffusion Coefficient (ADC) Analysis. DWI images were taken from the middle and apex of the heart for the evaluation of 6 middle and 4 apical AHA cardiac segments. The DWI images were evaluated via both qualitative and quantitative methods. For the qualitative evaluation, a radiologist and a cardiologist, who were both experienced in the field and blinded to the patients' history and other CMR sequences, independently observed the DWI images and classified the segments as fibrosis-positive and fibrosis-negative (intraobserver reproducibility: 0.89–0.92). In the case of disagreement between the 2 interpreters, the final decision was made by the senior radiologist in the ward. These visual assay findings were thereafter compared with

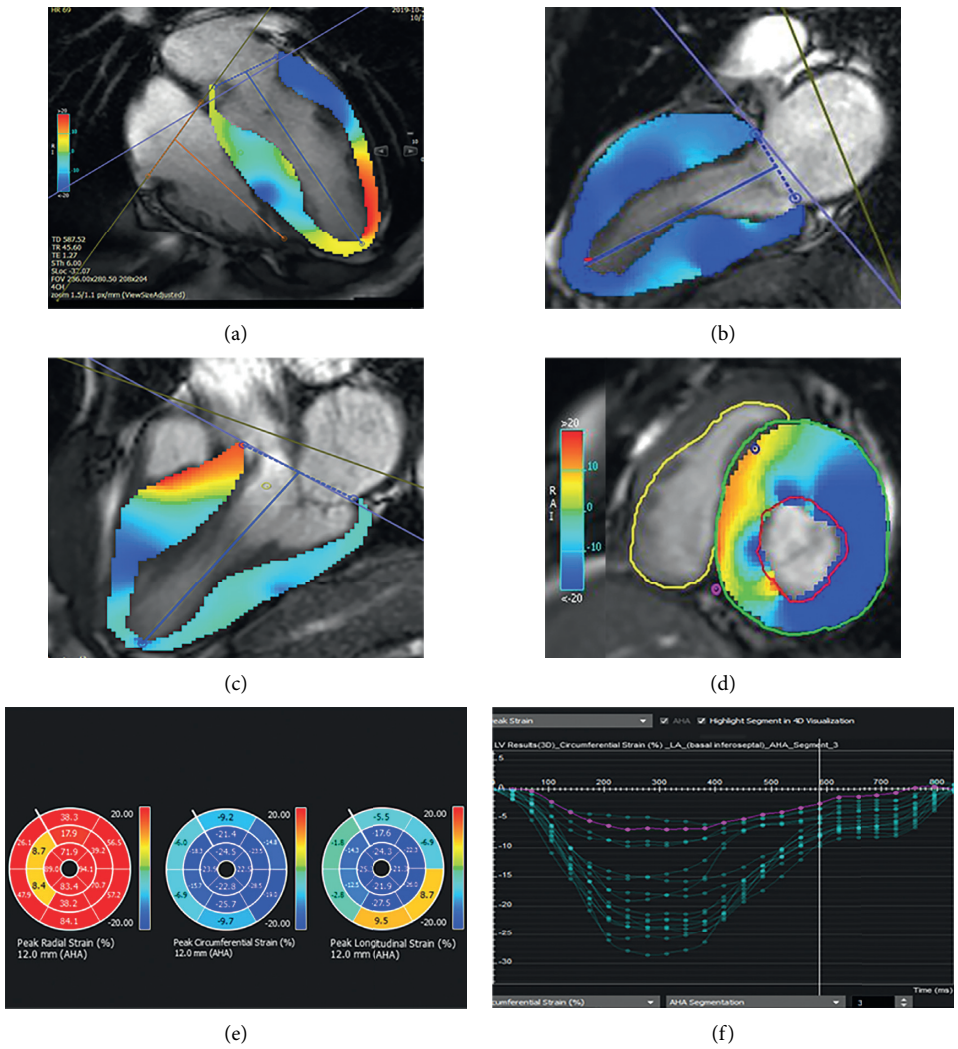

Figure 1: CMR feature-tracking technique for determining myocardial strain. (a) Four-chamber, (b) two-chamber, (c) three-chamber, and (d) short-axis images depict left ventricle endocardial (red) and epicardial (green) borders. (e) Bull's eye maps and (f) strain curves according to AHA myocardial segmentation.

those of segmental LGE. In the next step, ADC maps were calculated from the DWI dataset using MATLAB software, and the mean ADC value for each AHA segment was extracted (Figure 2).

2.5. Statistical Analysis. SPSS software, version 22.00, was used for the statistical analyses. Continuous variables with normal distributions were described as the mean ± the standard deviation (SD), while categorical variables were expressed as frequencies and percentages. Intergroup comparisons between LGE-positive and LGE-negative cases and between LGE < 15% and ≥15% were performed in terms of the quantitative variables by using an independent-samples *t*-test. The predictive power of regional strain parameters for regional LGE was tested using logistic regression models. A 2-tailed *P* value of less than 0.05 was considered statistically significant.

3. Results

3.1. Patients and Baseline Characteristics. The current study recruited 30 patients, of whom 4 were excluded due to severe motion artifacts. Twenty-six patients (female: 30.8%) at a mean (±SD) age of 46.5 (±14 y) were studied. The systolic anterior motion of mitral valve leaflets was seen in 13 patients (50%). Mild-to-moderate valvular abnormalities were seen in 11 patients (42.3%), with mitral regurgitation being the most common abnormality ($n = 9$), followed by pulmonary insufficiency ($n = 4$). LGE was present in 20 patients (76.9%: LGE-positive cases) and 52 out of 212 available segments (24.5%). Table 1 displays the baseline demographic

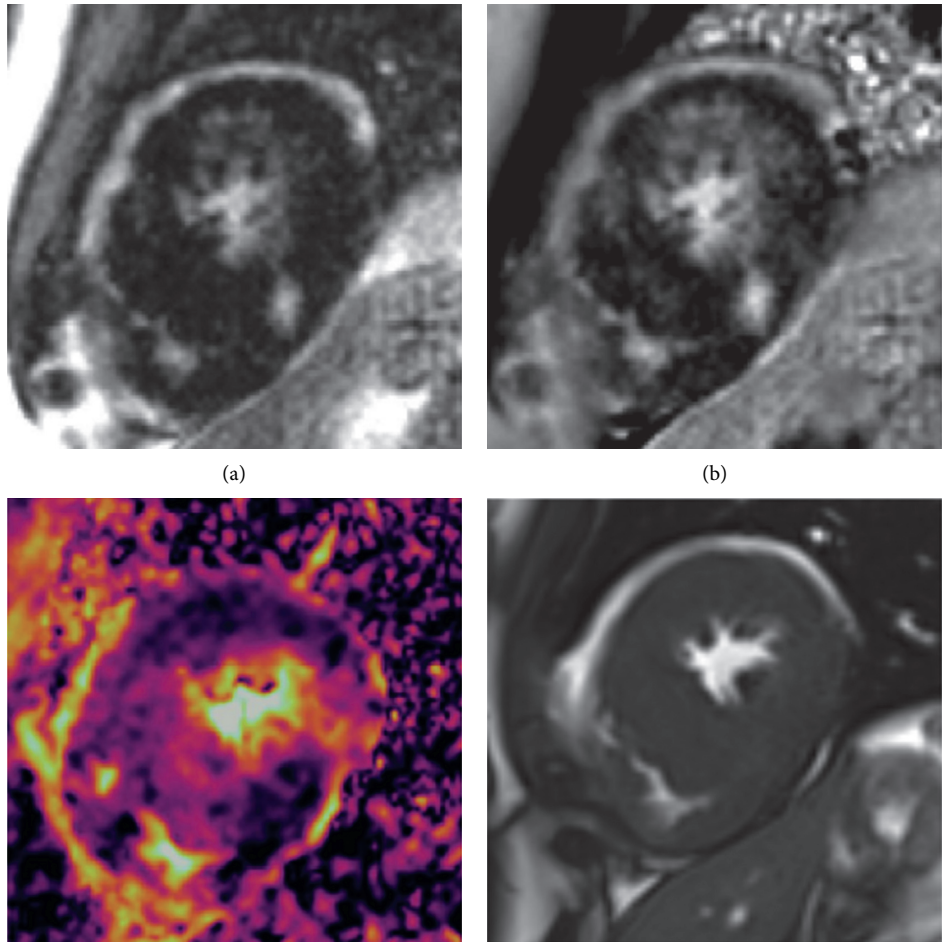

Figure 2: (a) Late gadolinium enhancement sequence (magnitude image), (b) late gadolinium enhancement sequence (phase image), (c) ADC map, and (d) true FISP image in a known case of hypertrophic cardiomyopathy. ADC: apparent diffusion coefficient; FISP: fast imaging with steady-state free precession.

Table 1: Baseline demographic and cardiac MRI characteristics of the study population.

Variables	All subjects ($n = 26$)	LGE < 15% ($n = 18$)	LGE ≥ 15% ($n = 8$)	P value
Age (y)	46.6 (±14)	47.1 (±13)y	45.2 (±19)	0.776
Gender (female)	8/26 (30.8%)	3/18 (16%)	5/8 (62%)	0.060
Body surface area (m^2)	1.91 (±0.21)	1.9 (±0.16)	1.7 (±0.23)	**0.006**
Positive family history	17/26 (68%)	14/18 (77%)	3/8 (37%)	0.078
Heart rate	64 (±8)	65 (±9)	63 (±6)	0.522
LVEF (%)	54 (±11)	58 (±8)	47 (±13)	**0.024**
LVESVI (mL/m^2)	34.7 (±18.3)	29 (±13)	46 (±23)	**0.032**
LVEDVI (mL/m^2)	74.7 (±20.8)	70 (±19)	84 (±22)	0.121
LV mass index (g/m^2)	84.1 (±39.1)	78 (±35)	96 (±46)	0.312
Cardiac output (L/m)	4.9 (±1.4)	5.3 (±1.4)	4.0 (±0.8)	**0.027**
Maximal wall thickness (mm)	19.5 (±5.7)	17 (±4.1)	24 (±6.2)	**0.003**

Values are mean (±SD) or n (%). LVEF: left ventricular ejection fraction; LVESVI: left ventricular end-systolic volume index; LVEDVI: left ventricular end-diastolic volume index; LV: left ventricle.

and cardiac MRI characteristics of the total study population and subgroup comparison based on the LGE percentage of greater or less than 15%. The patients with LGE percentage of 15% or greater had significantly lower LV ejection fraction ($47 \pm 13\%$ vs. $58 \pm 8\%$, $P = 0.024$) and cardiac output (4 ± 0.8 L/m vs. 5.3 ± 1.4 L/m, $P = 0.027$), as well as significantly higher LV end-systolic volume index (46 ± 23 ml/m^2 vs. 29 ± 13 ml/m^2, $P = 0.032$) and maximal wall thickness

(24 ± 6.2 mm vs. 17 ± 4.1 mm, $P = 0.003$). The LV mass index and LV end-diastolic volume index did not show a significant difference between the two groups ($P > 0.1$ for both).

3.2. FT-CMR Analysis. The comparison of global strain values between LGE-positive and LGE-negative patients demonstrated no significant difference in global longitudinal strain (GLS), global radial strain (GRS), and global circumferential strain (GCS) ($GLS = 11 \pm 3.5$ vs. 12.3 ± 4.5, $GCS = 14.3 \pm 3.0$ vs. 15.2 ± 4.4, and $GRS = 36.9 \pm 14.0$ vs. 31.3 ± 14.3, respectively; $P > 0.1$ for all). According to their LGE percentage, the patients were divided into 2 groups of LGE of less than 15% and LGE of 15% or greater so that global strain values could be compared between the groups. The intergroup analysis showed no significant difference in the absolute global strain values ($GLS = 10.60 \pm 3.60$ in LGE $\geq 15\%$ vs. 12.42 ± 3.72 in LGE $< 15\%$, $P > 0.1$; $GRS = 36.52 \pm 18.40$ in LGE $\geq 15\%$ vs. 35.20 ± 12.26 in LGE $< 15\%$, $P > 0.1$; and $GCS = 12.67 \pm 2.57$ in LGE $\geq 15\%$ vs. 15.33 ± 3.40 in LGE $< 15\%$, $P = 0.09$). Thereafter, a comparison of segmental longitudinal, circumferential, and radial strain values revealed significant differences concerning all 3 strain parameters between LGE-positive and LGE-negative segments (longitudinal strain $= 10.5 \pm 5.1$ vs. 15.5 ± 6.6, circumferential strain $= 11.8 \pm 5.7$ vs. 16.8 ± 6.3, and radial strain $= 24.8 \pm 26.6$ vs. 32.2 ± 28.1, respectively; $P < 0.001$ for all). As is shown in Table 2, the logistic regression models revealed that regional longitudinal and circumferential strain values had significant associations with regional LGE ($P < 0.001$ for both), and circumferential strain was the only independent predictor of segmental LGE (OR: 1.140, 95% CI: 1.073 to 1.207, $P < 0.001$).

3.3. DWI and ADC Analysis. In 12 patients, the DWI images of cardiac apical segments were excluded due to severe motion artifacts. In the total of 212/260 reviewed segments, a visual agreement between DWI and LGE images was reported in 193 segments (91%). In the remaining 19 segments, 5 LGE-positive segments were classified as fibrosis-negative by DWI images (false negative) and 14 LGE-negative segments were classified as fibrosis-positive by DWI images (false positive). In 11 out of the 19 discordant segments (57%), the timing of the cardiac cycle was dissimilar between LGE and DWI images. The mean ADC was 0.64 ± 0.25 for LGE-positive and 0.61 ± 0.23 for LGE-negative segments. The difference between the ADC values of LGE-positive and LGE-negative segments failed to constitute statistical significance ($P = 0.51$).

Table 2: The results of logistic regression analysis on the predictive role of regional strain values for regional fibrosis.

Variable	OR (95% CI)	P value
Regional longitudinal strain	1.121 (1.052–1.183)	**<0.001**
Regional circumferential strain	1.125 (1.052–1.183)	**<0.001**
Regional radial strain	1.005 (0.993–1.016)	0.386

4. Discussion

The main findings of our investigation are as follows:

(1) All regional strain values showed significant deterioration in fibrosis-containing segments

(2) Among the 3 regional strain values, circumferential strain was an independent predictor of fibrosis

(3) In patients with notable amounts of fibrosis, GCS showed relative impairment

(4) The qualitative assessment of DWI images revealed an excellent agreement with LGE sequences

(5) The quantitative assessment of ADC showed no difference between segments with or without LGE

Contractile dysfunction in HCM and its relationship with tissue characteristics have been the focus of some previous studies. Using speckle-tracking echocardiography, Popovic et al [19] demonstrated that regional and global longitudinal strain parameters had decreased absolute values in LGE-containing segments and patients, respectively. In their study, regional circumferential and radial strain values were comparable between LGE-positive and LGE-negative segments. Conversely, in a more recent study on 45 patients with HCM, Wu et al. [11] reported impairment in all 3 regional strain parameters in LGE-positive segments and segments with increased ECV values. Similarly, in a study on pediatric HCM, Bogarapu et al [20] demonstrated that all strains were significantly decreased in LGE-positive groups and introduced a cutoff point of −12.8% for GLS to differentiate between LGE-positive and LGE-negative patients. Scintillatingly, Swoboda et al [21] reported that segmental hypertrophy, LGE, and abnormal native T1 and ECV values were all associated with impairment in circumferential and radial strains. However, they showed that after correction for regional wall thickness, circumferential and radial strain values were significantly associated with native T1, but not with LGE and ECV. Therefore, they proposed that contractile abnormality was probably affected more by cellular changes and to a lesser extent by extracellular expansion.

In our study, global strains exhibited no significant difference between LGE-positive and LGE-negative cases. The regional strains, however, showed significant impairment in LGE-positive segments, and segmental circumferential strain proved to be an independent predictor of LGE. This might be due to the fact that, in HCM, myocardial fibrosis is typically midwall [4, 22, 23], and among the 3 strain axes, it is circumferential strain that is mainly generated by the circumferential fibers of the midwall myocardium [24]. Consequently, circumferential strain is diminished by the fibrous degeneration of these fibers. The mean maximal wall thickness of the patients in our study was low by comparison with that reported by some previous studies [20]. Given that the myocardial thickness is a major determinant of disease severity in HCM, it is probable that our study group consisted of individuals with milder disease. Thus, it could be postulated that, in the course of HCM, circumferential strain is the first strain to show impairment.

A few previous studies have utilized DWI to detect fibrosis in HCM hearts [10–12]. Our results demonstrated that the visual identification of fibrotic regions on b100 DWI images was consistent with LGE images in 91% of the reviewed segments, and more than half of the observed discordance was attributable to mismatched cardiac phases. Since no more than 2 segments were discordant in DWI with LGE images in each patient, the total visual estimation of fibrosis was comparable between LGE and DWI images. This is in line with the results of Nguyen et al [10], who reported a high visual agreement between ADC, ECV, and LGE images, not least for the detection of patch-like fibrosis. Nevertheless, in our study, ADC values did not show a significant difference between LGE-positive and LGE-negative segments. The broad SD of the ADC values in both normal and fibrotic regions indicates that low *b*-value DWI is not an efficient quantitative technique for the evaluation of myocardial changes. This finding does not chime in with that reported by a few investigations that demonstrated significantly increased ADC measures in fibrosis-positive segments defined by either LGE or ECV images [10–12]. One possible explanation for this discrepancy could be the fact that the low *b*-value diffusion also contains data regarding the perfusion characteristics of the myocardium [25, 26]. As long as resting-state dynamic contrast-enhanced myocardial perfusion images are close to normal, it is logical to observe no ADC value changes in the study group. On the other hand, according to previous studies, abnormal rest perfusion and reduction in capillary microcirculation are seen in a large percentage of patients with HCM and are mostly associated with areas of fibrosis shown in LGE images [27]. We, therefore, hypothesized that the reduction in the microcirculation in these areas might compensate for the increase in movements in the widened ECV and result in no significant change in the ADC values of these areas.

4.1. Limitations. The current study has some notable limitations, first and foremost among which is our small sample size, possibly explaining the indeterminate significance of some findings. In our view, similar studies with larger samples should be considered. Second, DWI sequences were based on segmented spin-echo EPI, which added to the susceptibility of the lung tissue over the LV lateral wall and caused distortion in some images. Third, EPI-based sequences usually have a low signal-to-noise ratio, adding to the complexity of image and data analysis. Thus, we recommend the evaluation of balanced steady-state free precession for DWI in larger studies on HCM.

5. Conclusions

FT-CMR can reliably show fibrosis-containing segments in HCM. Circumferential strain is probably the first strain parameter to exhibit impairment in LGE-positive patients. This is of paramount importance since this novel post-processing technique can serve as an available, easy, and fast method to show myocardial fibrosis in clinical practice and obviate the need for any additional CMR sequences or contrast injections. DWI can function as an efficient qualitative method for the estimation of the fibrosis extent in HCM, whereas low *b*-value DWI is not a reliable method to quantify the scar extent. Further large-scale multicentric studies are warranted to reliably propose these 2 novel noncontrast CMR methods for fibrosis prediction in patients suffering from HCM.

Data Availability

The datasets generated during the current research are available from the corresponding author upon reasonable request.

Conflicts of Interest

The authors declare that they have no conflicts of interest.

Authors' Contributions

Dr. AM, AN, and KK collected the data. Dr. YT, Dr. LH, and Dr. AMF prepared the primary draft. Dr. MSH, Dr. NR, and Dr.SA participated in data gathering and data analysis as well as writing the paper.

Acknowledgments

The authors would like to thank Dr. Maryam Khalili and Dr. Mohammad Mehdi Hemmati Komasi for their assistance in the data gathering.

References

[1] B. J. Maron, M. S. Maron, and C. Semsarian, "Genetics of hypertrophic cardiomyopathy after 20 years," *Journal of the American College of Cardiology*, vol. 60, no. 8, pp. 705–715, 2012.

[2] B. J. Maron, J. M. Gardin, J. M. Flack, S. S. Gidding, T. T. Kurosaki, and D. E. Bild, "Prevalence of hypertrophic cardiomyopathy in a general population of young adults," *Circulation*, vol. 92, no. 4, pp. 785–789, 1995.

[3] B. J. Gersh, B. J. Maron, R. O. Bonow et al., "2011 ACCF/AHA guideline for the diagnosis and treatment of hypertrophic cardiomyopathy," *Circulation*, vol. 124, no. 24, pp. e783–e831, 2011.

[4] A. Rudolph, H. Abdel-Aty, S. Bohl et al., "Noninvasive detection of fibrosis applying contrast-enhanced cardiac magnetic resonance in different forms of left ventricular hypertrophy," *Journal of the American College of Cardiology*, vol. 53, no. 3, pp. 284–291, 2009.

[5] J. J. Green, J. S. Berger, C. M. Kramer, and M. Salerno, "Prognostic value of late gadolinium enhancement in clinical outcomes for hypertrophic cardiomyopathy," *JACC: Cardiovascular Imaging*, vol. 5, no. 4, pp. 370–377, 2012.

[6] G. Moravsky, E. Ofek, H. Rakowski et al., "Myocardial fibrosis in hypertrophic cardiomyopathy," *JACC: Cardiovascular Imaging*, vol. 6, no. 5, pp. 587–596, 2013.

[7] W. G. Rehwald, D. S. Fieno, E.-L. Chen, R. J. Kim, and R. M. Judd, "Myocardial magnetic resonance imaging contrast agent concentrations after reversible and irreversible ischemic injury," *Circulation*, vol. 105, no. 2, pp. 224–229, 2002.

[8] S. R. Ommen, "AHA/ACC guideline for the diagnosis and treatment of patients with hypertrophic cardiomyopathy: a report of the american college of cardiology/american heart association joint committee on clinical practice guidelines," *Circulation*, vol. 145, 2020.

[9] M. Pop, N. R. Ghugre, V. Ramanan et al., "Quantification of fibrosis in infarcted swine hearts byex vivolate gadolinium-enhancement and diffusion-weighted MRI methods," *Physics in Medicine and Biology*, vol. 58, no. 15, pp. 5009–5028, 2013.

[10] C. Nguyen, "Contrast-free detection of myocardial fibrosis in hypertrophic cardiomyopathy patients with diffusion-weighted cardiovascular magnetic resonance," *Journal of Cardiovascular Magnetic Resonance*, vol. 17, no. 1, pp. 1–7, 2015.

[11] R. Wu, D.-A. An, R.-Y. Shi et al., "Myocardial fibrosis evaluated by diffusion-weighted imaging and its relationship to 3D contractile function in patients with hypertrophic cardiomyopathy," *Journal of Magnetic Resonance Imaging*, vol. 48, no. 4, pp. 1139–1146, 2018.

[12] L.-M. Wu, B.-H. Chen, Q.-Y. Yao et al., "Quantitative diffusion-weighted magnetic resonance imaging in the assessment of myocardial fibrosis in hypertrophic cardiomyopathy compared with T1 mapping," *The International Journal of Cardiovascular Imaging*, vol. 32, no. 8, pp. 1289–1297, 2016.

[13] M. Reindl, "Prognostic implications of global longitudinal strain by feature-tracking cardiac magnetic resonance in st-elevation myocardial infarction," *Circulation: Cardiovascular Imaging*, vol. 12, no. 11, Article ID e009404, 2019.

[14] I. Eitel, T. Stiermaier, T. Lange et al., "Cardiac magnetic resonance myocardial feature tracking for optimized prediction of cardiovascular events following myocardial infarction," *JACC: Cardiovascular Imaging*, vol. 11, no. 10, pp. 1433–1444, 2018.

[15] N. Rezaeian, "Comparison of global strain values of myocardium in beta-thalassemia major patients with iron load using specific feature tracking in cardiac magnetic resonance imaging," *The International Journal of Cardiovascular Imaging*, vol. 36, no. 7, 2020.

[16] U. Neisius, "Cardiovascular magnetic resonance feature tracking strain analysis for discrimination between hypertensive heart disease and hypertrophic cardiomyopathy," *PLoS One*, vol. 14, no. 8, Article ID e0221061, 2019.

[17] Z. U. Rahman, P. Sethi, G. Murtaza et al., "Feature tracking cardiac magnetic resonance imaging: a review of a novel non-invasive cardiac imaging technique," *World Journal of Cardiology*, vol. 9, no. 4, p. 312, 2017.

[18] F. Jafari, A. M. Safaei, L. Hosseini et al., "The role of cardiac magnetic resonance imaging in the detection and monitoring of cardiotoxicity in patients with breast cancer after treatment: a comprehensive review," *Heart Failure Reviews*, vol. 26, pp. 1–19, 2020.

[19] Z. B. Popović, D. H. Kwon, M. Mishra et al., "Association between regional ventricular function and myocardial fibrosis in hypertrophic cardiomyopathy assessed by speckle tracking echocardiography and delayed hyperenhancement magnetic resonance imaging," *Journal of the American Society of Echocardiography: Official Publication of the American Society of Echocardiography*, vol. 21, no. 12, pp. 1299–1305, 2008.

[20] S. Bogarapu, M. D. Puchalski, M. D. Everitt, R. V. Williams, H.-Y. Weng, and S. C. Menon, "Novel cardiac magnetic resonance feature tracking (CMR-FT) analysis for detection of myocardial fibrosis in pediatric hypertrophic cardiomyopathy," *Pediatric Cardiology*, vol. 37, no. 4, pp. 663–673, 2016.

[21] P. P. Swoboda, "Effect of cellular and extracellular pathology assessed by T1 mapping on regional contractile function in hypertrophic cardiomyopathy," *Journal of Cardiovascular Magnetic Resonance*, vol. 19, no. 1, pp. 1–10, 2017.

[22] W. Hindieh, R. Chan, and H. Rakowski, "Complementary role of echocardiography and cardiac magnetic resonance in hypertrophic cardiomyopathy," *Current Cardiology Reports*, vol. 19, no. 9, p. 81, 2017.

[23] J. C. C. Moon, E. Reed, M. N. Sheppard et al., "The histologic basis of late gadolinium enhancement cardiovascular magnetic resonance in hypertrophic cardiomyopathy," *Journal of the American College of Cardiology*, vol. 43, no. 12, pp. 2260–2264, 2004.

[24] D. Muser, S. A. Castro, P. Santangeli, and G. Nucifora, "Clinical applications of feature-tracking cardiac magnetic resonance imaging," *World Journal of Cardiology*, vol. 10, no. 11, pp. 210–221, 2018.

[25] S. Rapacchi, H. Wen, M. Viallon et al., "Low b-value diffusion-weighted cardiac magnetic resonance imaging," *Investigative Radiology*, vol. 46, no. 12, pp. 751–758, 2011.

[26] D. Le Bihan, E. Breton, D. Lallemand, P. Grenier, E. Cabanis, and M. Laval-Jeantet, "MR imaging of intravoxel incoherent motions: application to diffusion and perfusion in neurologic disorders," *Radiology*, vol. 161, no. 2, pp. 401–407, 1986.

[27] A. Chiribiri, S. Leuzzi, M. R. Conte et al., "Rest perfusion abnormalities in hypertrophic cardiomyopathy: correlation with myocardial fibrosis and risk factors for sudden cardiac death," *Clinical Radiology*, vol. 70, no. 5, pp. 495–501, 2015.